

Pigmy resonances, neutron skins and neutron stars

C.A. Bertulani



TEXAS A&M UNIVERSITY

COMMERCE

Collaboration



Dr. Paolo Avogadro



Prof. Andrew Sustich



Hiroyuki Sagawa
Professor



Prof. Thomas Aumann



Prof. Mahir Hussein



Dr. Hongliang Liu



Nathan Brady



James Thomas

Outline of this talk

- Disappointing start with pigmy
- Pigmy revival
- Pigmy inn stars
- Compressional modulus and symmetry energy
- Neutron skins
- Dipole polarizability
- Perspectives with electron-ion scattering

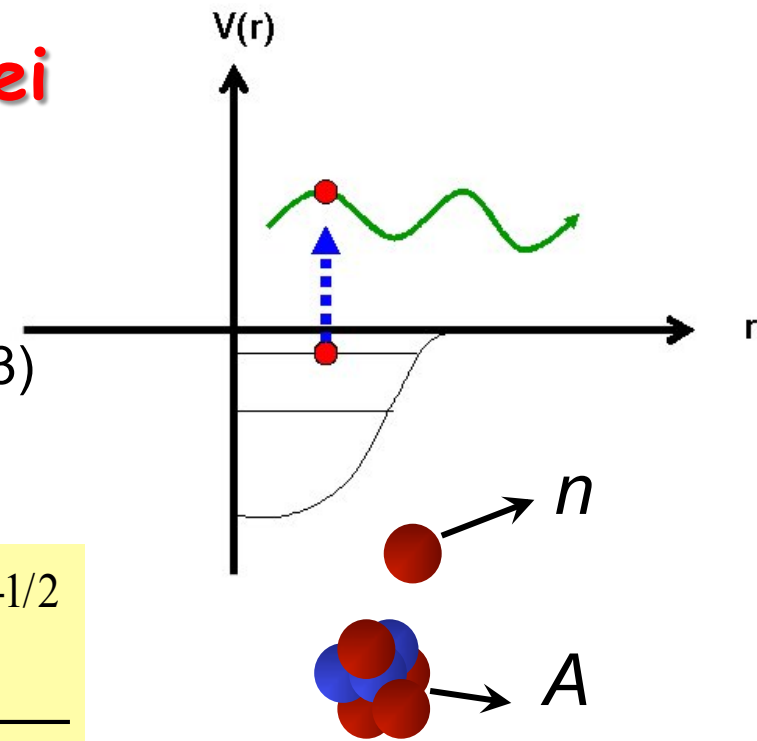
No Pigmy, no collective motion

E & M response in neutron-rich nuclei

First studies

Two-body cluster: CB, Baur, NPA 480, 615 (1988)

CB, Sustich, PRC 46, 2340 (1993)

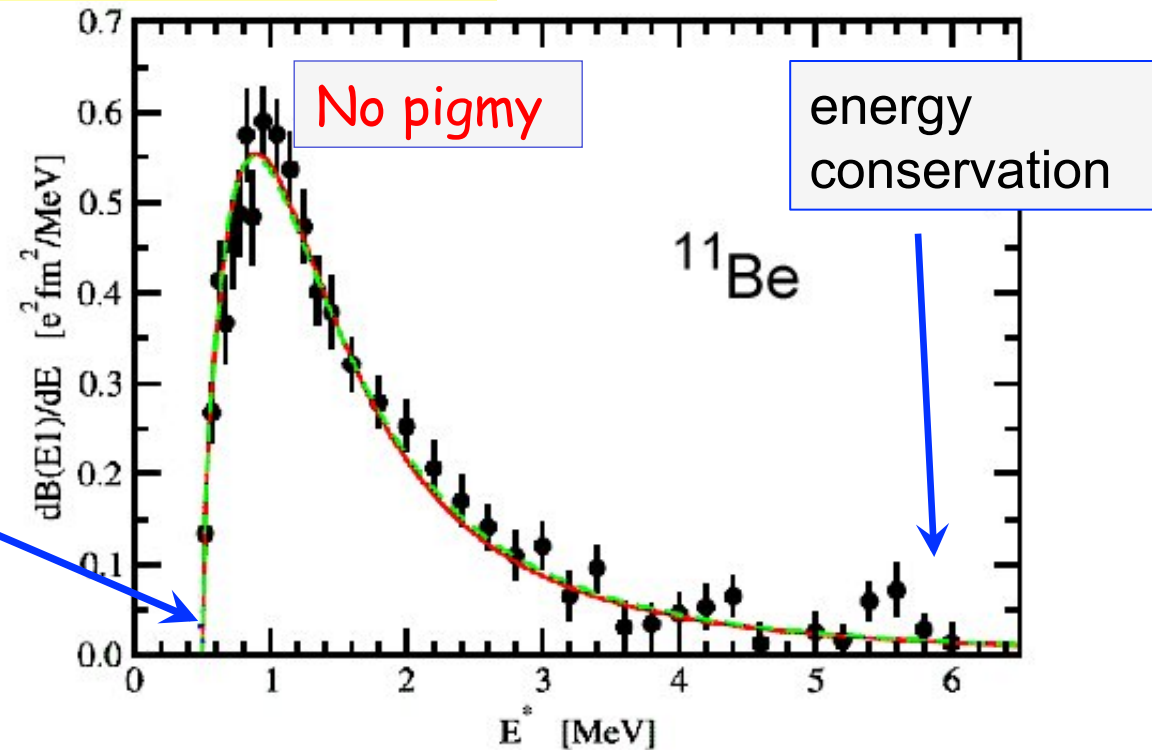


$$\frac{dB(EL)}{dE} \sim \left| \left\langle \Psi_f \left| r^L Y_L \right| \Psi_i \right\rangle \right|^2 \sim \frac{(E_x - S_n)^{L+1/2}}{E_x^{2L+2}}$$

$$E_r^{(EL)\text{peak}} \approx \frac{L+1/2}{L+3/2} S_n$$

$$E_r^{(E1)\text{peak}} \approx \frac{3}{5} S_n$$

phase space



3-body model

CB, PRC 75, 024606 (2007)
NPA 790, 467 (2007)

$$\Psi(\mathbf{x}, \mathbf{y}) = \frac{1}{\rho^{5/2}} \sum_{\text{KLS}1_x1_y} \Phi_{\text{KLS}}^{1_x1_y}(\rho) \left[\Gamma_{\text{KL}}^{1_x1_y}(\Omega_5) \otimes \chi_S \right]_{\text{JM}}$$

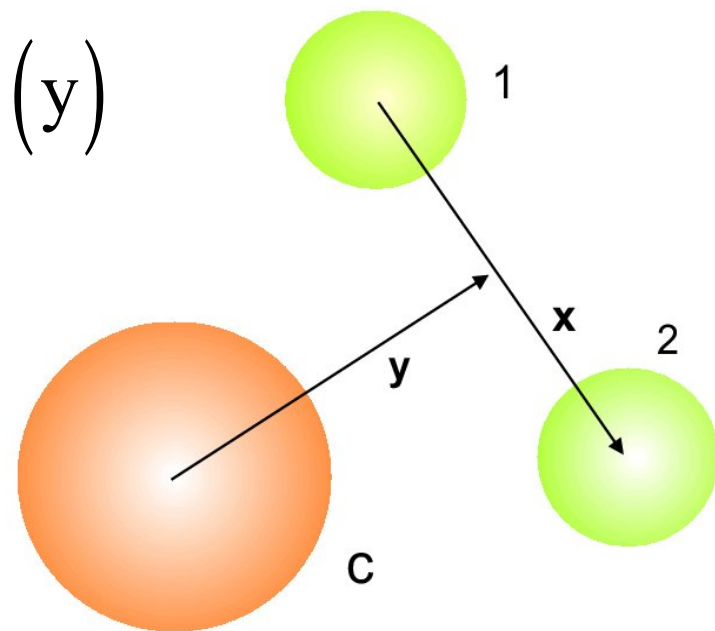
$$\Omega_5 = (\theta_x, \varphi_x, \theta_y, \varphi_y, \theta)$$

$$x = \rho \sin \theta, \quad y = \rho \cos \theta$$

$$\langle \Psi_f | r Y_1 | \Psi_i \rangle \propto \int dx dy \frac{\Phi_\alpha(\rho)}{\rho^{5/2}} y^3 x u_p(x) u_q(y)$$

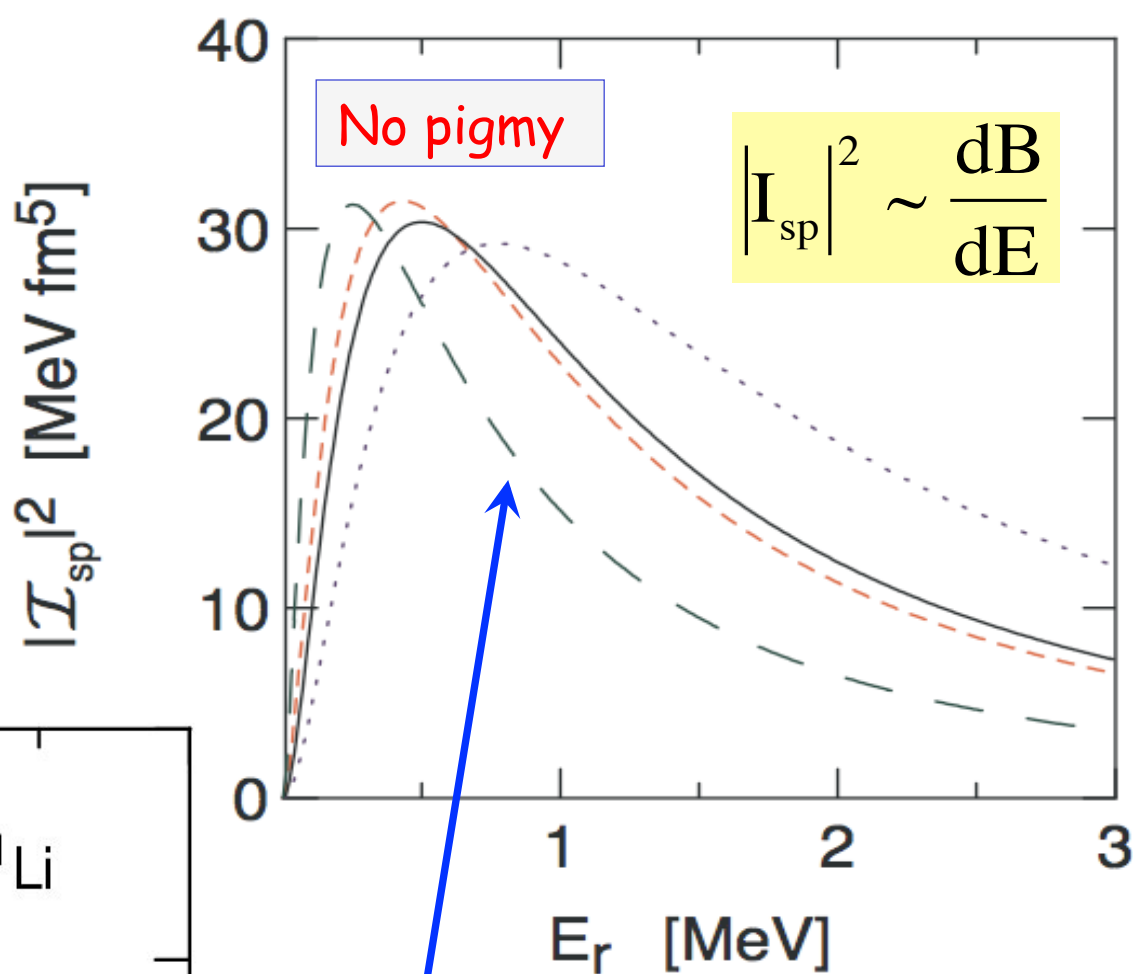
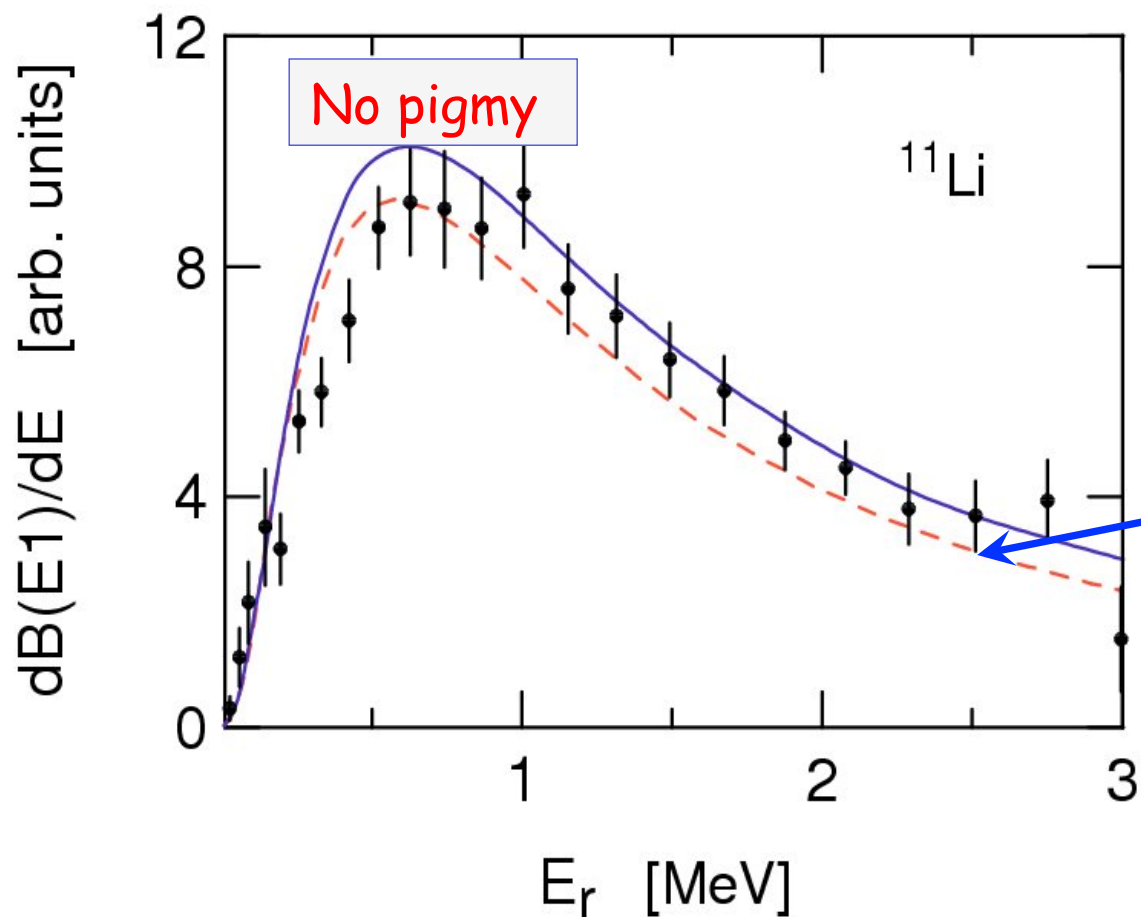
$$\frac{dB(E1)}{dE_r} \propto \frac{E_r^3}{(S_{2n}^{\text{eff}} + E_r)^{11/2}} (1 + \text{FSI})^2$$

$$S_{2n}^{\text{eff}} \cong 1.8 S_{2n}$$



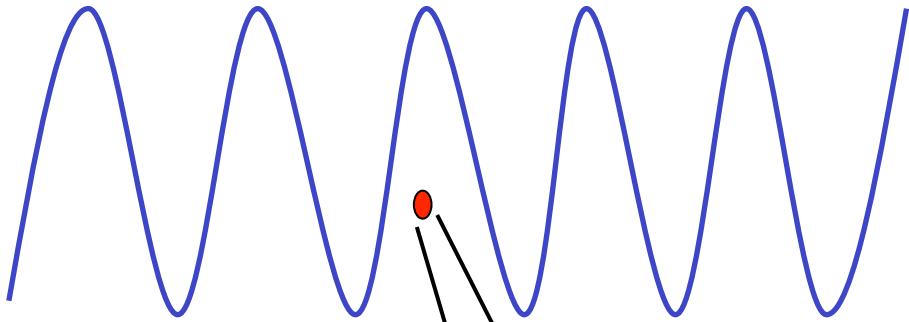
3-body model

3-body configurations and FSI widen $\frac{dB(E1)}{dE}$

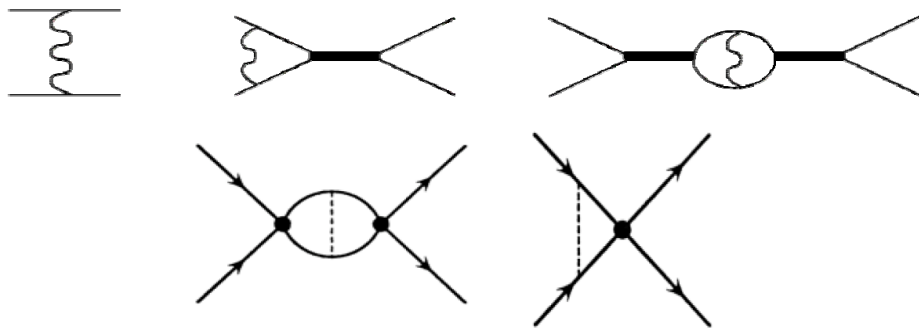


FSI: Different scattering lengths, effective ranges

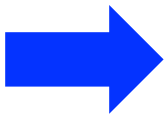
Halo EFT



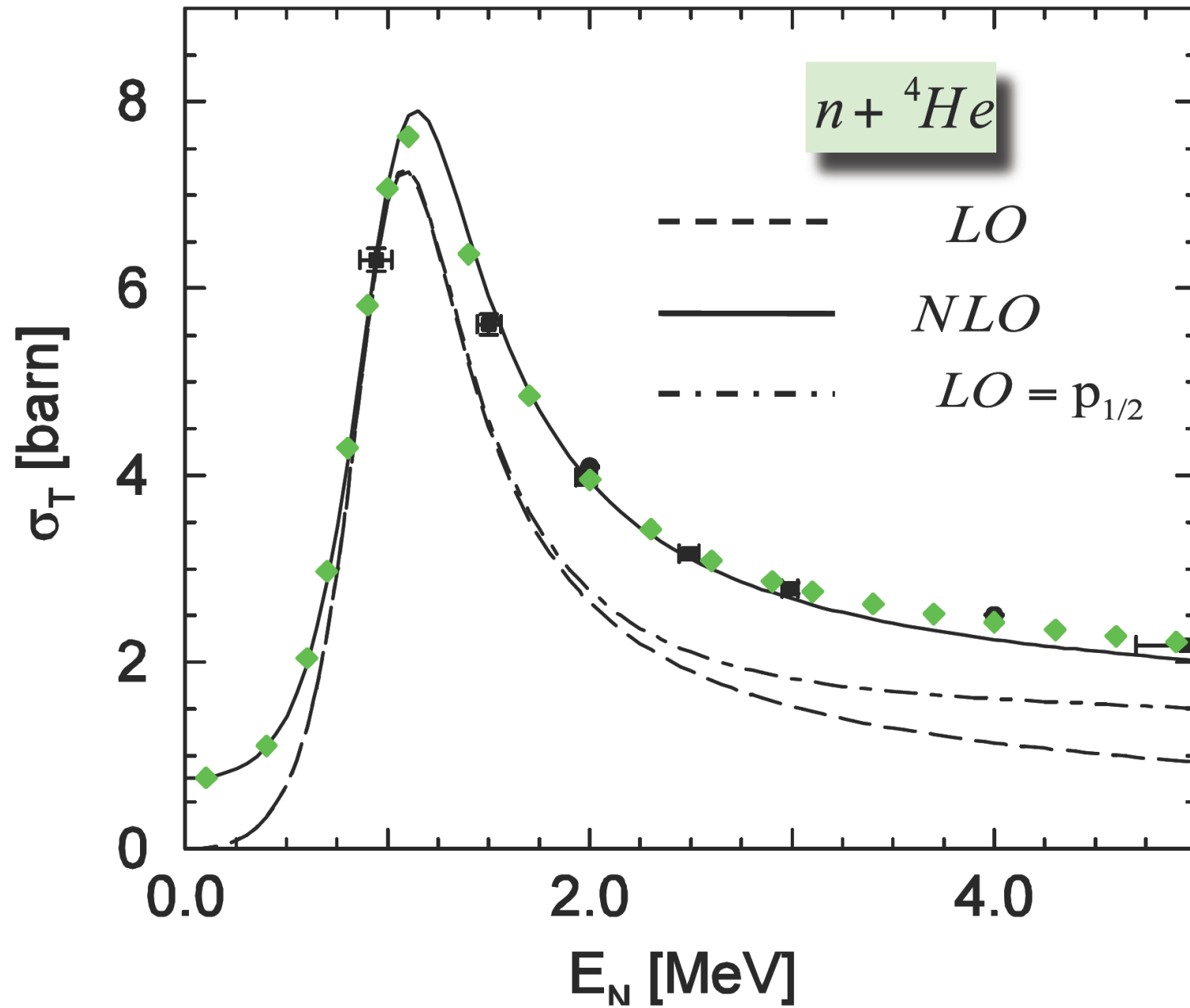
$$\begin{aligned} \mathcal{L}_{\text{EFT}} = & N^+ \left(i\partial_0 + \frac{\nabla^2}{2m_N} \right) N + C_0 N^+ N N^+ N \\ & + N^+ \frac{\nabla^4}{8m_N^3} N + C_2 N^+ N N^+ \nabla^2 N \\ & + C'_2 N^+ \vec{\nabla} N \cdot N^+ \vec{\nabla} N + \dots \end{aligned}$$



- Feynman diagrams
- particle exchange
- vacuum polarization
- loop integrals, divergences
- regularization, renormalization



Halo EFT



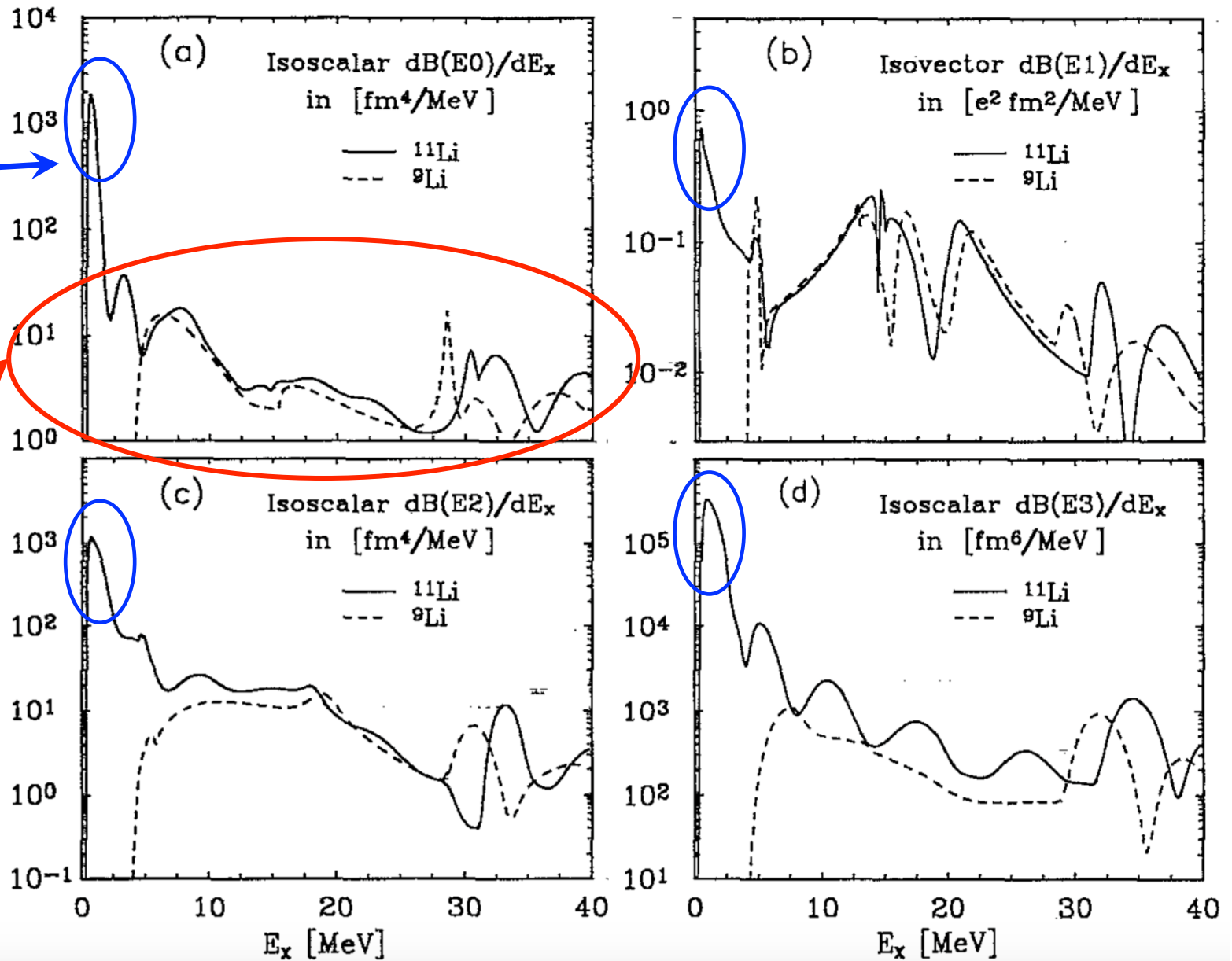
CB, H-W. Hammer, U. van Kolck, NPA 712, 37 (2002)

Many-body models

Continuum RPA: CB, Sustich, PRC 46 , 2340 (1992)

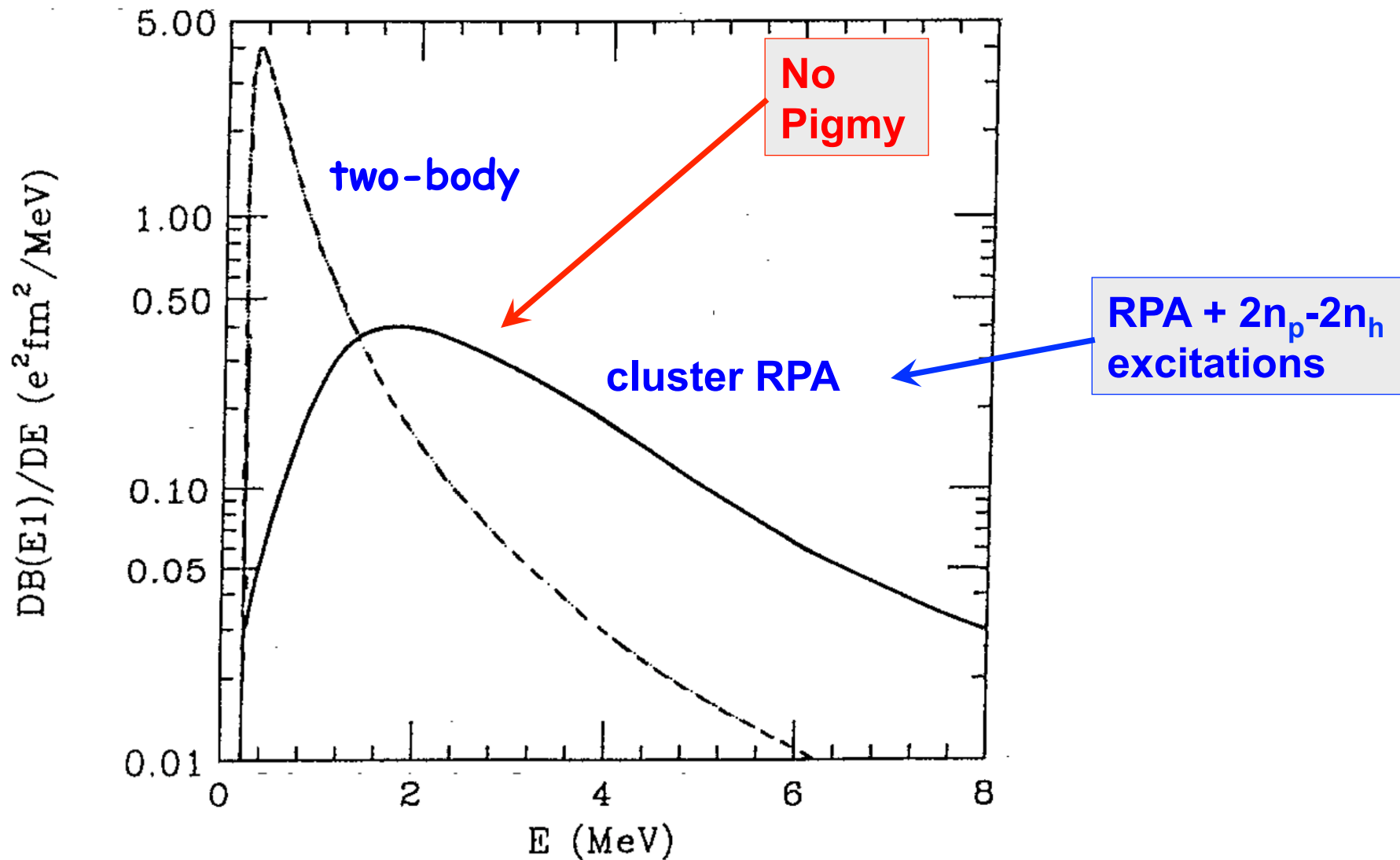
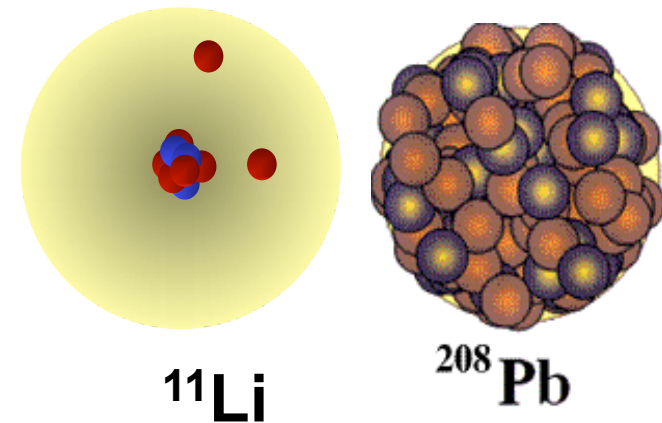
No
Pigmy

Core
excitations



Many-body models

Cluster RPA: Teruya, CB, Krewald, Dias, Hussein,
PRC 43, 2049 (1991)



Pigmy & collective motion

Origins of Pigmy Resonance

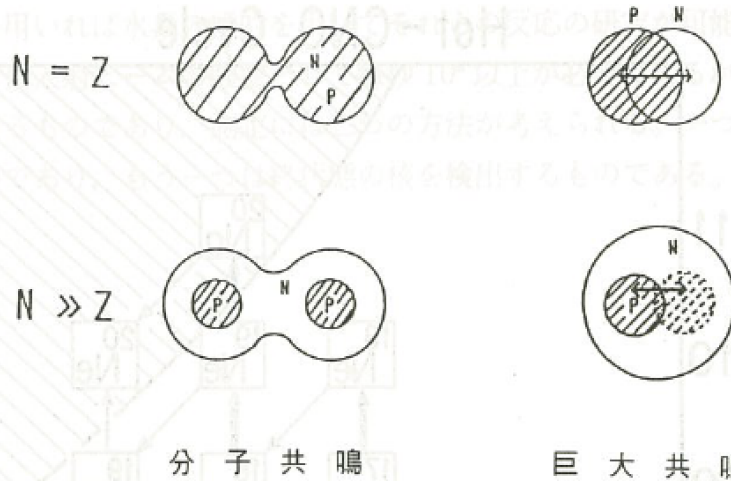
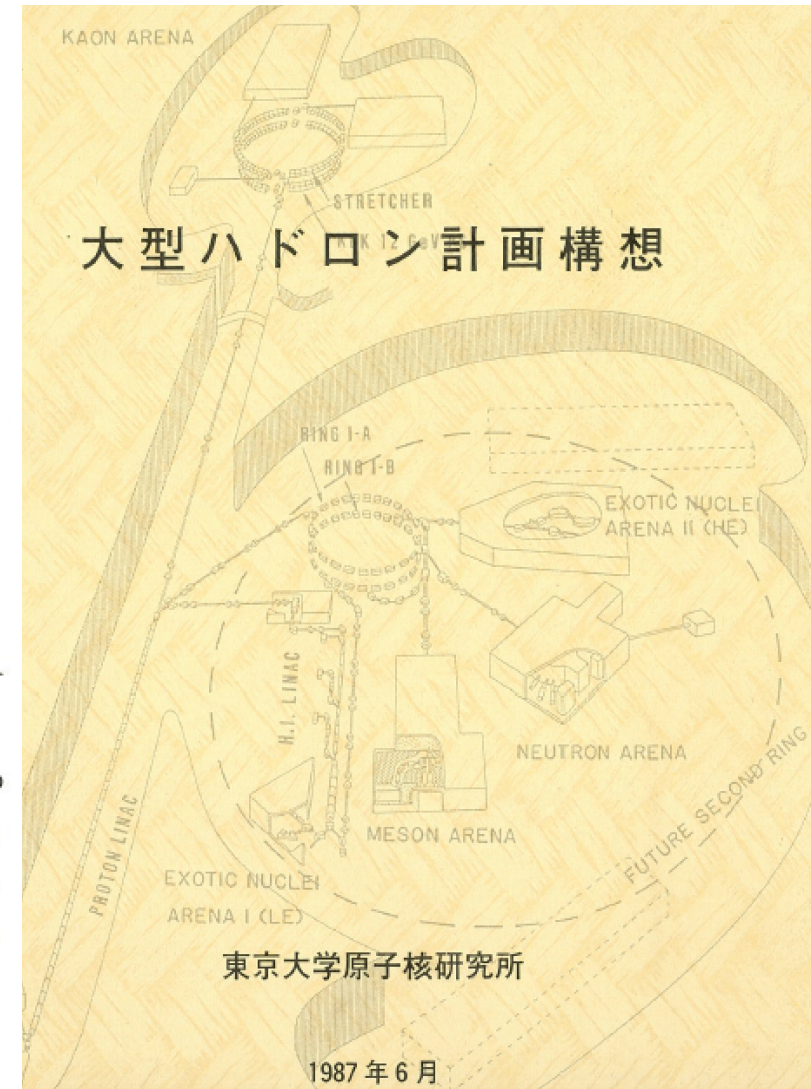


図 3E-6 N=Z 核と N>>Z 核の集団運動の例

なく、 $N \approx Z$ 領域の核物質の性質及び有効相互作用の研究に関連する課題である。また、関連するテーマとしては、中性子過剰核のアイソベクトル型巨大共鳴の探求も興味深い。

安定核領域の分子状態の研究において重要な問題の一つに、出口チャンネルの分子共鳴への寄与がある。出口チャンネルは、多くの場合不安定状態の二つの原子核からなるため、これまでその効果を明瞭に調べることができなかった。不安定核のビームを用いれば、出口チャンネルの分子共鳴への寄与が調べられ、ひいてはこれまで不明瞭だった共鳴の原因がどのチャンネルにあるか特定することができる。



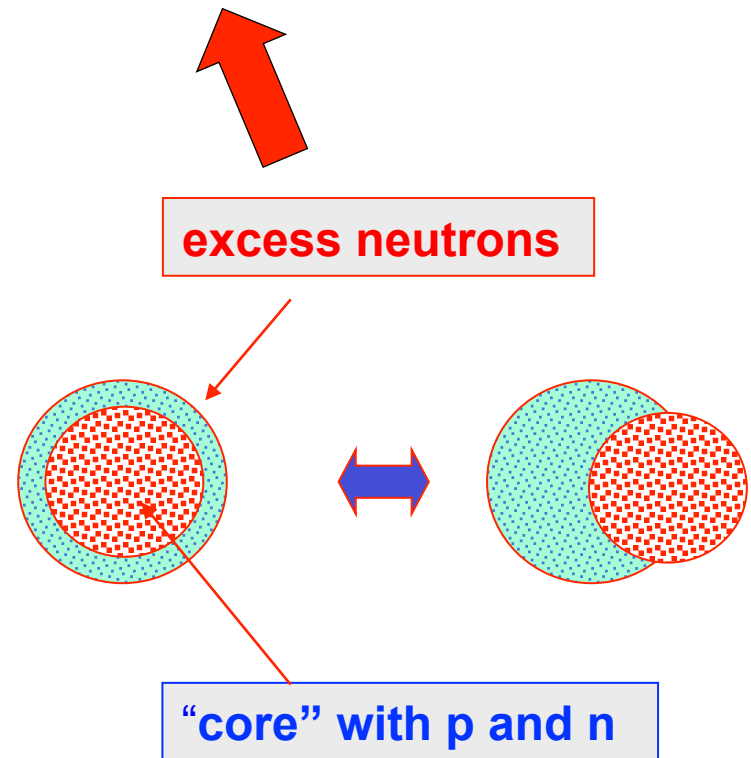
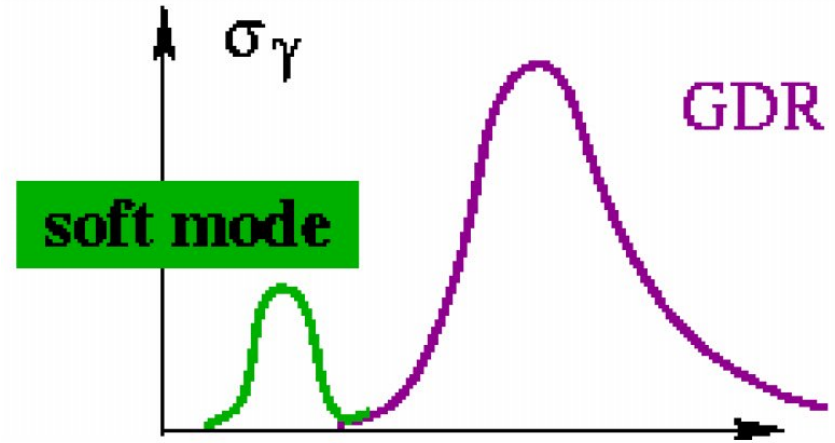
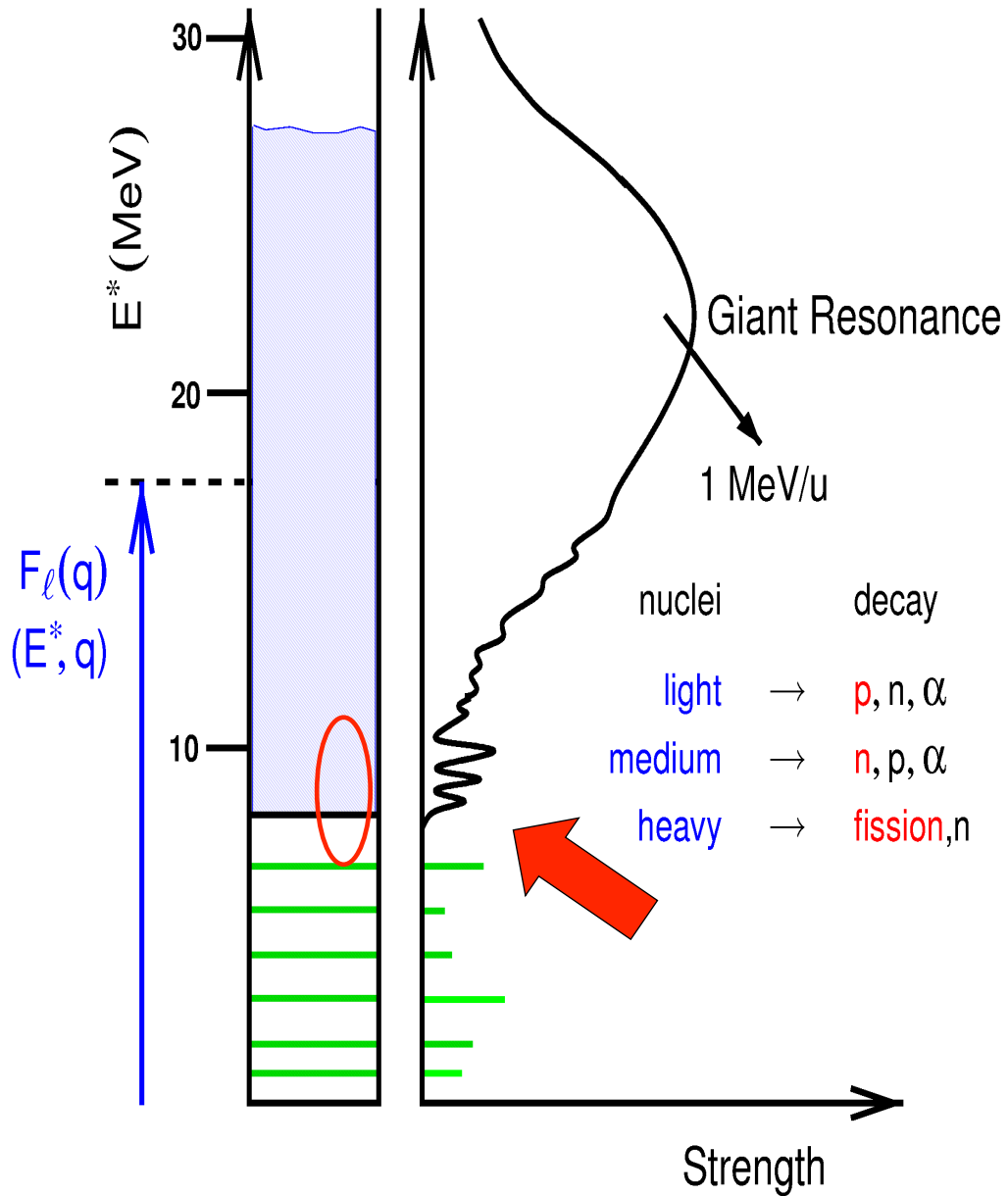
• June 1987

Nomura, Kubono, et al.

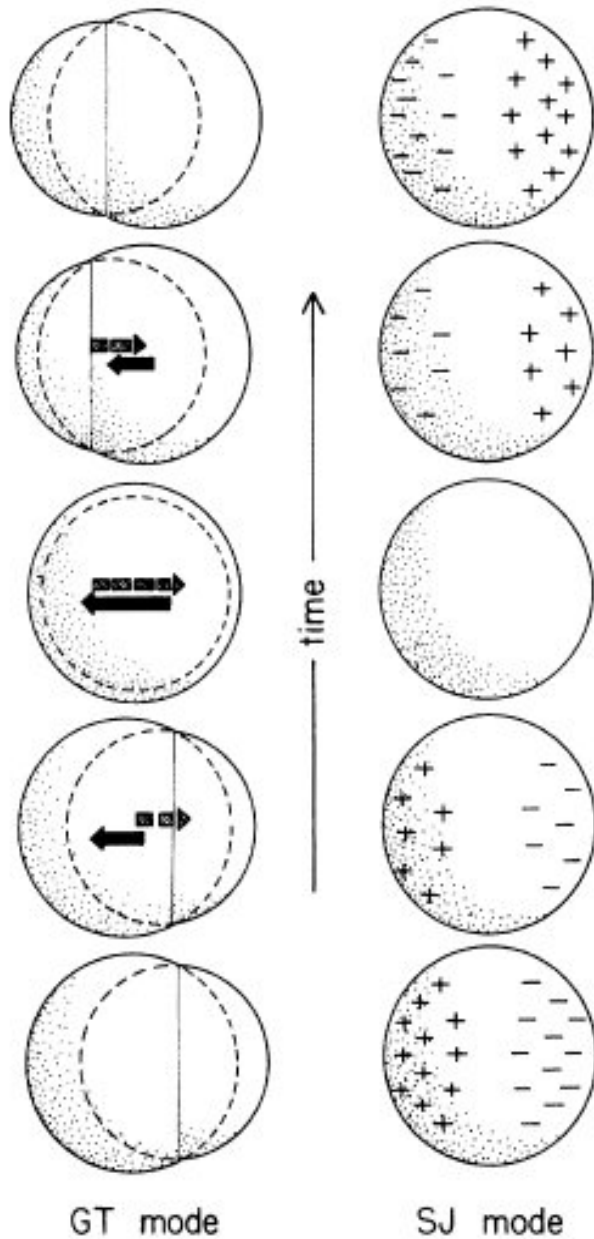
Experiment proposal (J-PARC)

Idea of Pigmy Resonance in N-rich nuclei

Collective vibrations



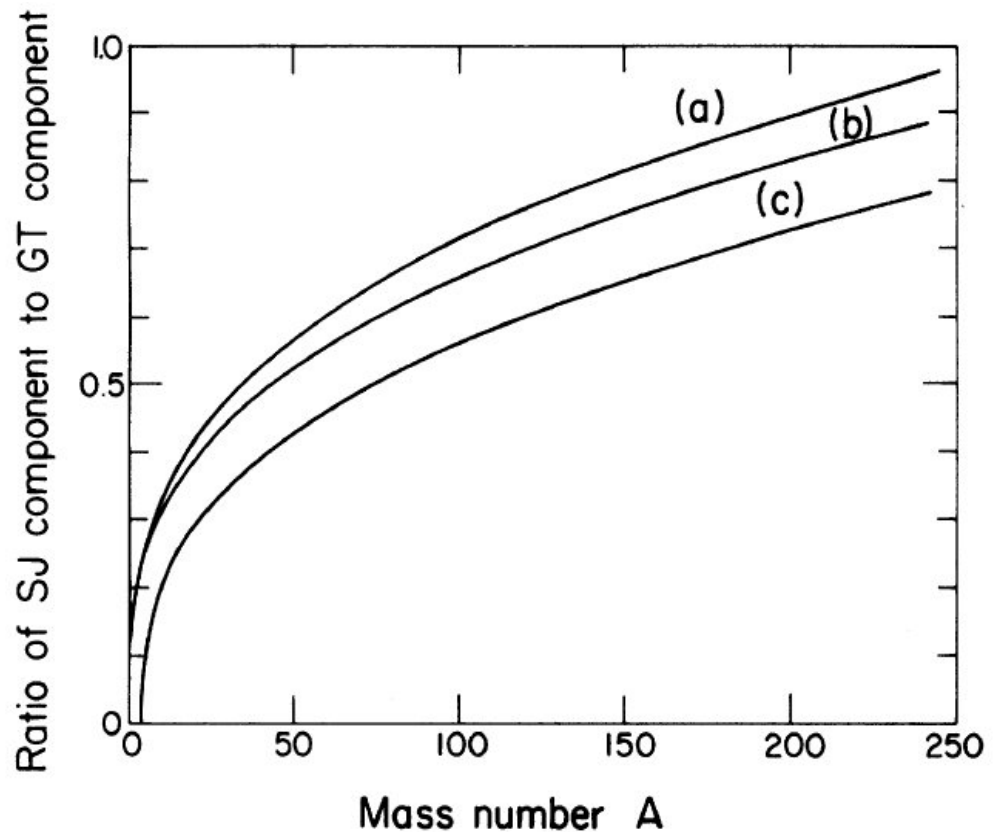
Hydrodynamics



$$T = \frac{1}{2} m^* \int \rho_p \left(\mathbf{v}_{\text{SJ}}^{(p)} + \mathbf{v}_{\text{GT}}^{(p)} \right)^2 + \rho_n \left(\mathbf{v}_{\text{SJ}}^{(n)} + \mathbf{v}_{\text{GT}}^{(n)} \right)^2$$

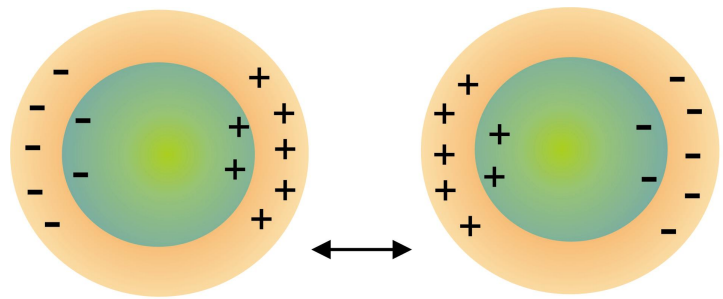
$$V = -\kappa \int d^3r \frac{(\rho_p - \rho_n)^2}{\rho_p + \rho_n} + \text{surf. terms}$$

$$\kappa \cong 30\text{-}40 \text{ MeV}$$

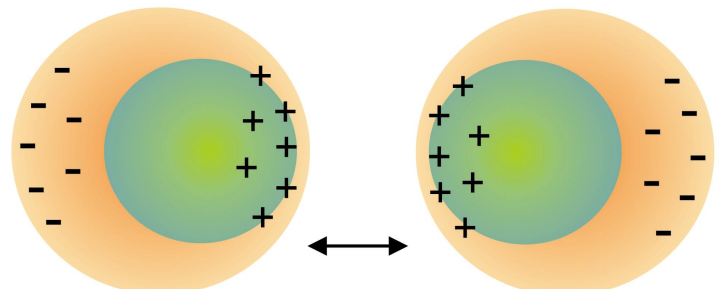


Myers et al, PRC 15, 2032 (1977)

Transition densities for pigmy resonances



SJ



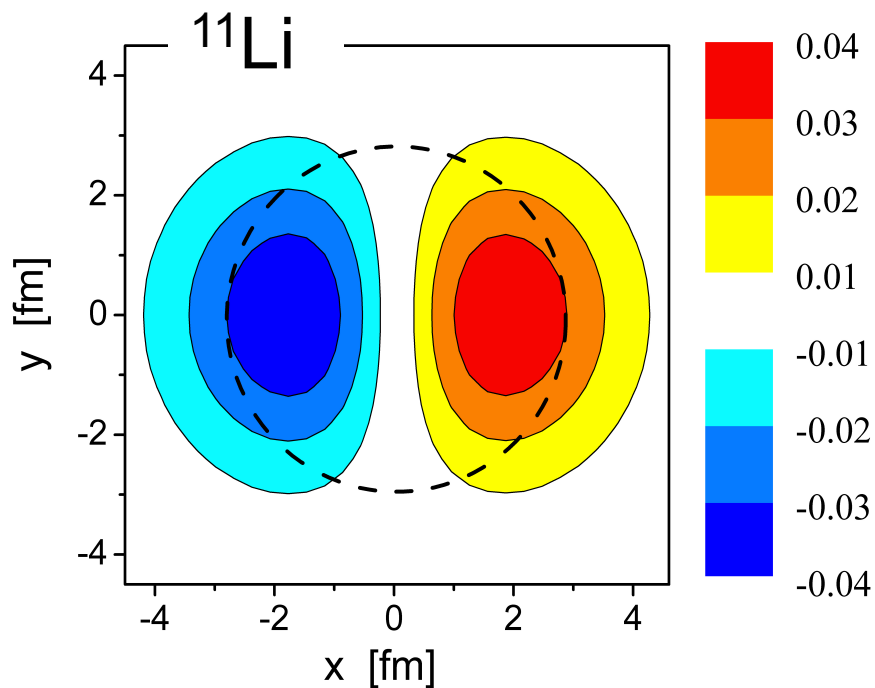
GT

$$\delta\rho = \sqrt{\frac{4\pi}{3}} R \left[Z_{\text{eff}}^{(\text{GT})} \alpha_{\text{GT}} \frac{d}{dr} + Z_{\text{eff}}^{(\text{SJ})} \alpha_{\text{SJ}} \frac{K}{R} j_1(kr) \right] \rho_0(r)$$

$kR = 2.081, \quad K = 9.93$

GT

SJ



$$E_{\text{PR}} = \left[\frac{3S_n A \hbar^2}{2aRm_N A_c (A - A_c)} \right]^{1/2} \sim 1-3 \text{ MeV}$$

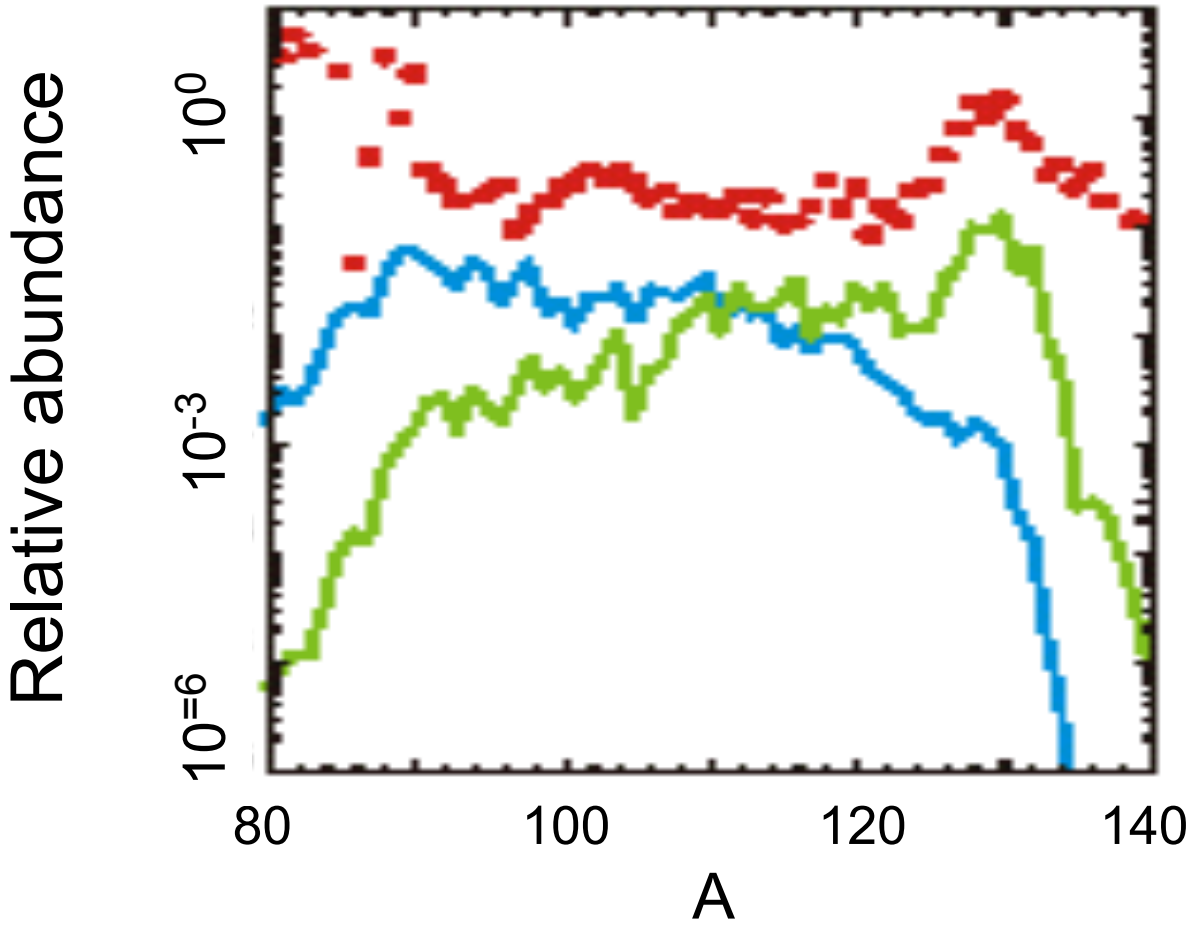
$$\Gamma_{\text{PR}} = \frac{\hbar \sqrt{\bar{v}_{\text{core}} \bar{v}_{\text{skin}}}}{R} \sim 3 \text{ MeV}$$

CB, PRC 75, 024606 (2007)
NPA 790, 467 (2007)

Pigmy & stars

Nucleosynthesis

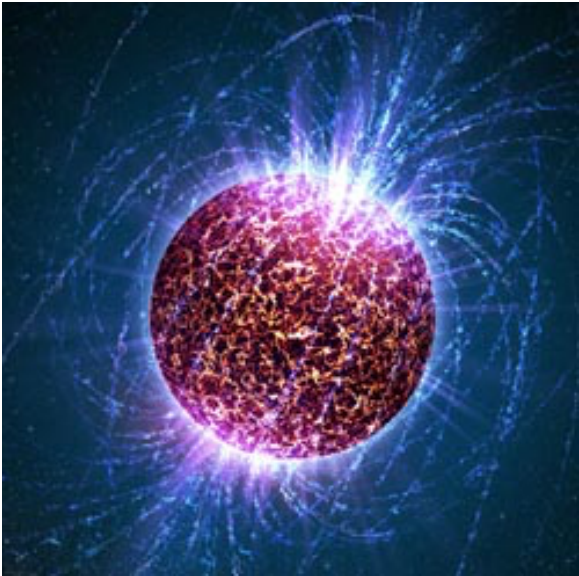
Nucleosynthesis: (γ,n) or (n,γ) cross sections in the r-process



Red: empirical
Blue: no pygmy
Green: with pygmy

S. Goriely, PLB 436, 10 (1998)

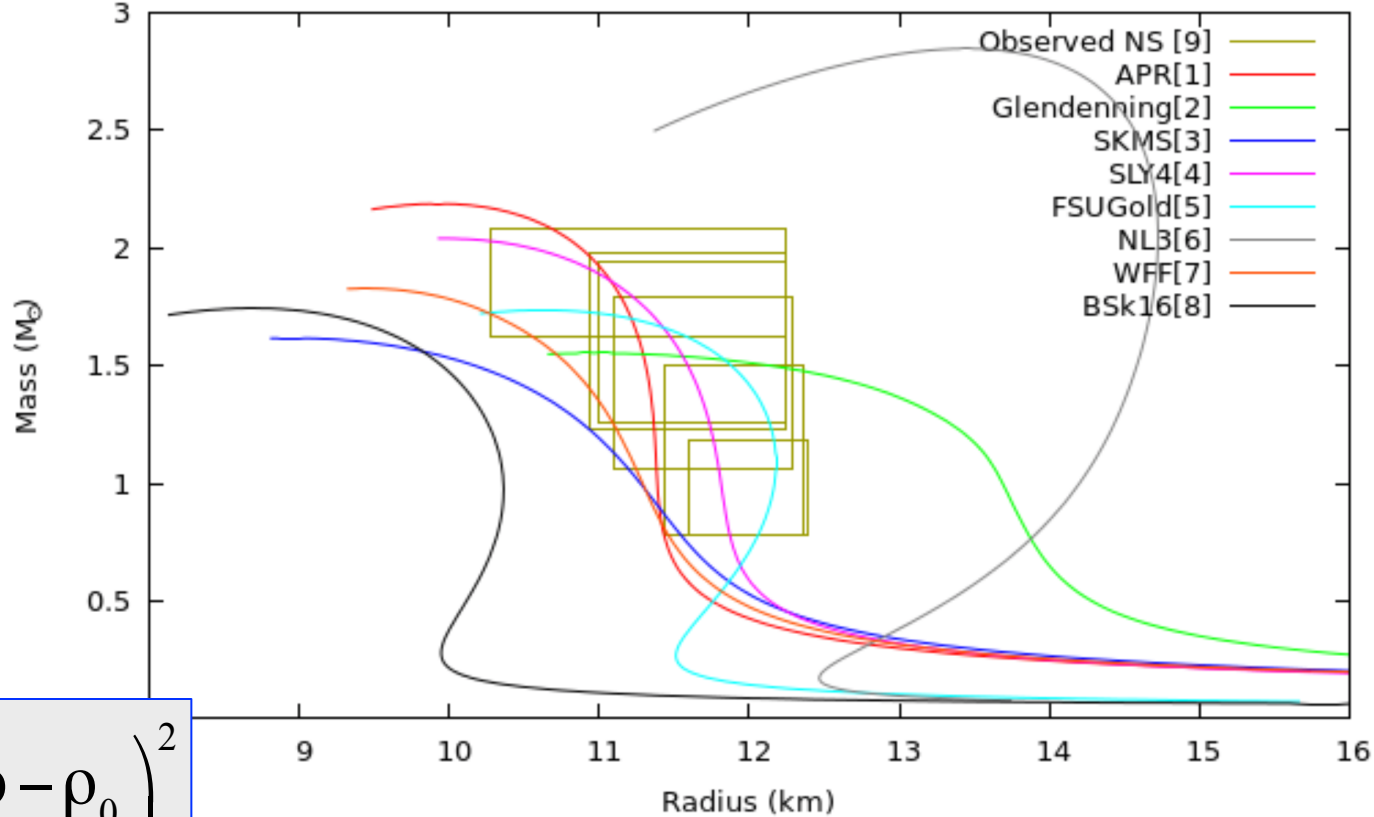
EOS & Neutron stars



$$\frac{dP}{dr} = -\frac{G\rho(r)M(r)}{r^2} \left[1 + \frac{P(r)}{\rho(r)} \right] \left[1 + \frac{4\pi r^3 P(r)}{M(r)} \right] \left[1 - \frac{2GM(r)}{r} \right]^{-1}$$

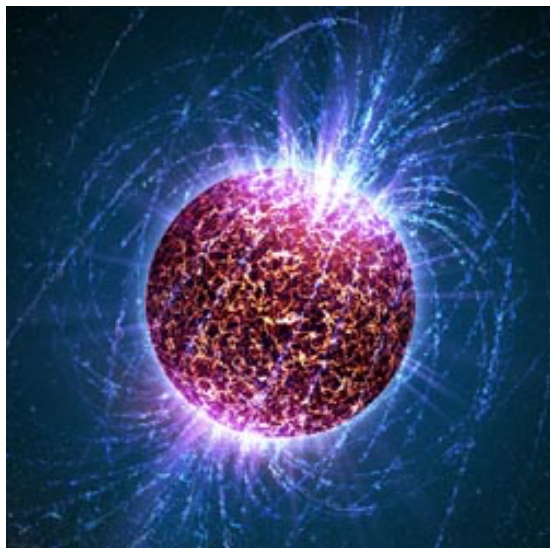
$$\frac{dM}{dr} = 4\pi r^2 \rho(r) \quad \text{Tolman-Oppenheimer-Volkoff}$$

$$K_\infty = 9\rho_0^2 \left. \frac{d^2 [E(\rho) / \rho]}{d\rho^2} \right|_{\rho_0}$$

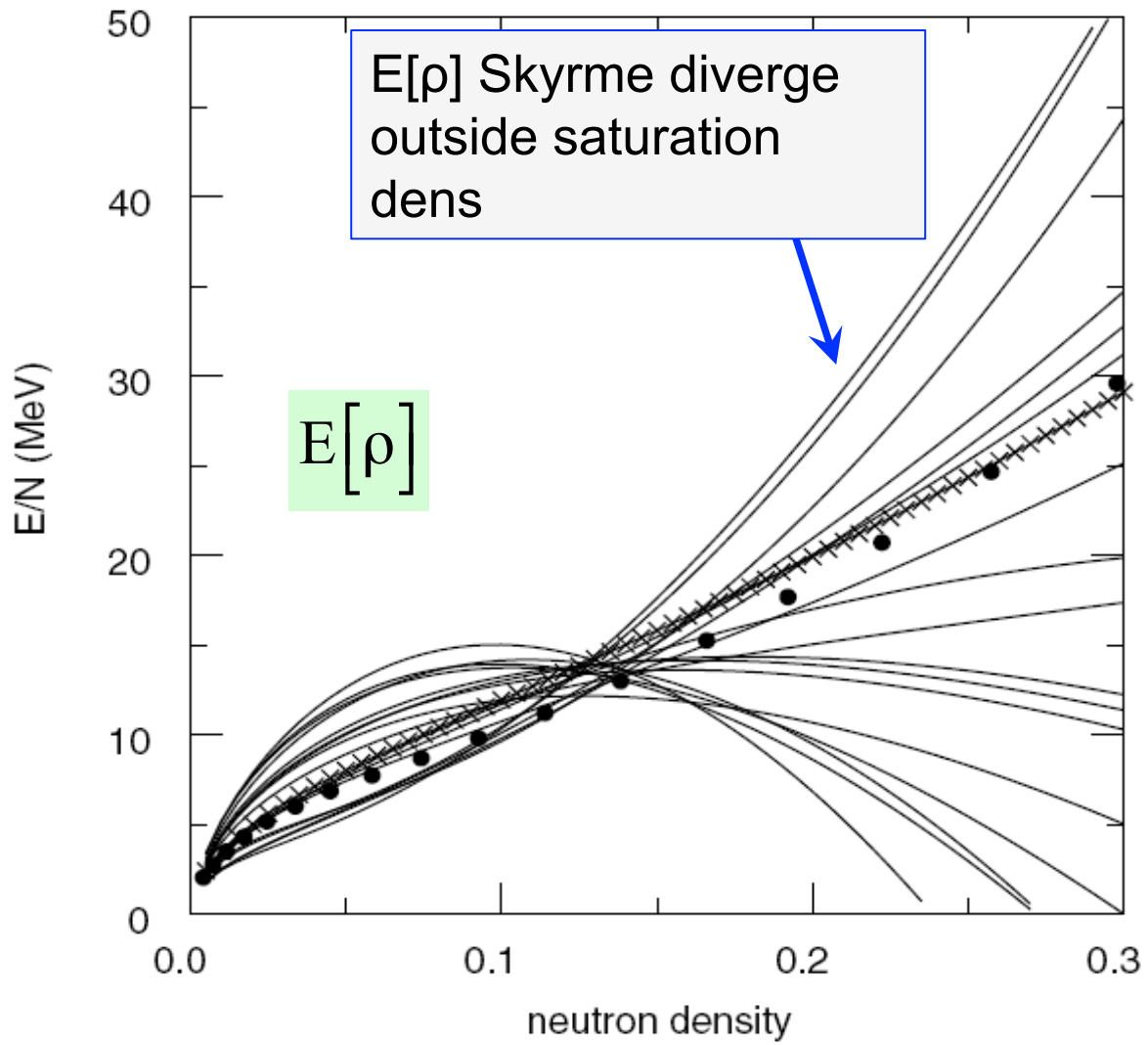


$$E[\rho] = E[\rho_0] + \frac{1}{18} K_\infty \left(\frac{\rho - \rho_0}{\rho_0} \right)^2$$

EOS & Neutron stars



$E[\rho]$ Skyrme diverges outside saturation
Brown, PRL 85 (2000) 5296



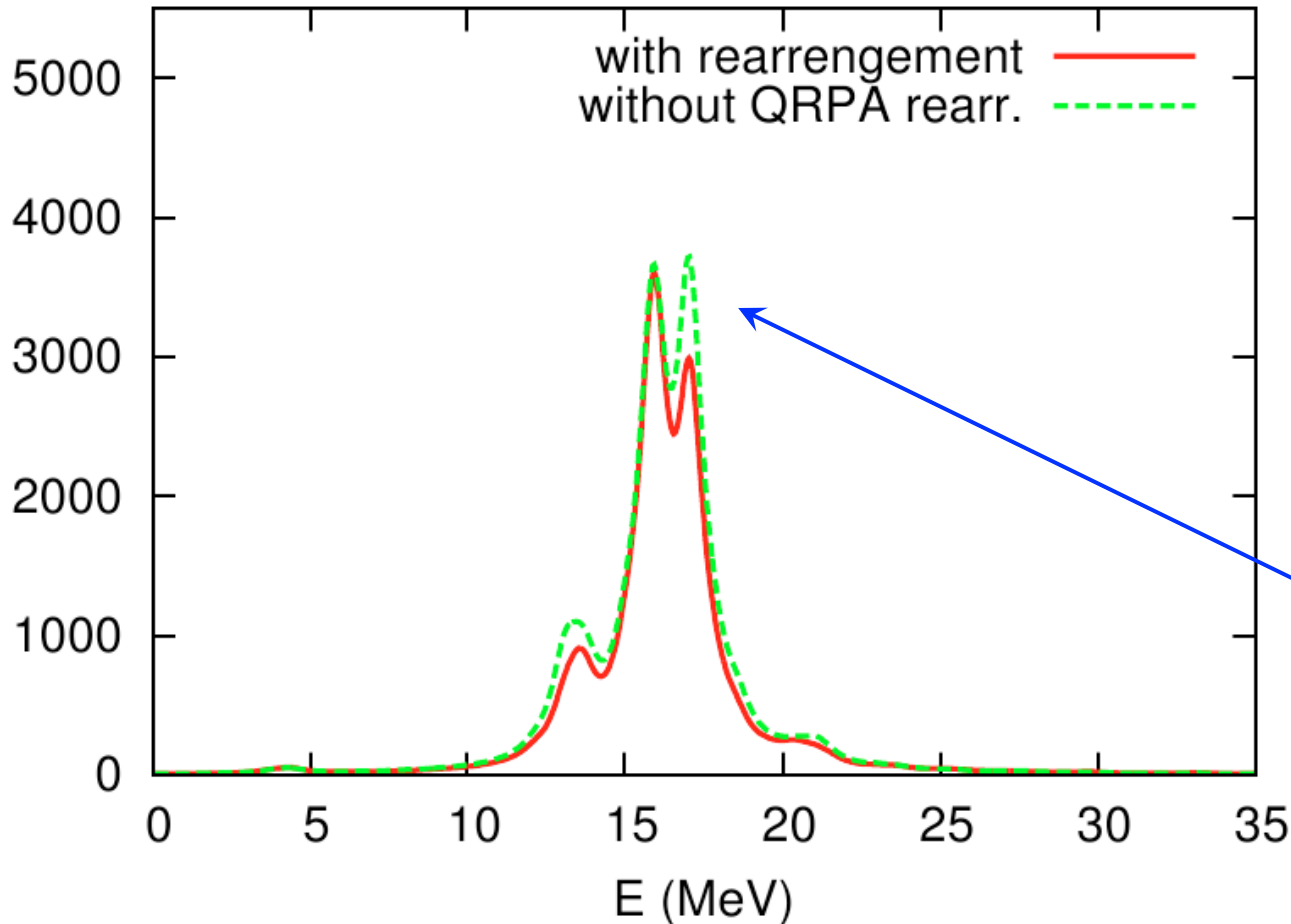
QRPA: pairing induces a rearrangement term

Avogadro, CB, PRC 88, 044319 (2013)

$$h = \frac{\delta E_{\text{kin}}}{\delta \rho} + \frac{\delta E_{\text{skyrme}}}{\delta \rho} + \frac{\delta E_{\text{pair}}}{\delta \rho} + \frac{\delta E_{\text{Coul}}}{\delta \rho}$$

- Fully self consistent EWSR = 99.2%
- Without rearrangement in EWSR = 116%

^{112}Sn , SkM* + surface



$$\frac{\delta h_{\text{rearr}}}{\delta \rho} = \frac{\delta}{\delta \rho} \left(\frac{\delta E_{\text{pair}}}{\delta \rho} \right)$$

$\neq 0$ if E_{pair} depends on density

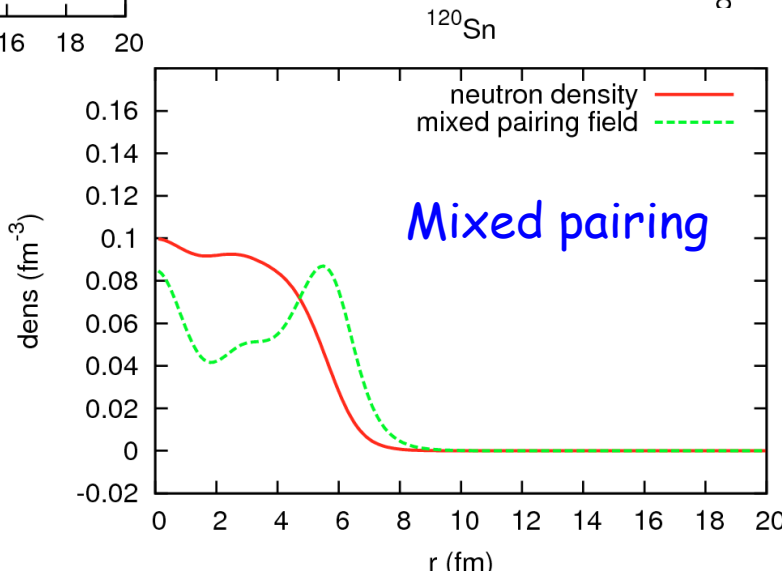
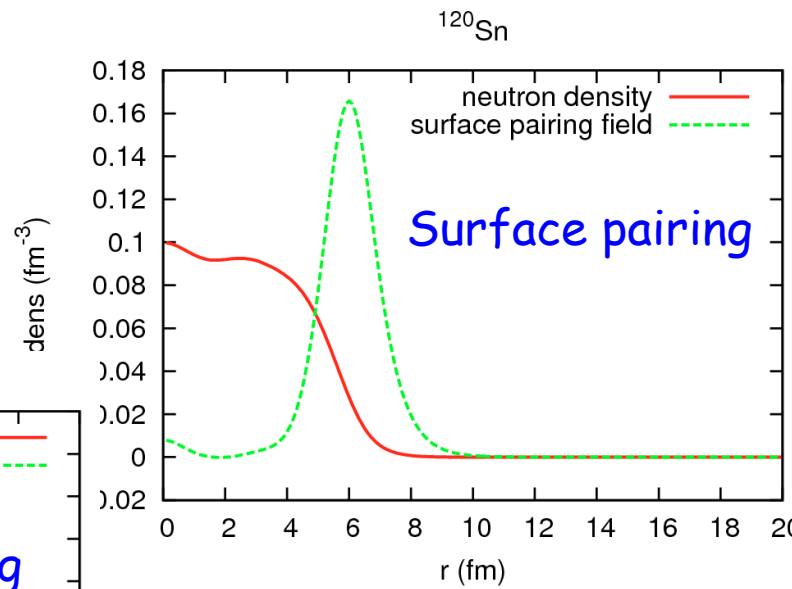
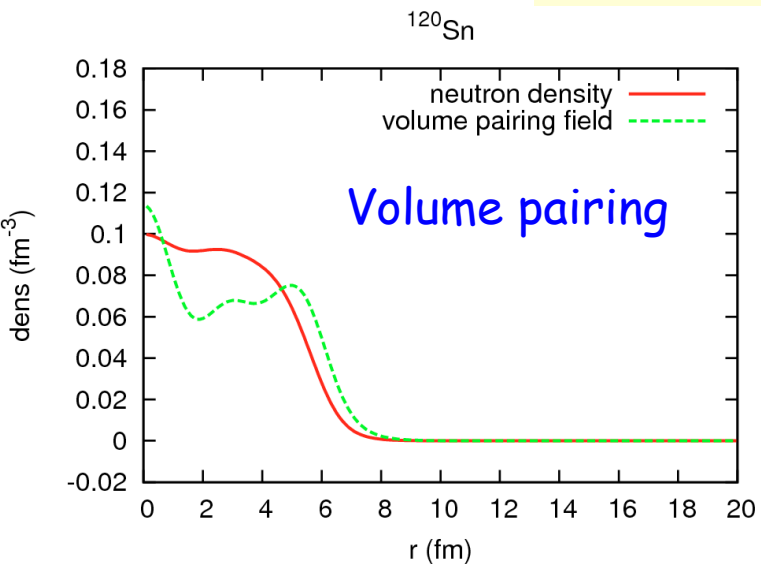
Calculations without rearrangements tend to return higher centroids respect to the fully self-consistent case.

Mean field + Pairing

A clear understanding of **the microscopic foundation of the pairing functional is still lacking.**

$$v(\mathbf{r}, \mathbf{r}') = v_0 \left[1 - \eta \left(\frac{\rho}{\rho_0} \right)^\gamma \right] \delta(\mathbf{r} - \mathbf{r}')$$

Skyrme	K_∞
SLy5	230
SkM*	216
Skxs20	202



EOS + symmetry energy

$$E[\rho] = E[\rho_0] + \frac{1}{18} K_\infty \left(\frac{\rho - \rho_0}{\rho_0} \right)^2 + S \left(\frac{\rho_n - \rho_p}{\rho} \right)^2 + \dots$$

$$S = \frac{1}{8} \frac{\partial^2 (E / \rho)}{\partial y^2} \Big|_{\rho, y=1/2}, \quad y = \frac{\rho_p}{\rho}$$

$$= J + Lx + \frac{1}{2} K_{\text{sym}} x^2 + O(x^3), \quad x = \frac{(\rho - \rho_0)}{3\rho_0}$$

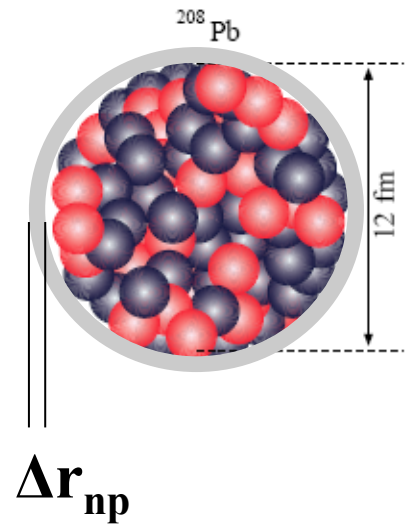
Skyrme	ρ_0	E_0	K_∞	J	L	K_{sym}
SLy5	0.161	-15.99	229.92	32.01	48.15	-112.76
SkM*	0.160	-15.77	216.61	30.03	45.78	-155.94
Skxs20	0.162	-15.81	201.95	35.50	67.06	-122.31

Neutron skins

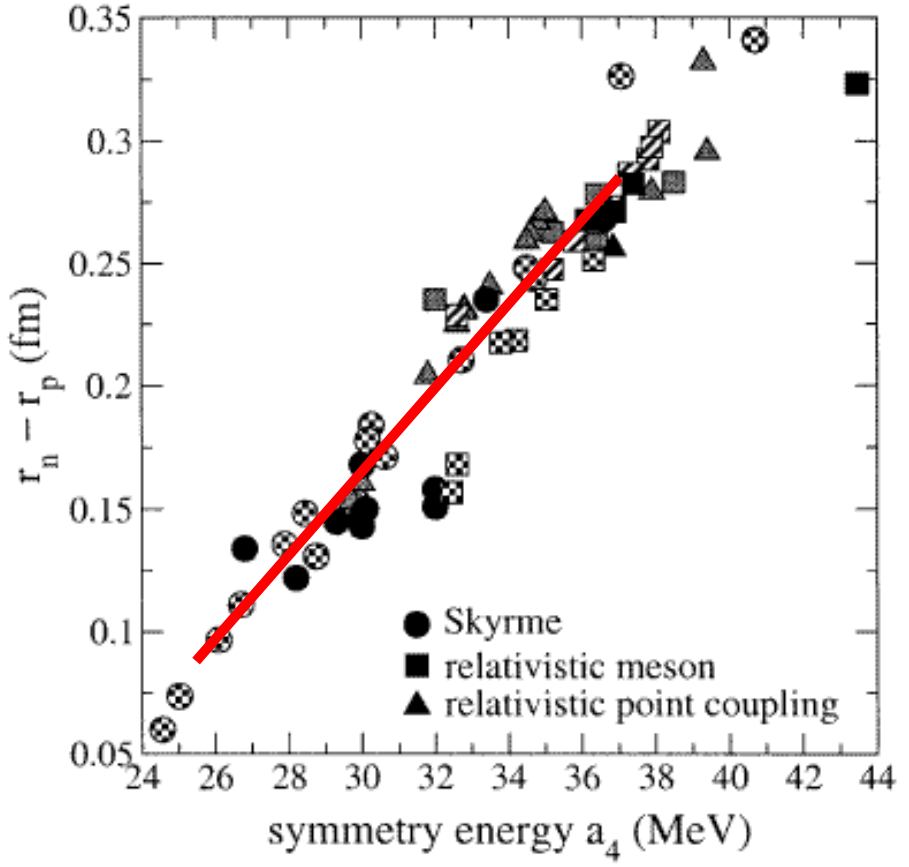
Symmetry energy & neutron skin

$$S = J + Lx + \frac{1}{2} K_{\text{sym}} x^2 + \dots,$$

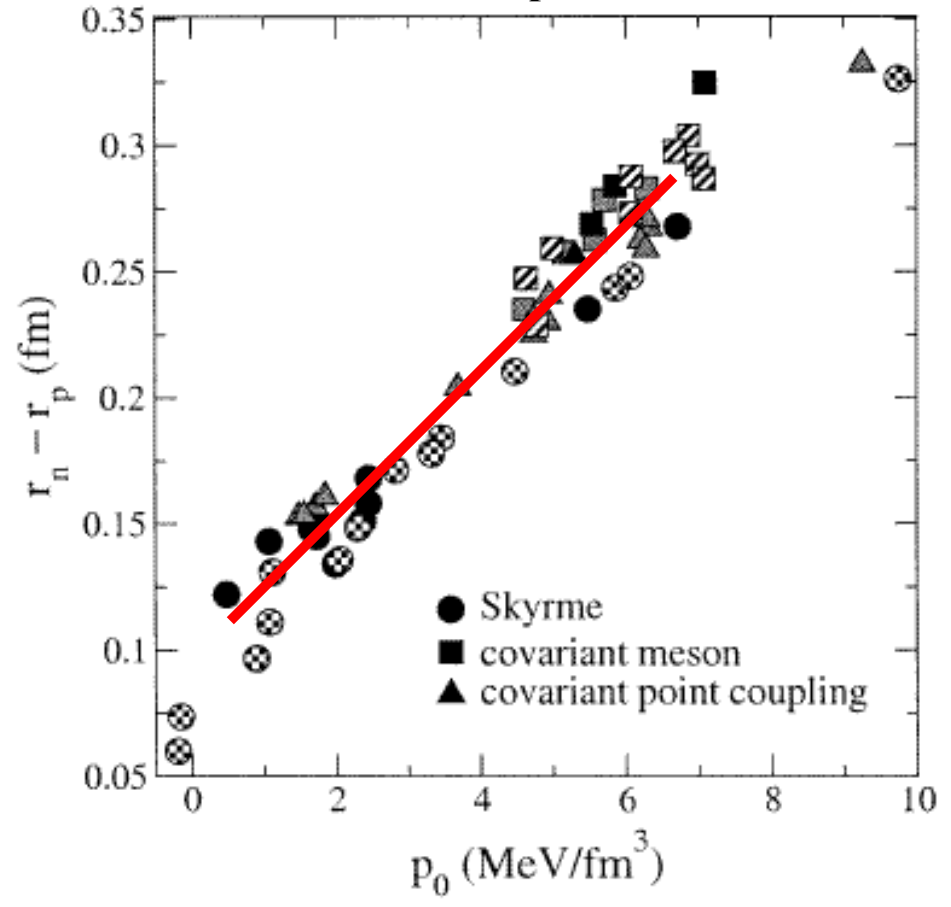
$$x = \frac{(\rho - \rho_0)}{3\rho_0}$$



Furnstahl, NPA 706, 85 (2002)



$$a_4 \sim J$$



$$\rho_0 \sim L$$

Isvector pairing

$$v(\mathbf{r}, \mathbf{r}') = v_0 \left[1 - \eta \left(\frac{\rho}{\rho_0} \right)^\gamma \right] \delta(\mathbf{r} - \mathbf{r}')$$

$$v_{\text{pair}}^{\text{MSH}}(\mathbf{r}, \mathbf{r}') = v_0 \left[1 - (1 - \delta) \eta_s \left(\frac{\rho}{\rho_0} \right)^{\alpha_s} - \delta \eta_n \left(\frac{\rho}{\rho_0} \right)^{\alpha_n} \right] \delta(\mathbf{r}, \mathbf{r}')$$

Margueron, Sagawa, Hagino, PRC 76, 064316 (2007)

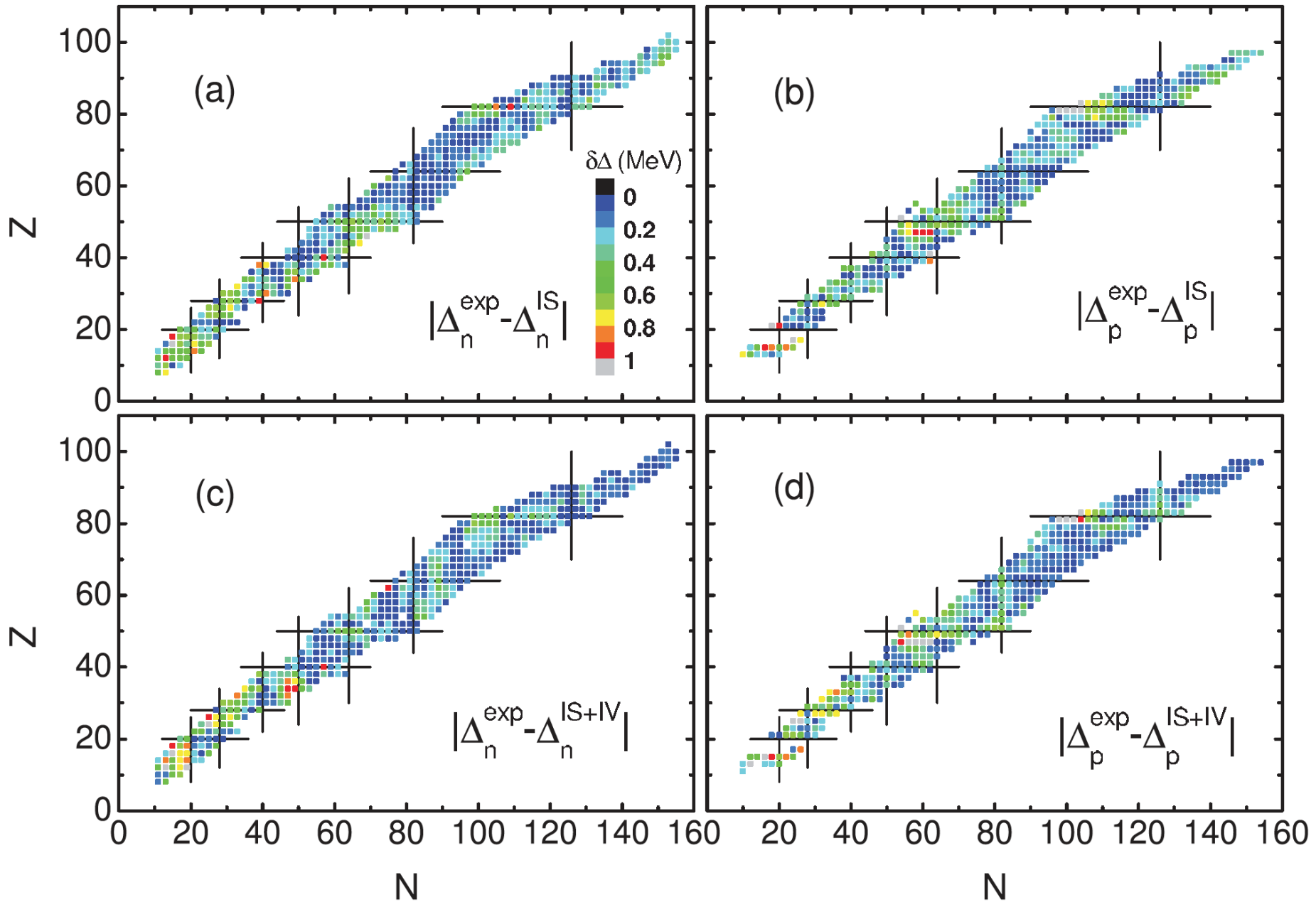
$$v_{\text{pair}}^{\text{MSH}}(\mathbf{r}, \mathbf{r}') = v_0 \left[1 - \left(\eta + \eta_1 \tau_3 \delta \right) \frac{\rho}{\rho_0} - \eta_2 \left(\delta \frac{\rho}{\rho_0} \right)^2 \right] \delta(\mathbf{r}, \mathbf{r}')$$

Yamagami, Shimizu, Nakatsukasa, PRC 80, 064301 (2009)

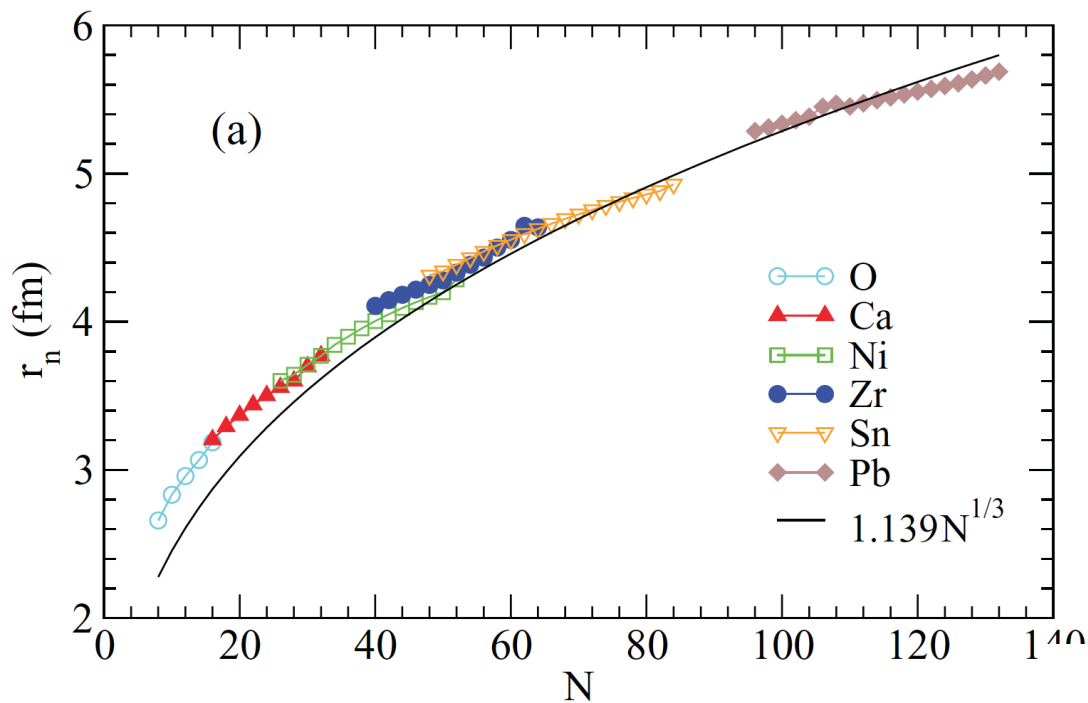
$$\rho = \rho_n + \rho_p$$

$$\delta = \frac{\rho_n - \rho_p}{\rho}$$

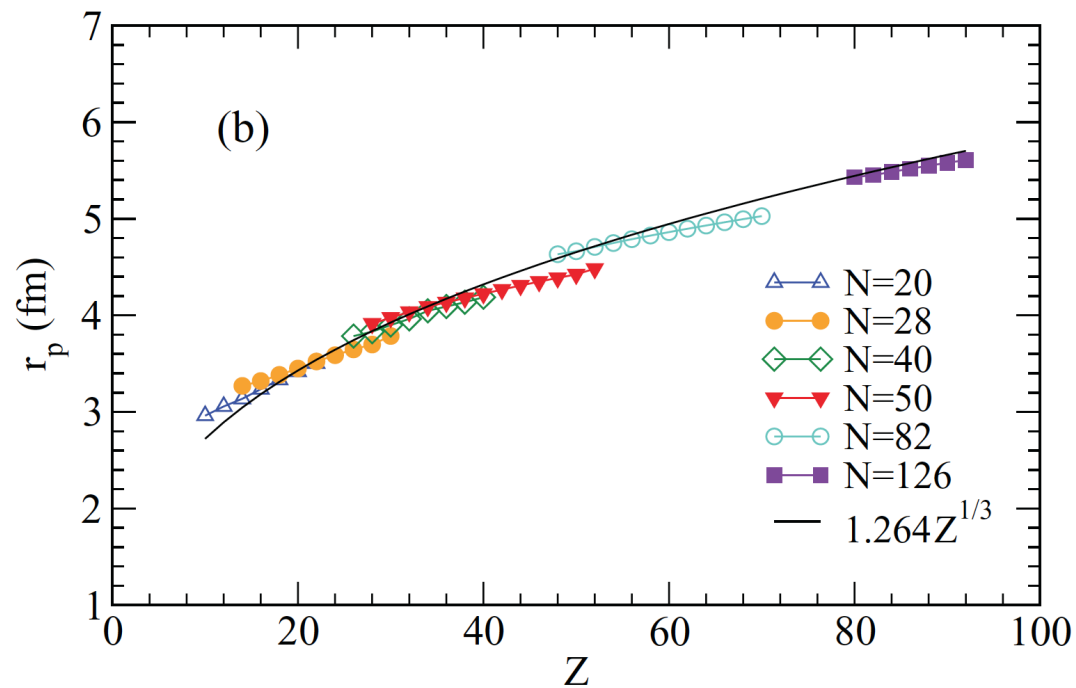
Isvector pairing - Good global fits to pairing gaps



Skyrme + Isovector pairing & nuclear radii

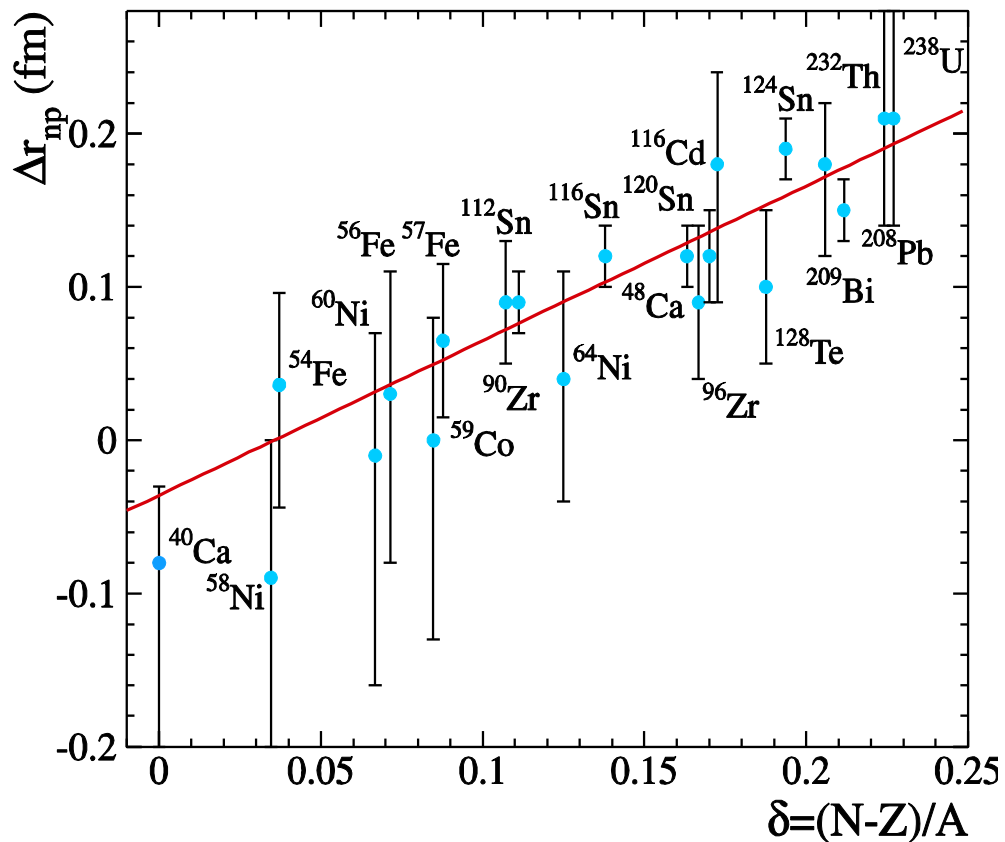


CB, Hongliang Liu, Sagawa,
PRC 85, 014321 (2012)



Neutron Skins

CB, Hongliang Liu, Sagawa,
PRC 85, 014321 (2012)



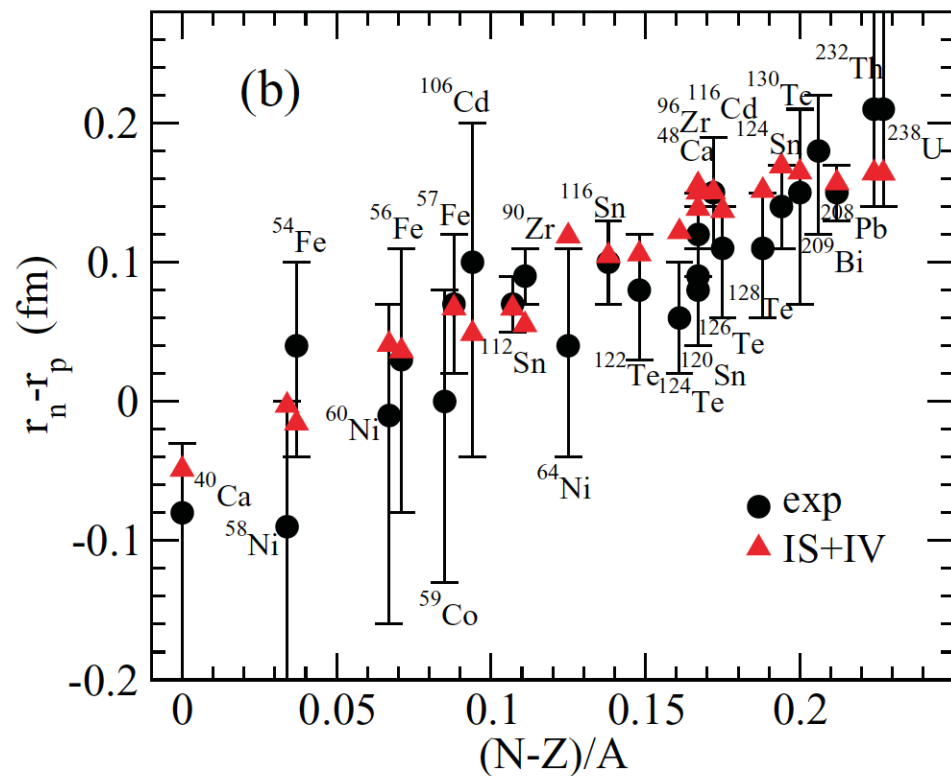
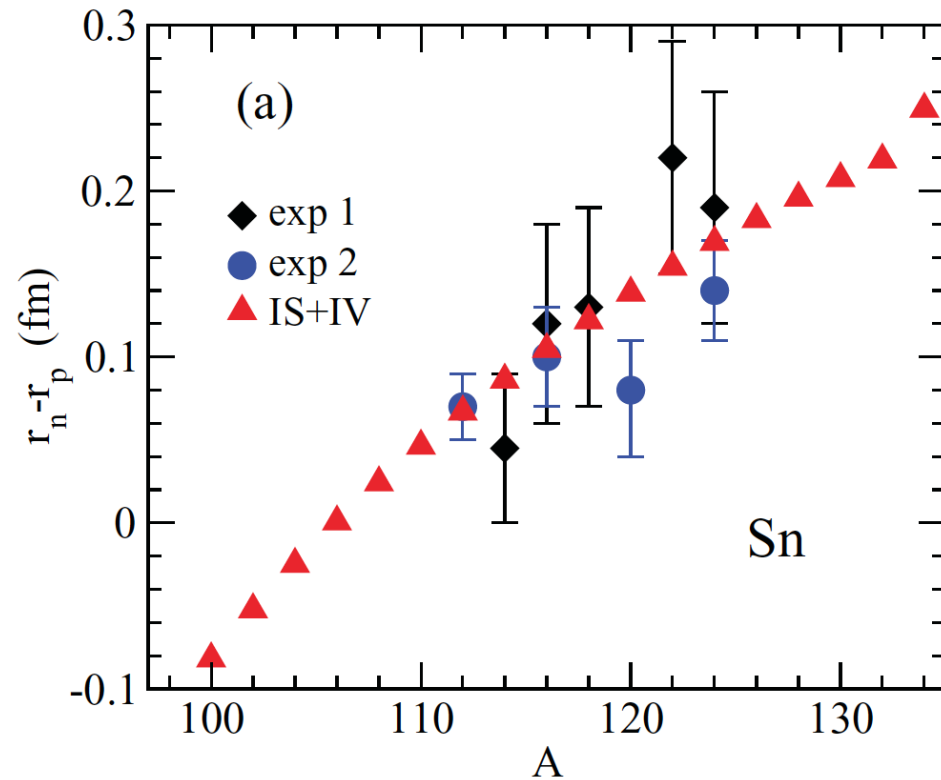
Radii from spin-dipole resonances

Krasznahorkay et al., PRL 82, 3216 (1999)

&

Antiprotonic atoms

Trzcinska et al., PRL 87, 082501 (2001)

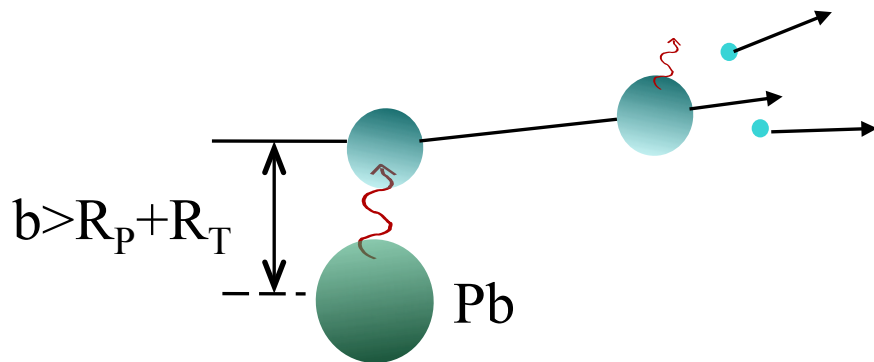


Dipole polarizability

Dipole polarizability

Rossi et al.
PRL 111 (2013) 242503

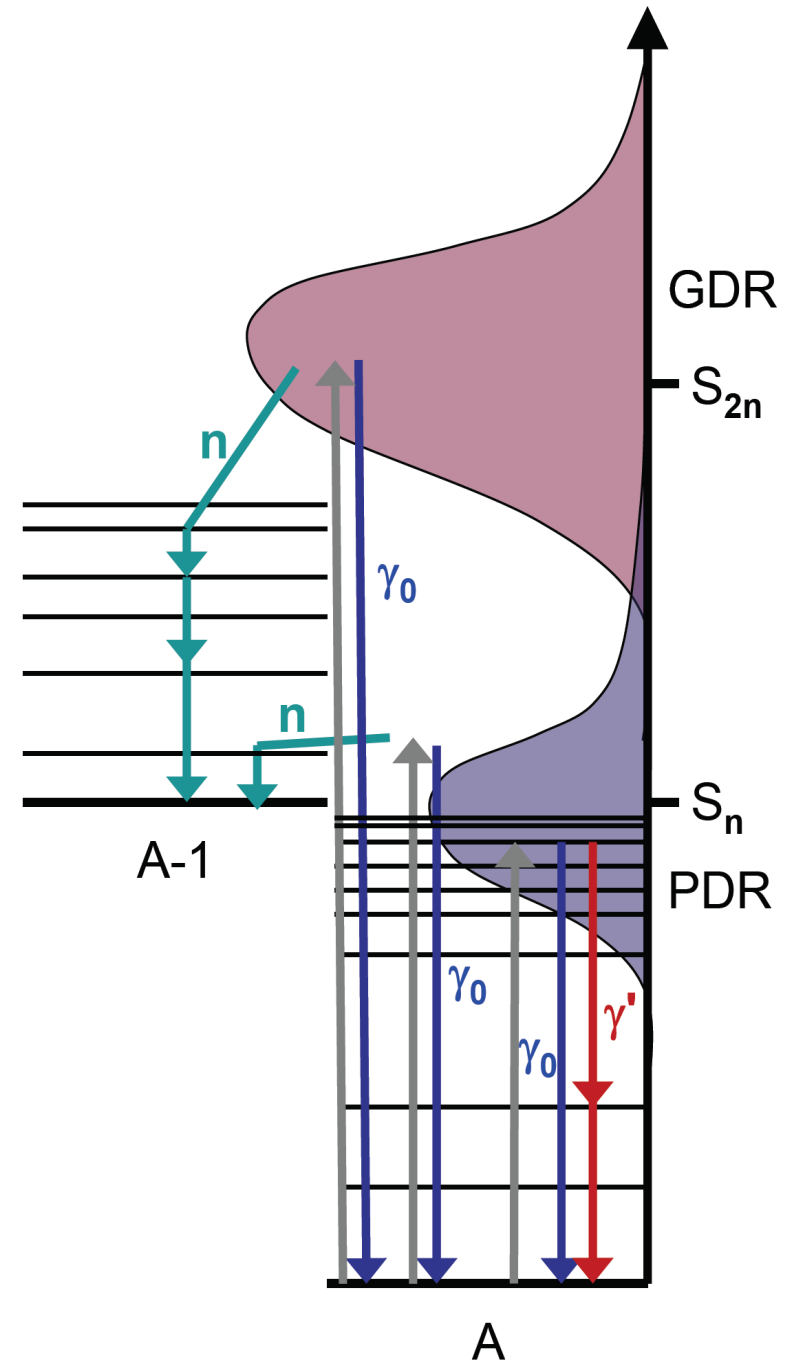
Wieland et al.
PRL 102, 092502 (2009)



Dipole polarizability

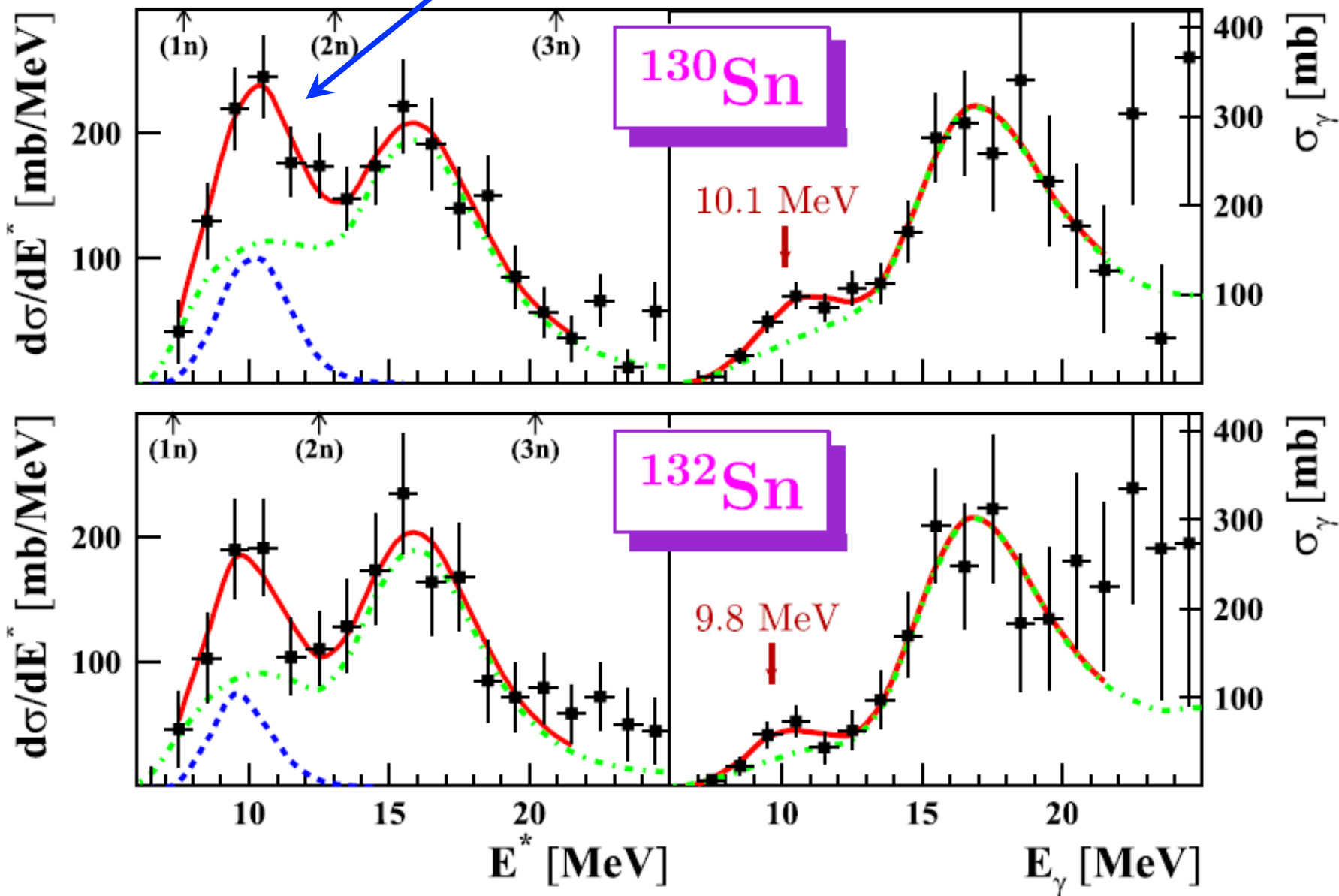
$$\alpha_D = \frac{\hbar c}{2\pi^2} \int_0^\infty \frac{\sigma_\gamma(E)}{E^2} dE$$

$$= \frac{8\pi}{9} \int \frac{B(E1, E_x)}{E_x} dE_x \propto \sigma_C$$



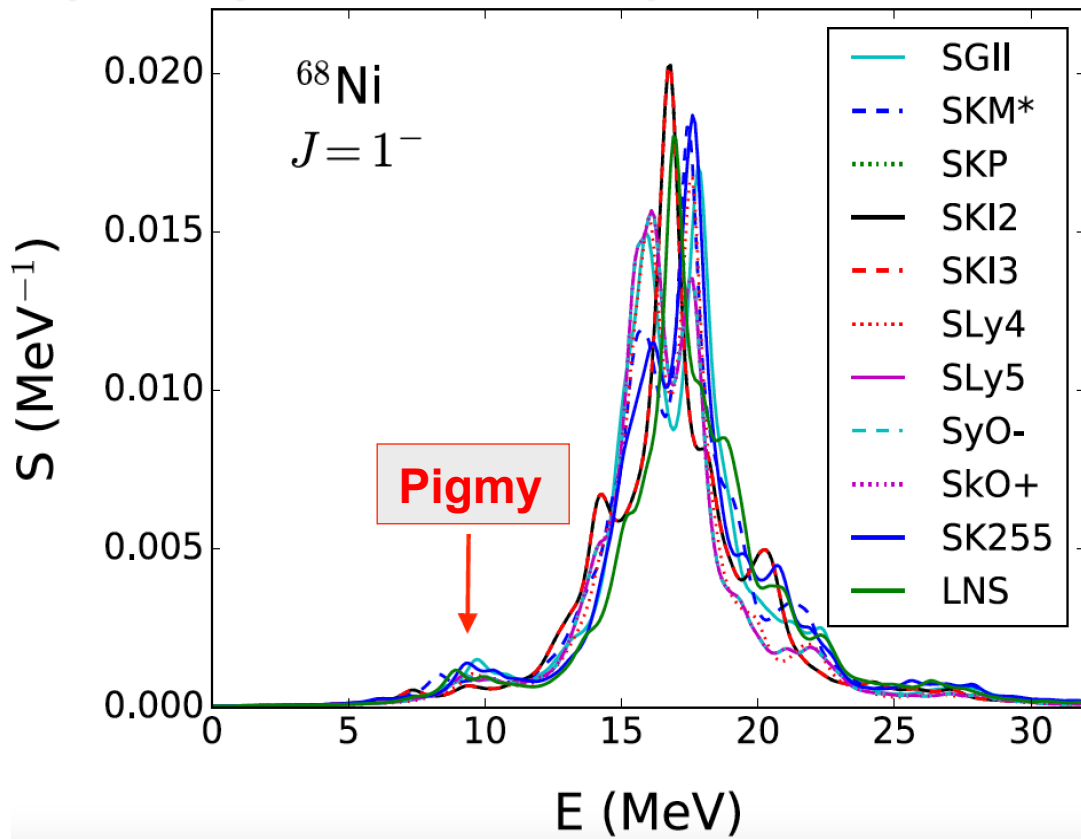
Dipole polarizability

Pigmy



Adrich et al., PRL 95, 132501 (2005)

Dipole polarizability

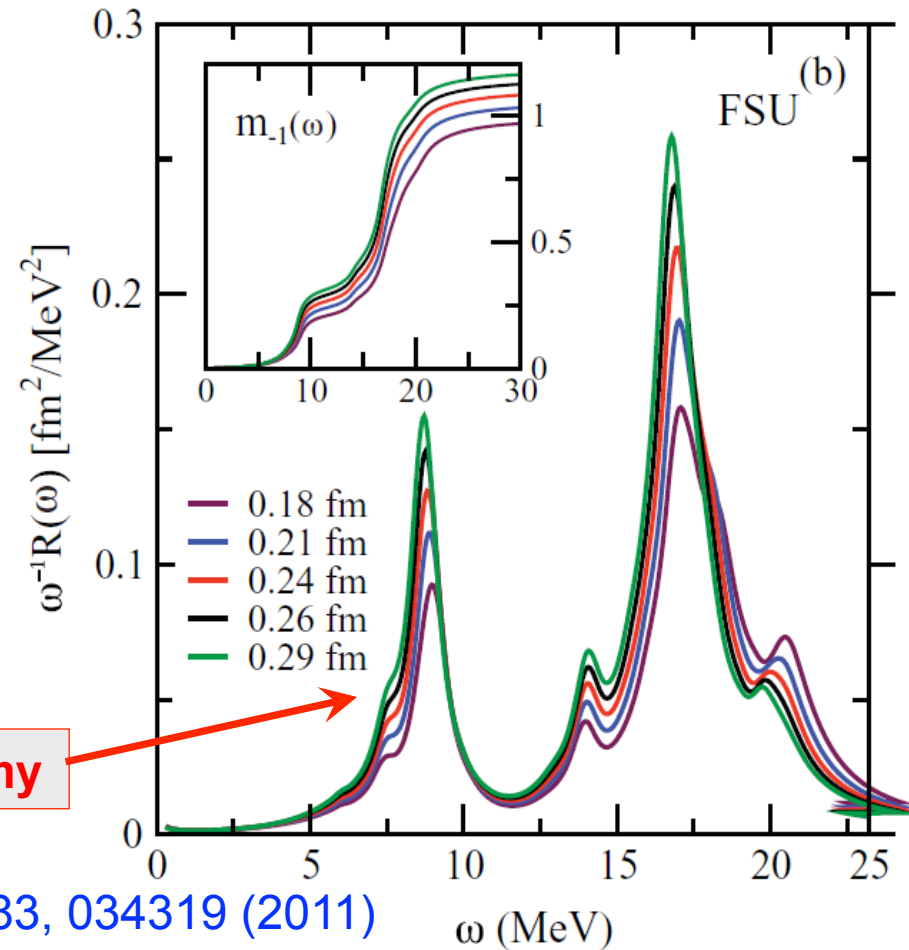


$$S(E) = \sum_{\nu} \left| \left\langle \nu \left\| j_L \left(\frac{Er}{\hbar c} \right) \right\| 0 \right\rangle \right|^2 \delta(E - E_{\nu})$$

Brady, Aumann, CB, Thomas
Phys. Lett. B 757, 553 (2016)

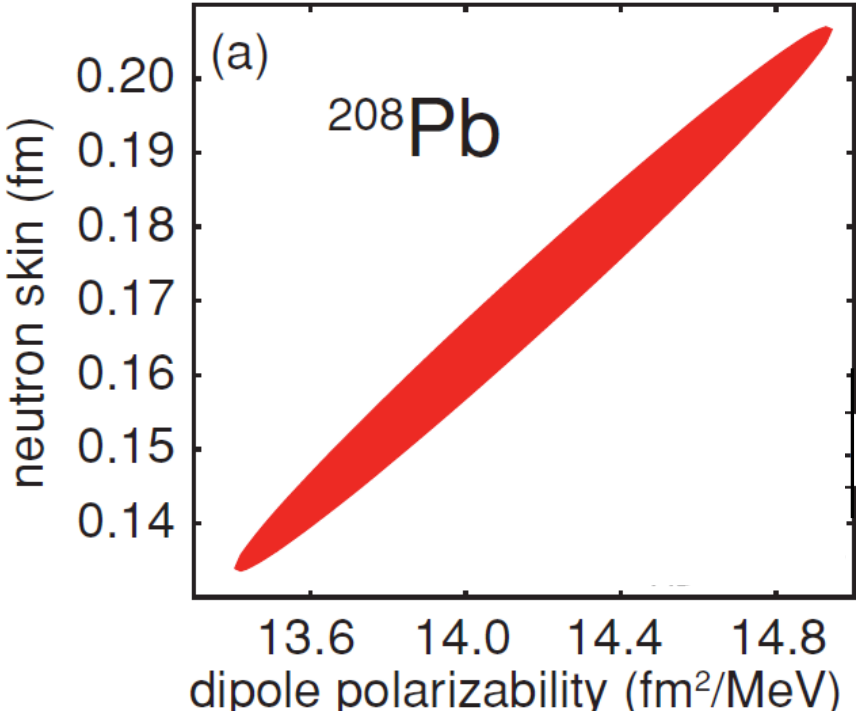
$$\alpha_D = \frac{\hbar c}{2\pi^2} \int_0^{\infty} \frac{\sigma_{\gamma}(E)}{E^2} dE$$

Dipole polarizability



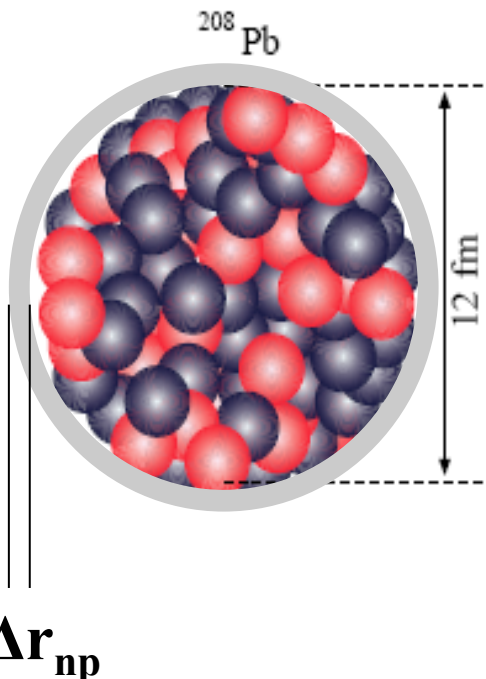
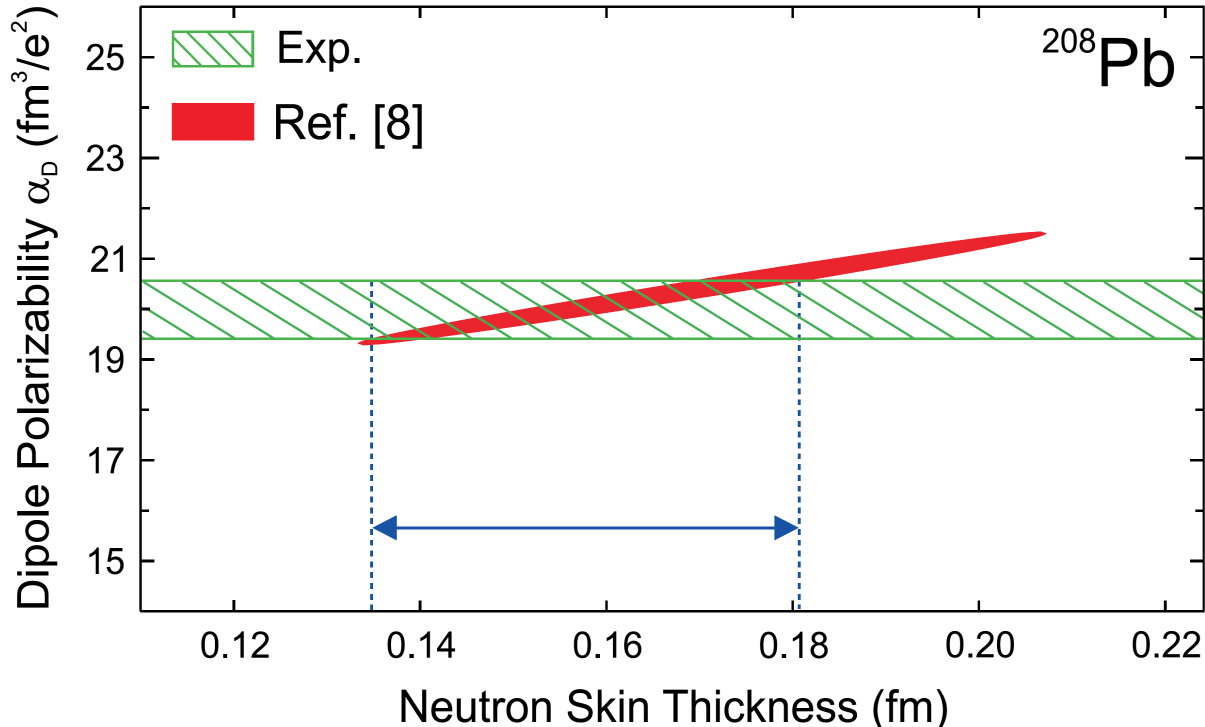
Piekarewicz, PRC 83, 034319 (2011)

Dipole polarizability & neutron skin



Strong correlation between neutron skin and S_2

Reinhard, Nazarewicz, PRC 81 (2010) 051303

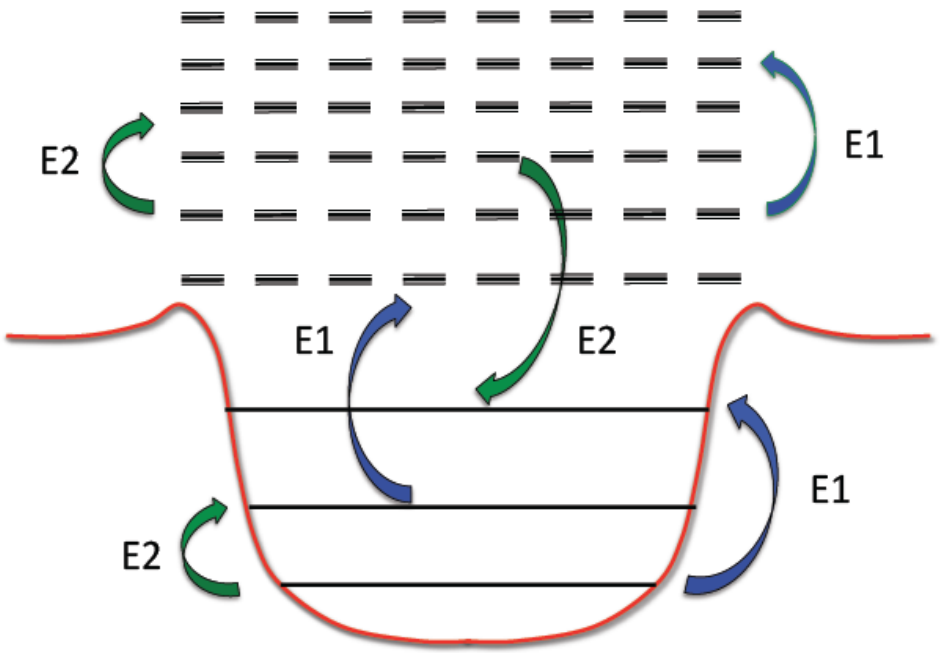


Tamii et al., PRL 107, 062502 (2011)

Reaction theory

Reaction theory of PR excitation

with higher-order effects and relativistic corrections

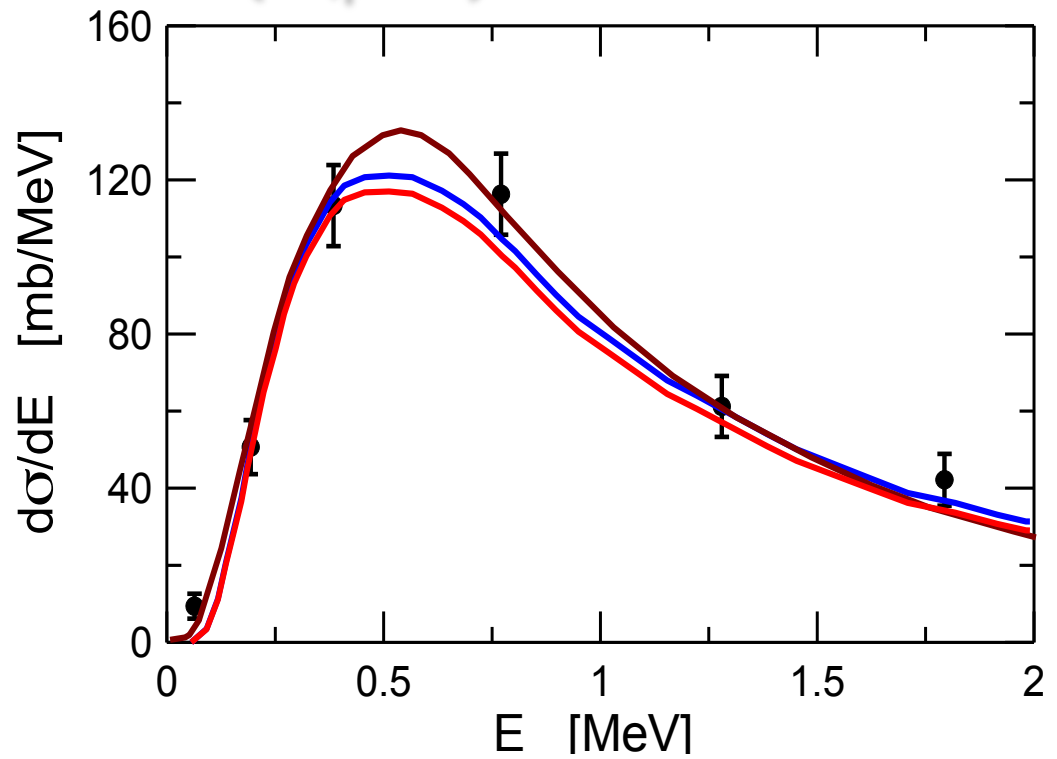


- LO
- all orders
- all orders relativistic

Relativistic CDCC
 CB, PRL 94, 072701 (2005)

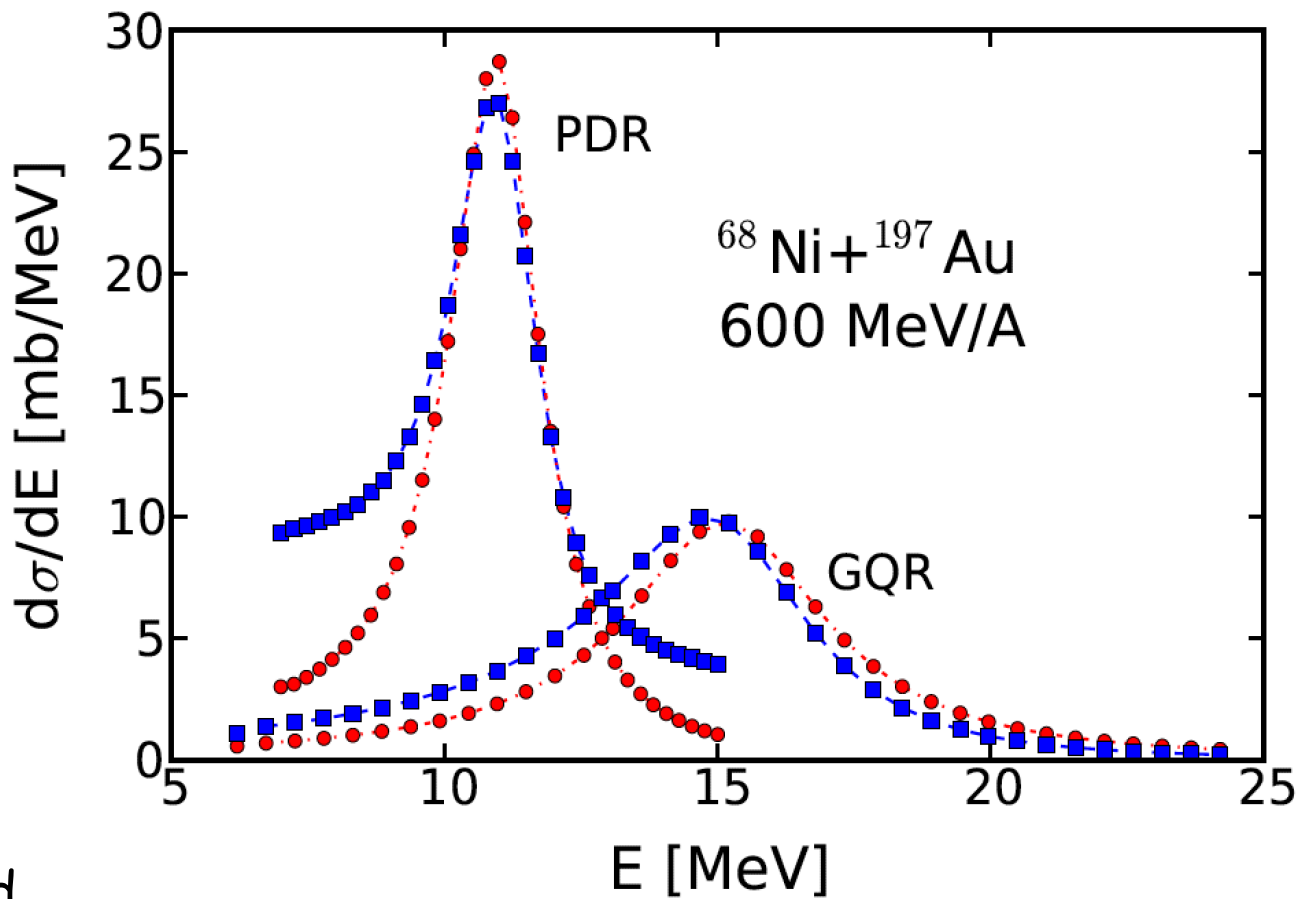
Ogata, CB, PTP 121 (2009), 1399
 PTP 123 (2010) 701

Pb ($^8\text{B}, p^7\text{Be}$) at 83 MeV/nucleon



Dynamical coupling of PDR, GDR and GQR

Brady, Aumann, CB, Thomas
PLB 757, 553 (2016)



- Nuclear response discretized
- Coupled Channels calculations

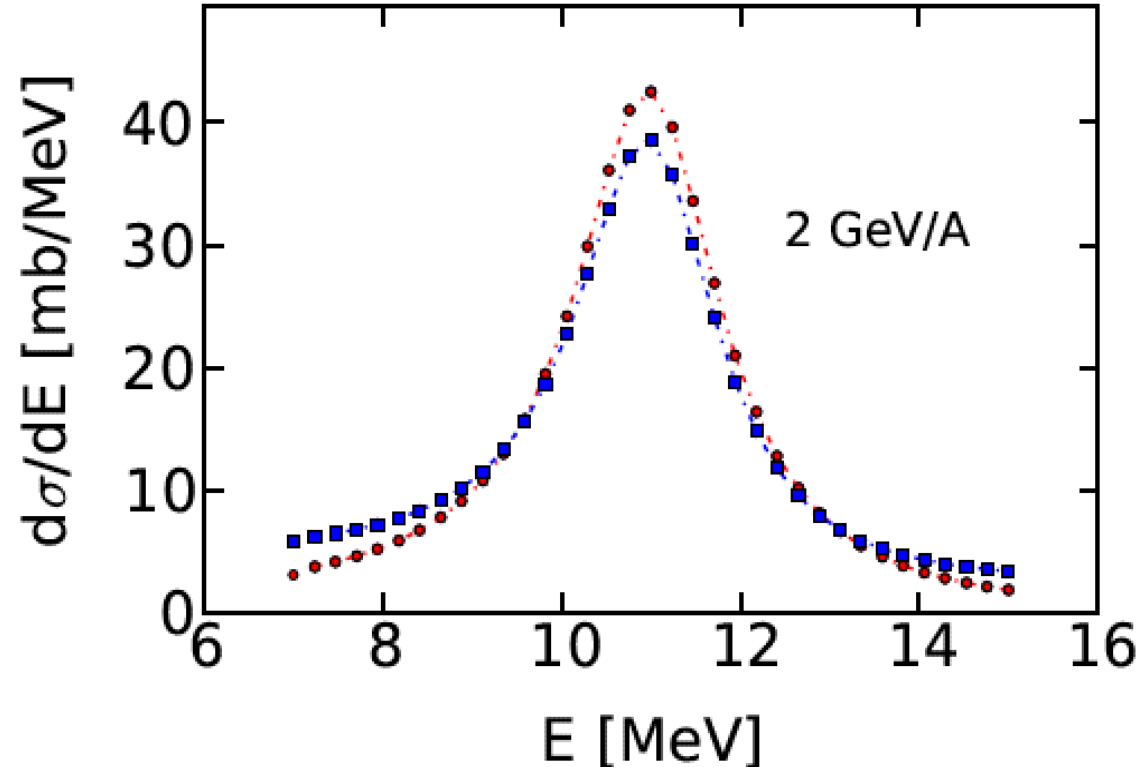
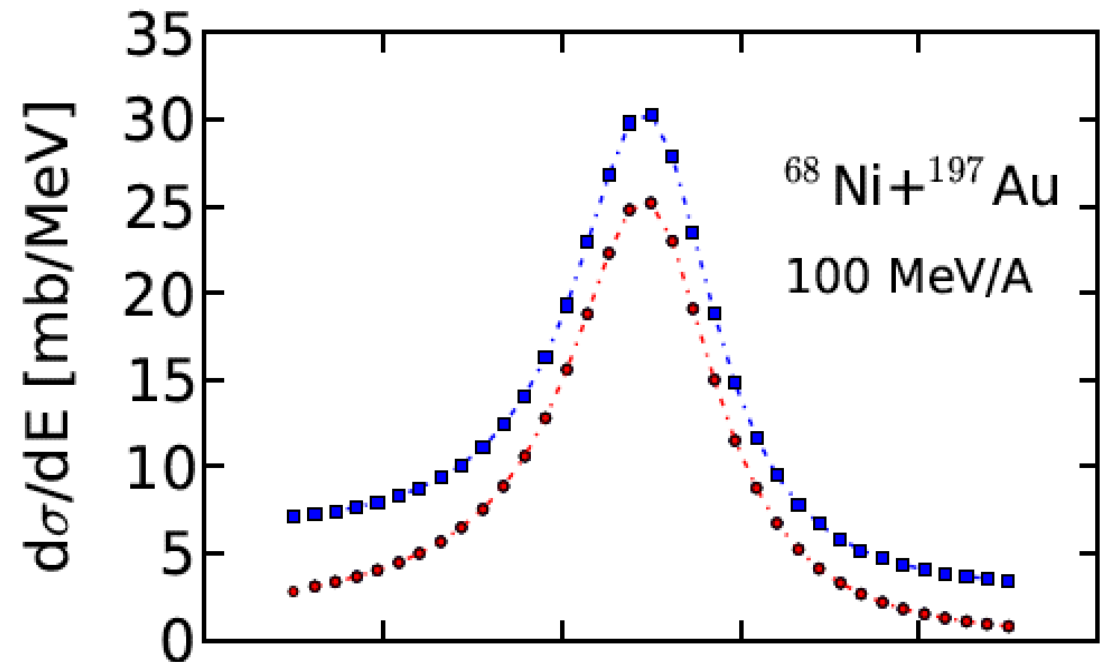
- First order
- all orders relativistic

Dynamical coupling of PDR, GDR and GQR

Brady, Aumann, CB, Thomas
PLB 757, 553 (2016)

- Nuclear response discretized
- Coupled Channels calculations

- First order
- all orders relativistic



Dynamical coupling of PDR, GDR and GQR

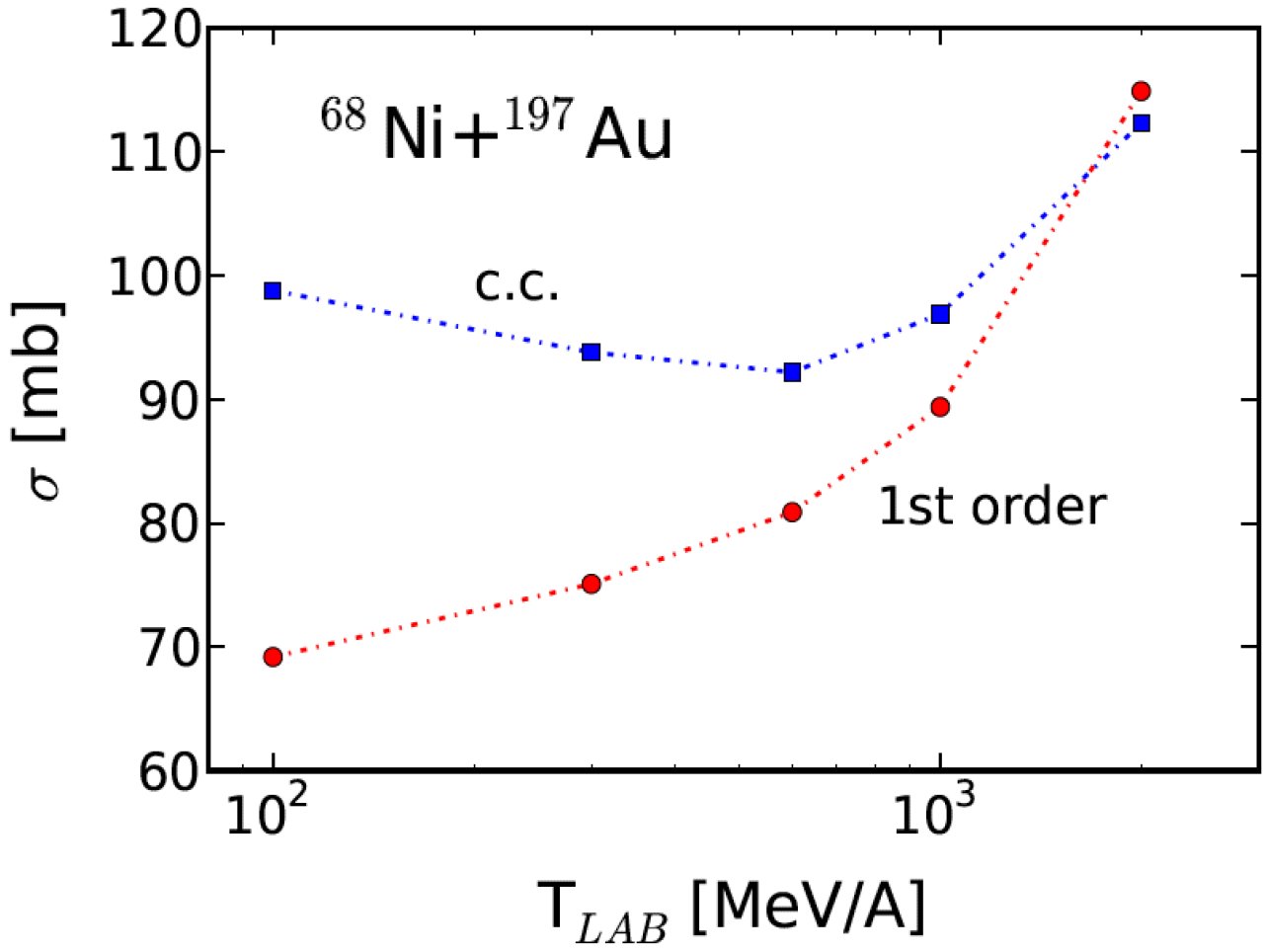
Rossi et al.,
PRL 111, 242503 (2013)

→ $\alpha_D = 3.40 \text{ fm}^3$

Our new analysis
→ $\alpha_D = 3.16 \text{ fm}^3$

Neutron skin
→ $\Delta r_n = 0.17 \text{ fm}$

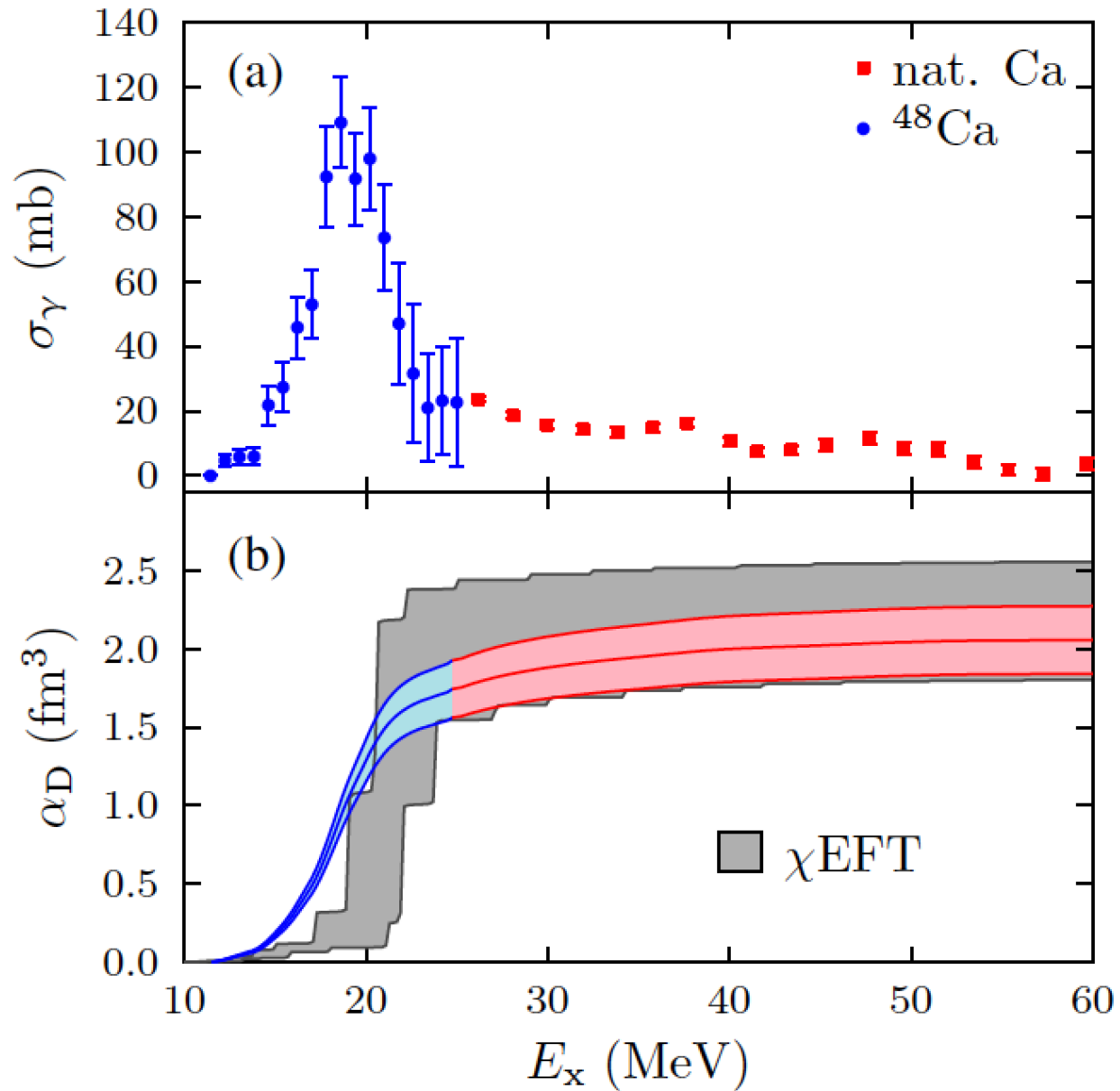
Our new analysis
→ $\Delta r_n = 0.16 \text{ fm}$



BUT, experimental error
= 7% for α_D and
= 0.2 for Δr_n

Recent experiments on dipole polarizability

Birkhan et al.,
PRL 118, 252501 (2017)



Experiment:

$$\alpha_D(^{40}\text{Ca}) = 1.50(2) \text{ fm}^3$$

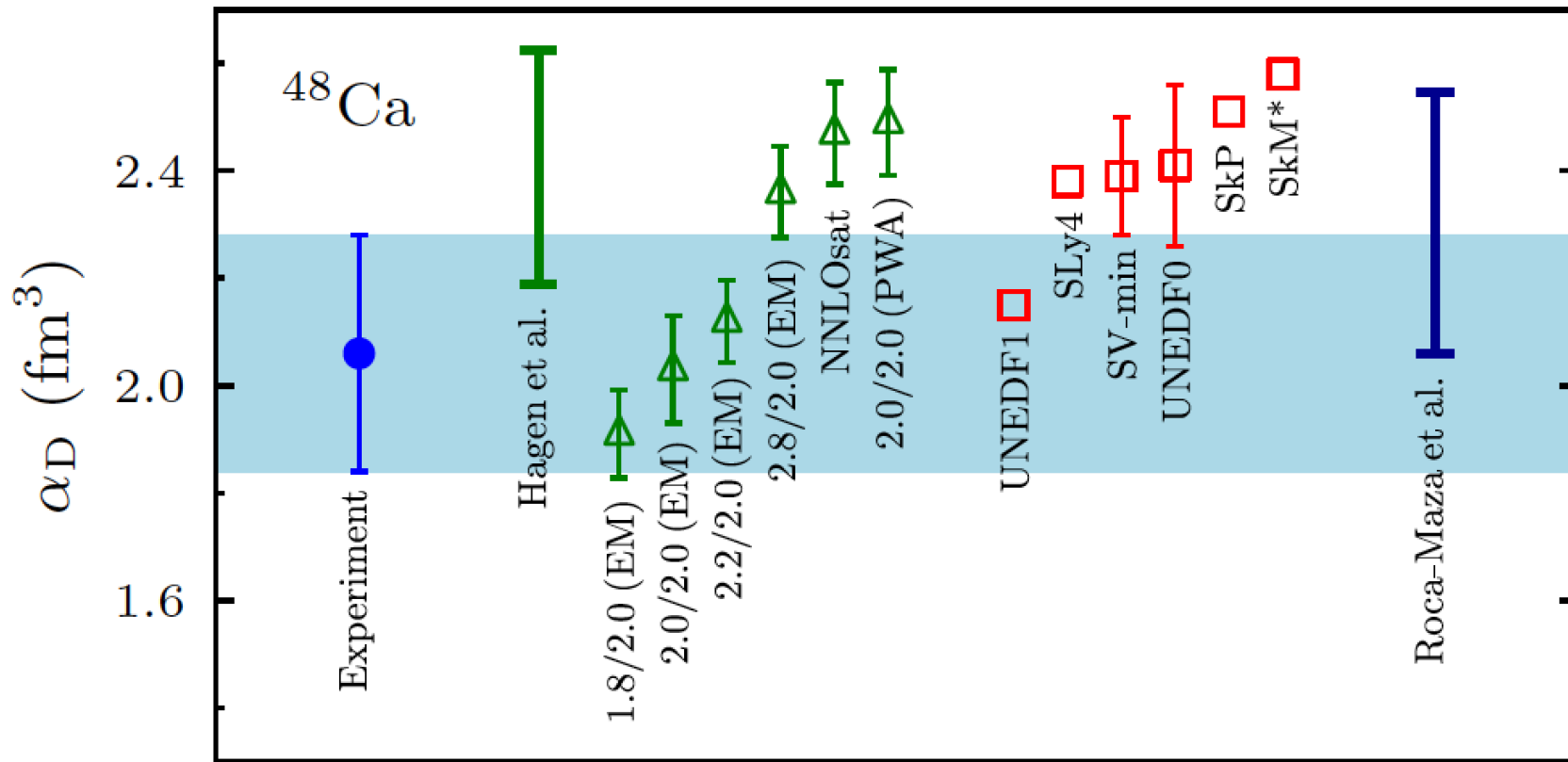
$$\alpha_D(^{48}\text{Ca}) = 2.07(22) \text{ fm}^3$$

Theory:

$$\alpha_D(^{40}\text{Ca}) = 1.87(3) \text{ fm}^3$$

Neutron skin:

0.14 - 0.20 fm



Experimental electric dipole polarizability in ^{48}Ca (blue band) and predictions from EFT (green triangles) and χ EDFs (red squares)

Hagen, et al., Nature Phys. 12, 186 (2016)

Electron scattering

Elastic Electron Scattering

$$\left\langle \Phi_i \left| \sum_1^Z e^{i\mathbf{q}\cdot\mathbf{r}_k} \right| \Phi_i \right\rangle = \int d^3r \rho_{\text{ch}}(\mathbf{r}) e^{i\mathbf{q}\cdot\mathbf{r}} \equiv F(\mathbf{q}) \quad \text{charge form-factor}$$

Point nucleus

Mott cross section

$$\frac{d\sigma}{d\Omega} = \left(\frac{Ze^2}{2E} \right)^2 \frac{\cos^2 \theta/2}{\sin^4 \theta/2} \frac{1}{1 + \frac{2E}{Mc^2} \sin^2 \theta/2} \equiv \sigma_M$$

$$F(\mathbf{q}) = \frac{4\pi}{q} \int dr r \sin(qr) \rho_{\text{ch}}(r)$$

spherical nuclei

$$\frac{d\sigma}{d\Omega} = \frac{\sigma_M(\theta)}{Z^2} |F(\mathbf{q})|^2$$

Nuclear physics

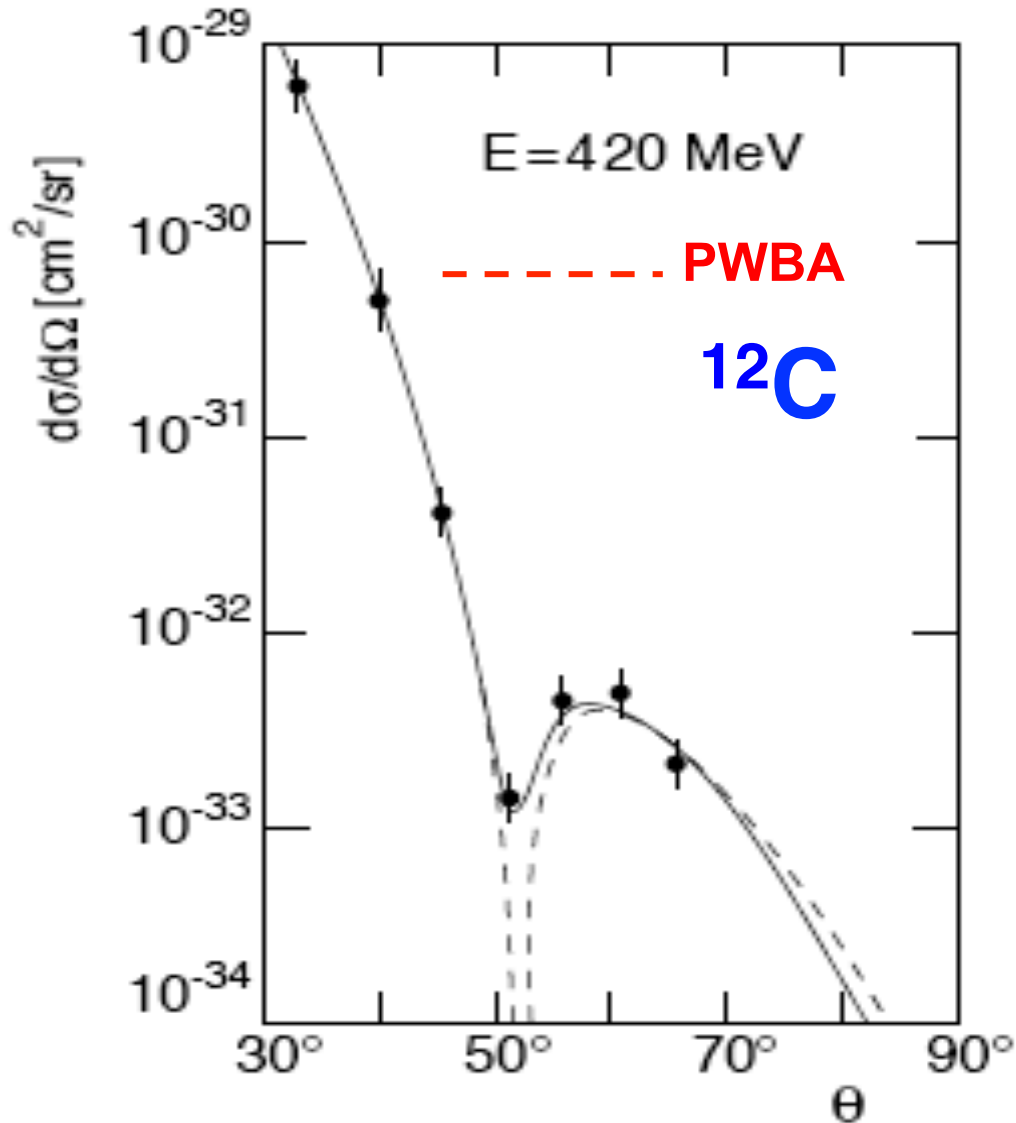
$$\rho_{\text{ch}}(\mathbf{r}) = \int \rho_p(\mathbf{r}') f_{\text{Ep}}(\mathbf{r} - \mathbf{r}') d\mathbf{r}' + \int \rho_n(\mathbf{r}') f_{\text{En}}(\mathbf{r} - \mathbf{r}') d\mathbf{r}'$$

f_{Ep} = charge dist. in proton

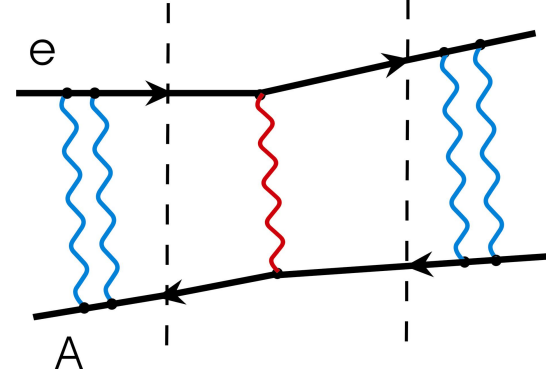
f_{En} = charge dist. in neutron

10% effect, mainly surface

DWBA corrections



Hofstadter, 1953



• electron wavefunction attracted to the nucleus

• a measured q probes a larger $q = q_{\text{eff}}$ in $F(q)$



$$\frac{d\sigma}{d\Omega} = \frac{\sigma_M(\theta)}{Z^2} |F(q_{\text{eff}})|^2$$

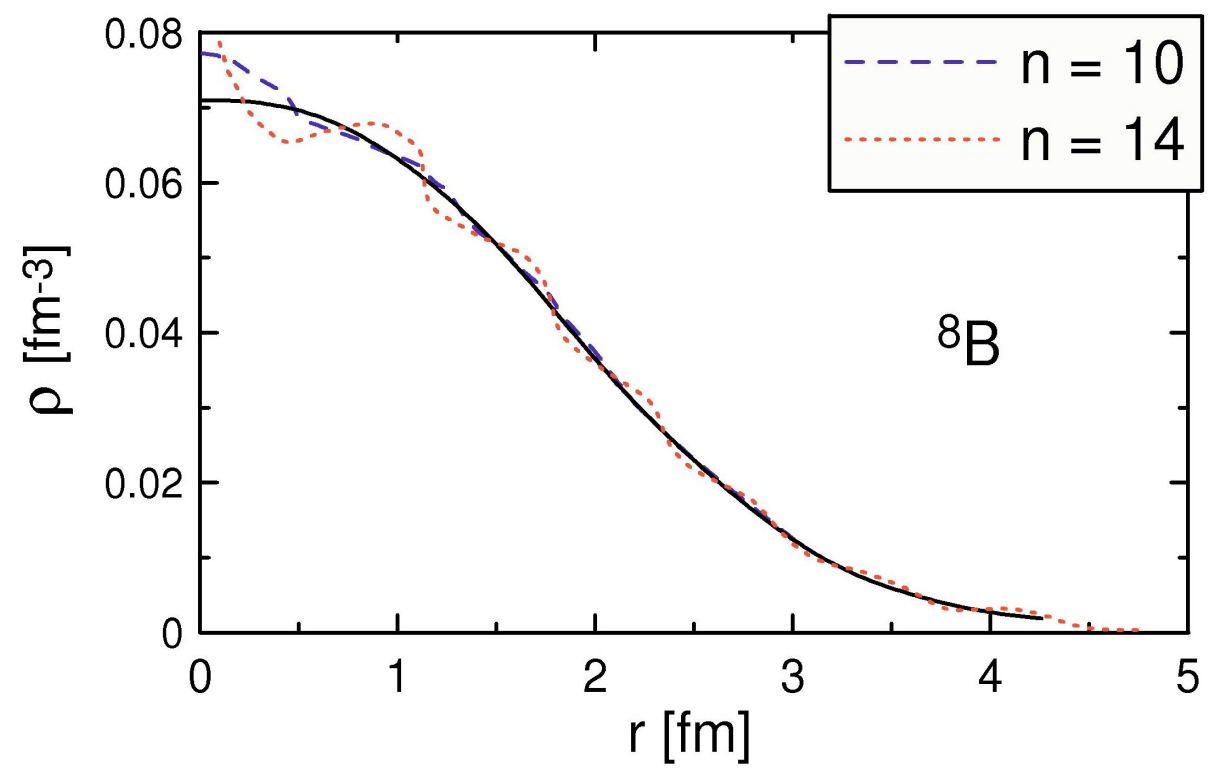
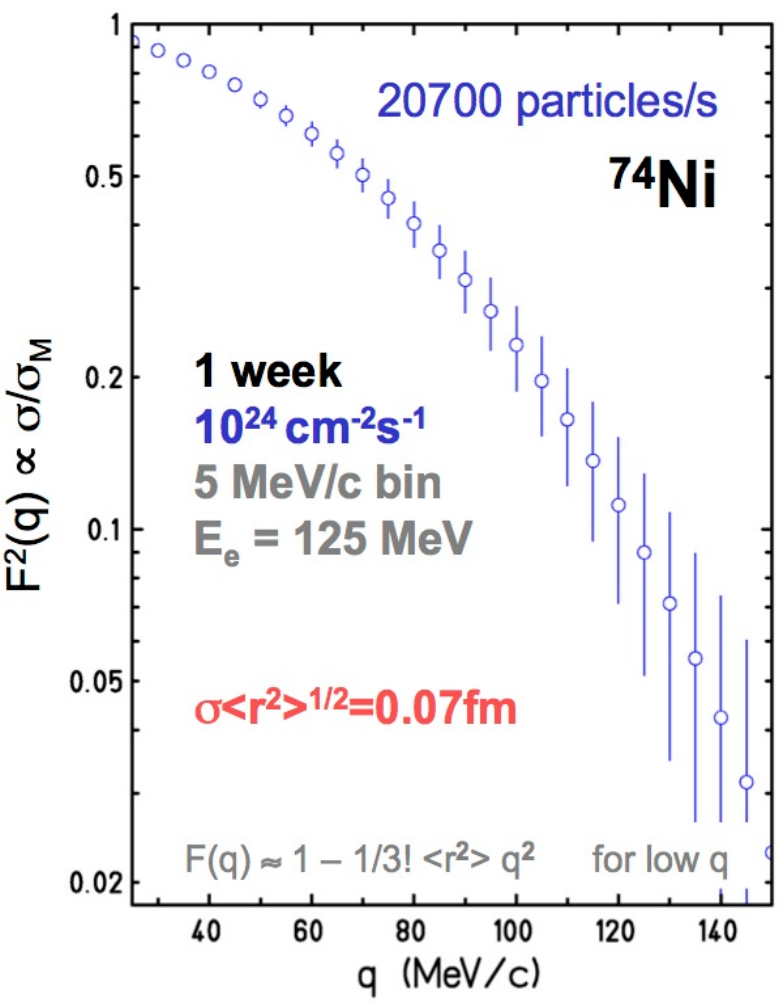
$$q_{\text{eff}} = q \left(1 - \frac{V(0)}{E} \right)$$

$$= q \left(1 + 1.5 \frac{Ze^2}{ER} \right), \quad R \cong 1.2A^{1/3} \text{ fm}$$

Inversion of experimental data

inverse scattering problem

experimental precision



test case: ^8B

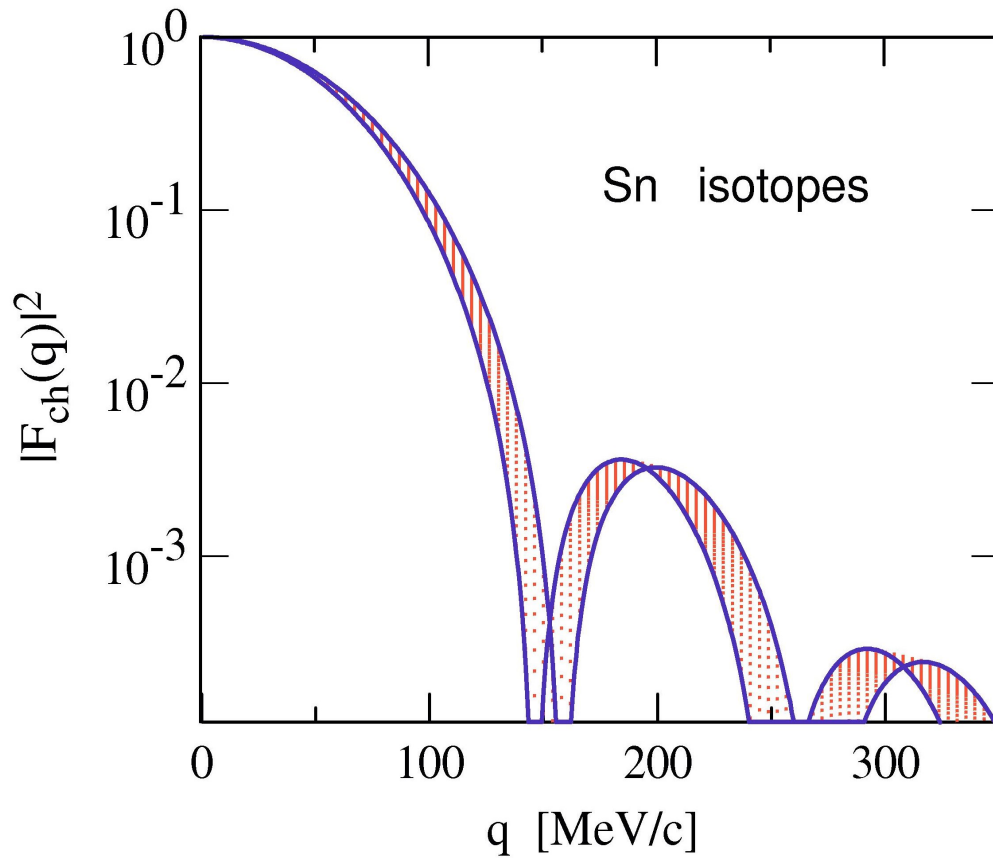
$$q_n = \frac{n\pi}{R_{\max}}$$

CB, JPG 34, 315 (2007)

Fourier-Bessel expansion

$$\rho_{\text{ch}}(r) = \Theta(R_{\max} - r) \sum_{n=1}^{\infty} a_n j_0(q_n r) \longleftrightarrow F_{\text{ch}}(q) = \frac{4\pi}{q} \sum_n a_n \frac{(-1)^n}{q^2 - q_n^2} \sin(q R_{\max})$$

Expectations from electron-ion scattering

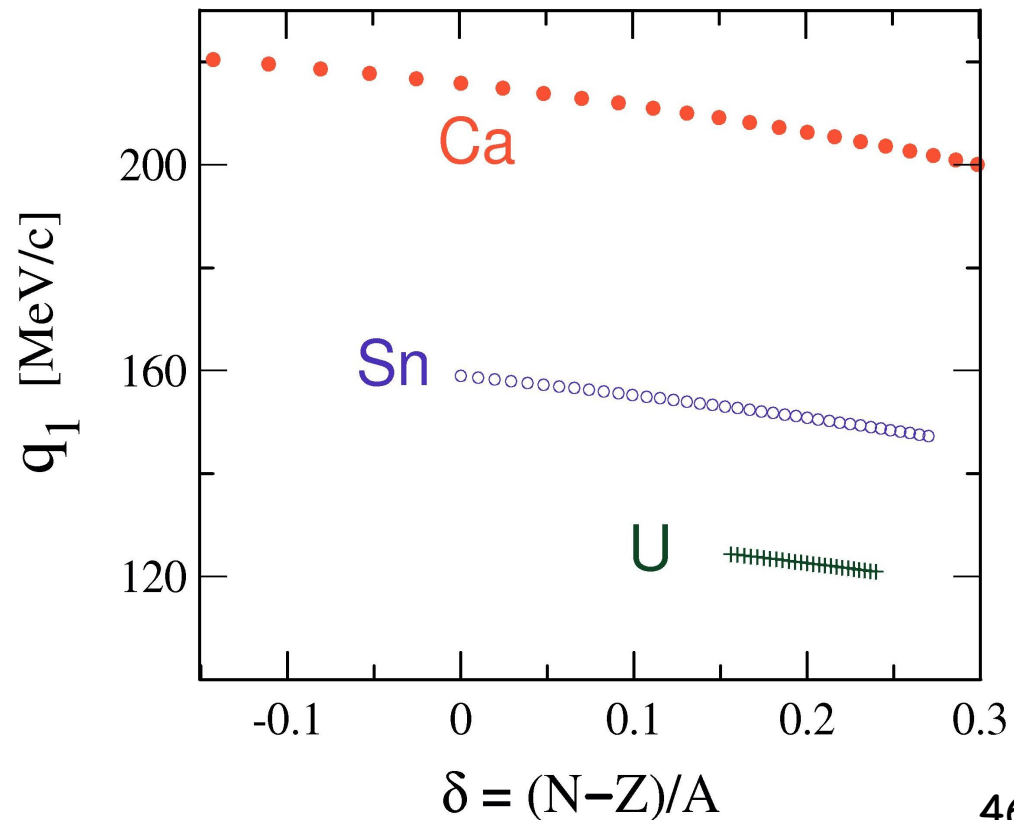


$$\exp(-q^2 a^2)$$

CB, JPG 34, 315 (2007)

In electron-ion scattering:

$$q_1 \cong \frac{3.74}{A^{1/3}} \left[1 - 0.535 \frac{\delta}{A^{1/3}} \right] \text{ fm}^{-1}$$



Inelastic electron scattering: multipoles

$$\langle f, \mathbf{p}' | H | i, \mathbf{p} \rangle = \frac{4\pi e^2}{q^2} \left\langle f \left| \sum_1^Z e^{i\mathbf{q} \cdot \mathbf{r}_k} \left[(\mathbf{u}_f^* \mathbf{u}_i) (U_f^* U_i) - (\mathbf{u}_f^* \vec{\alpha}_e \mathbf{u}_i) \cdot (U_f^* \vec{\alpha}_N U_i) \right] \right| i \right\rangle$$

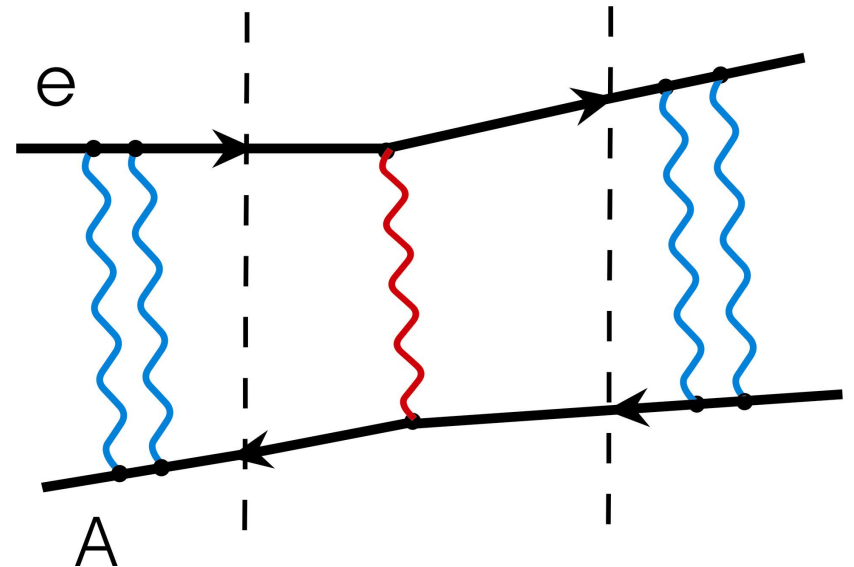
- expand $\exp(i\mathbf{q} \cdot \mathbf{r})$ into multipoles
- average over initial and sum over final spins

$$\left(\frac{d\sigma}{d\Omega} \right)_{\text{inel}} = \frac{\sigma_M(\theta)}{Z^2} \left[\sum_L |F_{\text{CL}}(q_{\text{eff}})|^2 + \left(\frac{1}{2} + \tan^2 \theta / 2 \right) \sum_{\lambda} |F_{\text{EML}}(q_{\text{eff}})|^2 \right]$$

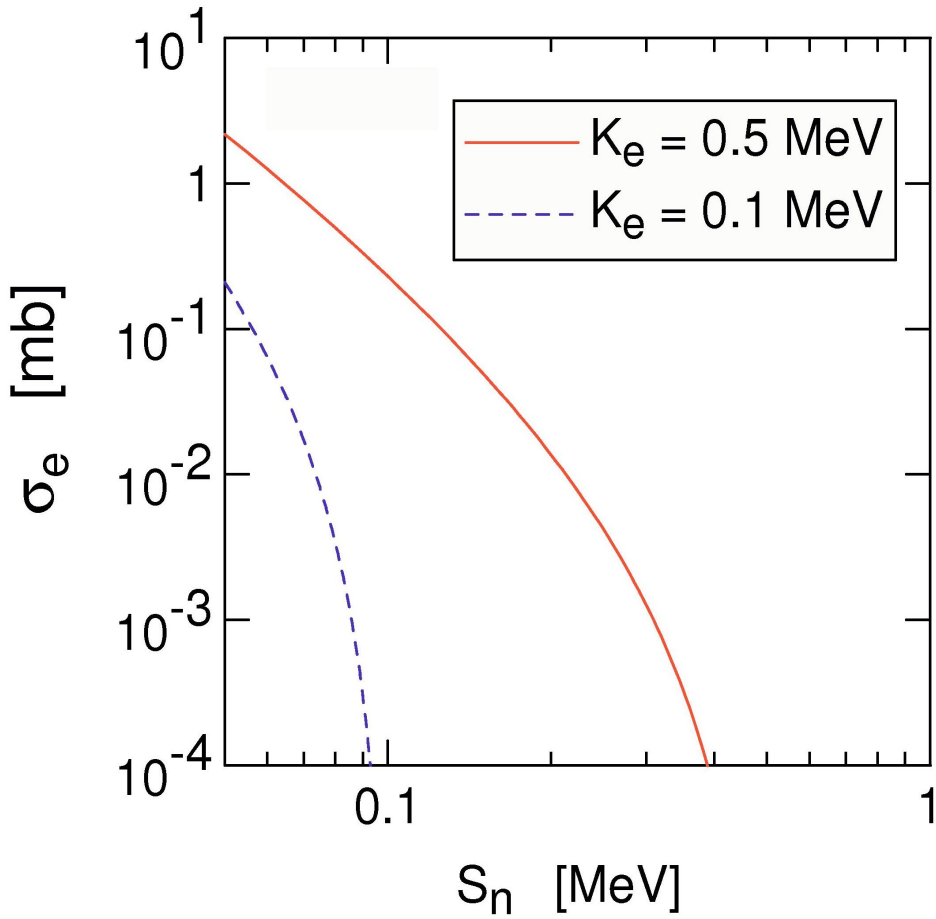
$$F_{\text{CL}}(q) \propto \int dr r^2 j_L(qr) \delta\rho_{fi}(r)$$

$$F_{\text{EML}}(q) \propto \int dr r^2 J_{L,L+1}^{\text{if}}(r) j_{L+1}(qr)$$

$$J_{L,L+1}^{\text{if}}(r) = \langle f | \mathbf{J}_{\text{if}} \cdot \mathbf{Y}_{LL'1} | i \rangle$$

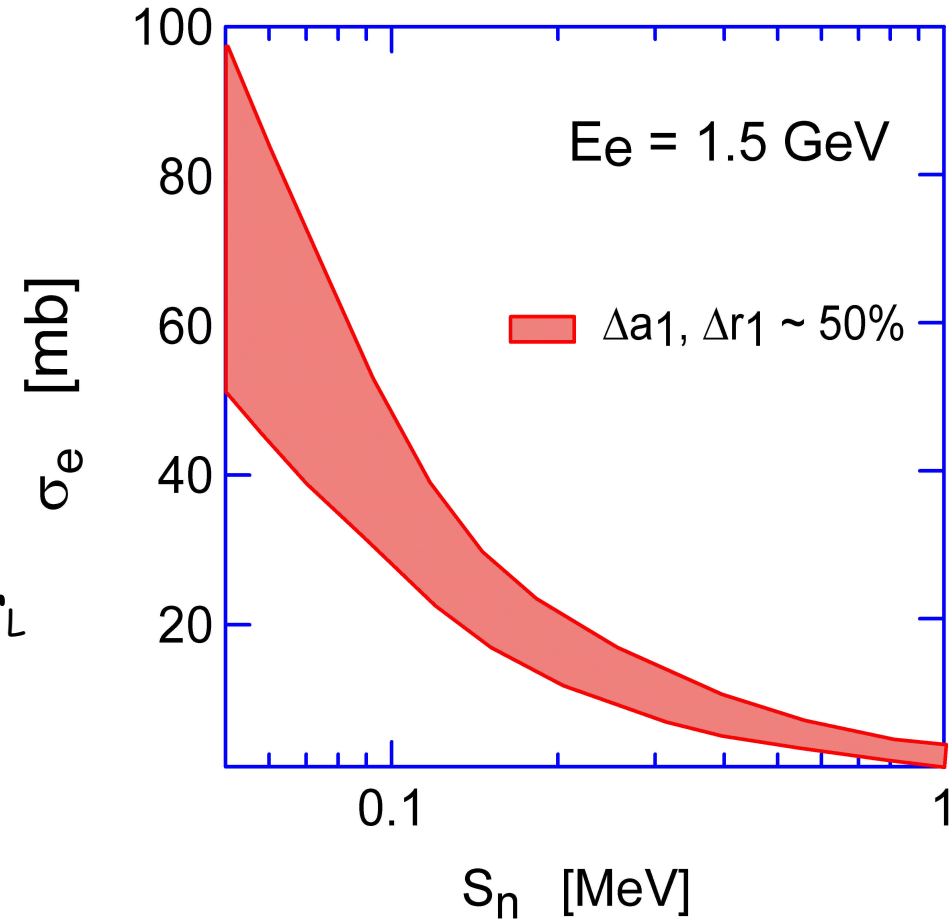


FSI in dissociation of halo nuclei



$$\frac{d\sigma}{dE_e d\Omega} \sim |f_L(q)|^2$$

$$f_L \equiv f_L(q, S_n, a_L, r_L)$$



Halo nuclei: very strong dependence on effective range expansion parameters, a_L, r_L

CB, PLB 624, 203 (2005)

Inelastic electron scattering: multipoles

$$E_x \ll E, \quad \theta \ll 1 \quad \text{Siegert's theorem}$$

$$qR \ll 1$$

$$F_{\text{CL}}(q) \cong \frac{E_x / \hbar}{q} \sqrt{\frac{L+1}{L}} F_{\text{EL}}(q)$$

$$\frac{d\sigma}{d\Omega dE_\gamma} = \sum_L \frac{dN^{(\text{EL})}(E, E_\gamma, \theta)}{d\Omega dE_\gamma} \sigma_\gamma^{(\text{EL})}(E_\gamma)$$

CB, PLB 624, 203 (2005)

virtual photon spectrum

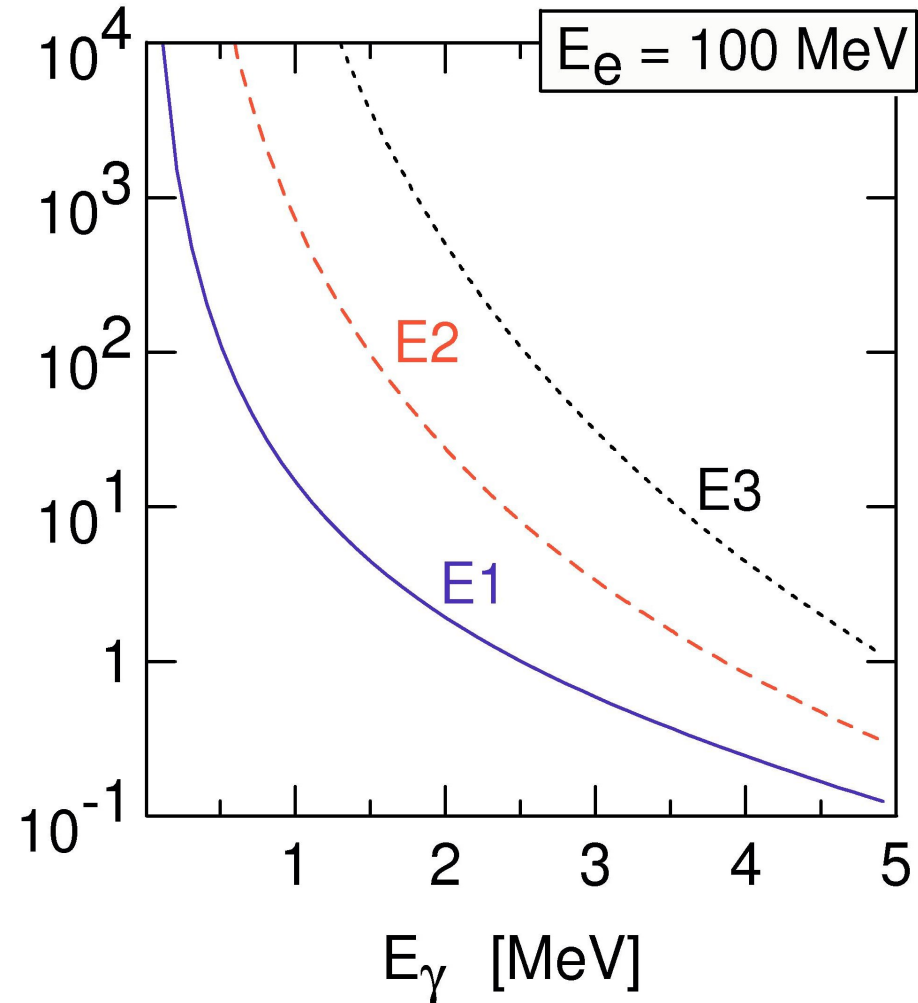
$$\frac{dN^{(\text{EL})}(E, E_\gamma)}{dE_\gamma} = \int_{E_\gamma/E}^{\theta_m} \frac{dN^{(\text{EL})}(E, E_\gamma, \theta)}{d\Omega dE_\gamma}$$

response function

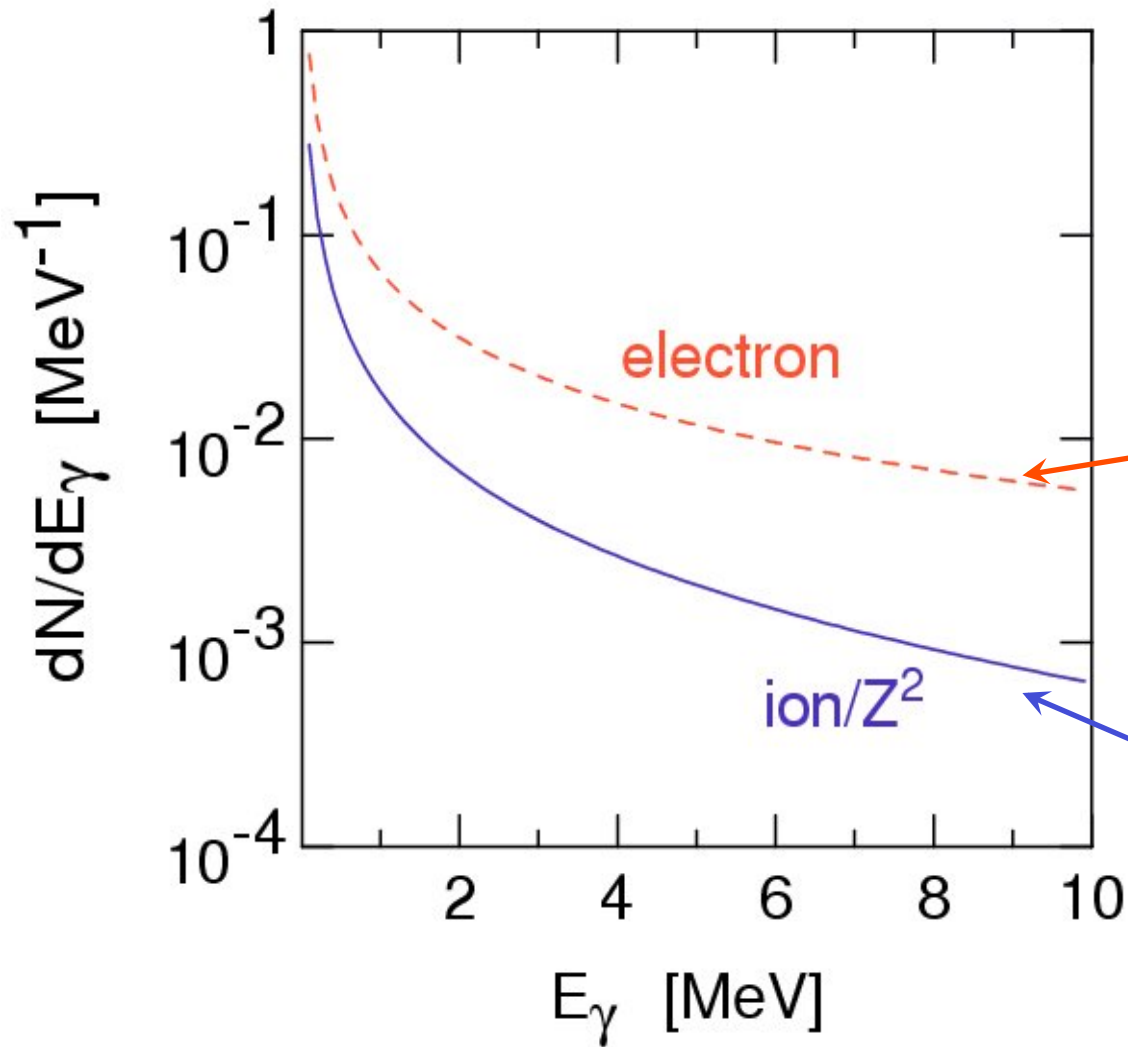
$$\sigma_\gamma^{(\text{EL})}(E_\gamma) \propto \frac{dB(\text{EL})}{dE_x}$$

$$\frac{dB(\text{EL})}{dE_x} \propto \int dr r^2 r^L \delta\rho_{\text{if}}(r)$$

dN_e/dE_γ [MeV⁻¹]



Coulomb vs. Electron Scattering



comparison with Coulomb excitation

$$E_e = 1 \text{ GeV}$$

$$E_{\text{ion}} = 1 \text{ GeV/nucleon}$$

CB, PLB 624, 203 (2005)
PRC 75, 024606 (2007)

Summary:

- Pigmy resonances

- Halos \leftrightarrow no pigmy

- Skins \rightarrow pigmy

- Experimental precision - needs to improve

- Low energies and high excitation probabilities

- \rightarrow Higher order effects crucial for experimental analyses of PDR strength

- Electron scattering could enlighten many of the above features

Backup slides

EOS - mean field

- Build an energy functional $E[\rho]$ using an mean field calculation
Each such a functional characterizes a K_∞

- Get excitations such as the ISGMR from a self-consistent QRPA calculation

For the nucleon-nucleon interaction

$$V(\mathbf{r}_i, \mathbf{r}_j) = V_{ij}^{\text{NN}} + V_{ij}^{\text{Coul}}$$

$$V_{ij}^{\text{Coul}} = -\frac{e^2}{4} \sum_{i,j=1}^A \frac{\tau_{ij}^2 + \tau_{ij}}{|\mathbf{r}_i - \mathbf{r}_j|},$$

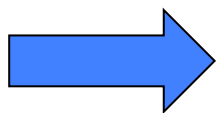
$$\tau_{ij} = \tau_i + \tau_j$$

$$V_{ij}^{\text{NN}} = t_0 (1 + x_0 P_{ij}^\sigma) \delta(\mathbf{r}_i - \mathbf{r}_j) + \frac{1}{2} t_1 (1 + x_1 P_{ij}^\sigma) [\hat{\mathbf{k}}_{ij}^2 \delta(\mathbf{r}_i - \mathbf{r}_j) + \delta(\mathbf{r}_i - \mathbf{r}_j) \vec{\mathbf{k}}_{ij}^2] +$$

$$t_2 (1 + x_2 P_{ij}^\sigma) \hat{\mathbf{k}}_{ij} \delta(\mathbf{r}_i - \mathbf{r}_j) \vec{\mathbf{k}}_{ij} + \frac{1}{6} t_3 (1 + x_3 P_{ij}^\sigma) \rho^\alpha \left(\frac{\mathbf{r}_i + \mathbf{r}_j}{2} \right) \delta(\mathbf{r}_i - \mathbf{r}_j) +$$

$$iW_0 \hat{\mathbf{k}}_{ij} \delta(\mathbf{r}_i - \mathbf{r}_j) (\vec{\sigma}_i + \vec{\sigma}_j) \vec{\mathbf{k}}_{ij},$$

t_i, x_i, α, W_0 are 10 **Skyrme** parameters



$$\mathcal{E}[\rho] = \langle \Phi | T + V_{ij}^{\text{Coul}} + V_{ij}^{\text{NN}} | \Phi \rangle$$

+ pairing

HF + BCS

$$\Delta_i = \frac{1}{2} \sum_j \frac{G_{ij} \Delta_j}{\sqrt{(\varepsilon_j - \lambda)^2 + \Delta_j^2}}$$

HFB

$$\begin{pmatrix} h_{HF} - \lambda & \Delta \\ -\Delta & -h_{HF} + \lambda \end{pmatrix} \begin{pmatrix} u_k \\ v_k \end{pmatrix} = E_k \begin{pmatrix} u_k \\ v_k \end{pmatrix}$$

$\mathbf{v}_{NN}^{\text{eff}} = \text{Skyrme} + \text{pairing force}$

$$V = V_0 \left[1 - \eta \left(\frac{\rho(\mathbf{r})}{\rho_0} \right)^\alpha \right] \delta(\mathbf{r}_1 - \mathbf{r}_2), \quad \rho_0 = 0.16 \text{ fm}, \quad \alpha = 1$$

$$\eta = \begin{cases} 0, & \text{"volume" pairing} \\ 1, & \text{"surface" pairing} \\ 1/2, & \text{"mixed" pairing} \end{cases}$$

Pairing Measure

three-point

$$\Delta^{(3)} = \frac{1}{2}(-1)^N [B(N-1) + B(N+1) - 2B(N)]$$

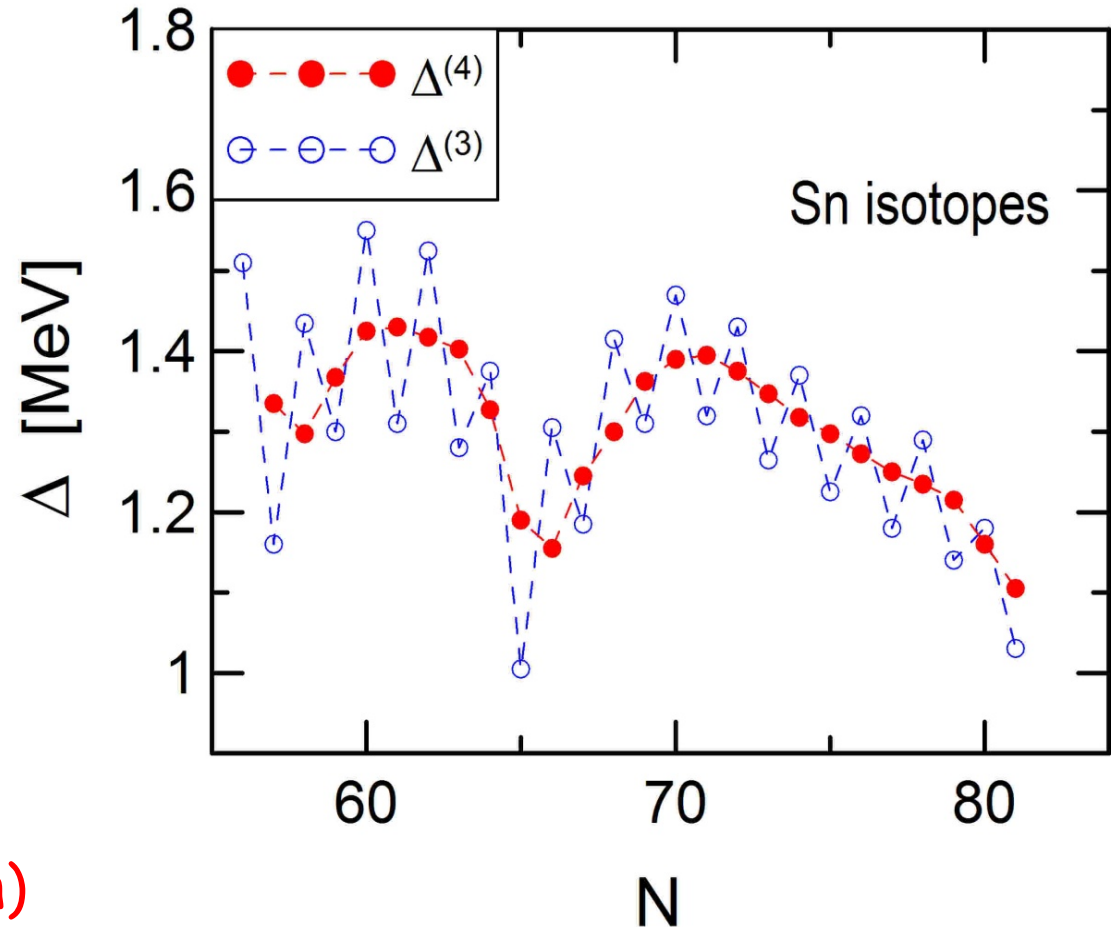
four-point

$$\Delta^{(4)} = \frac{1}{4}(-1)^N [3B(N-1) - 3B(N) - B(N-2) + B(N+1)]$$

or higher ?

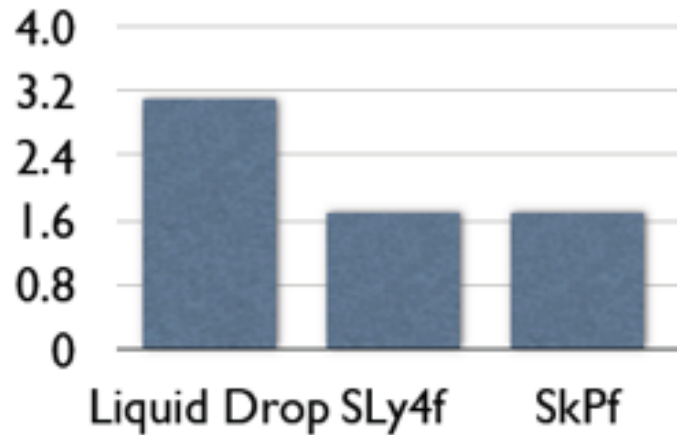
From experiment:

- $\Delta^{(3)}$ larger for $(-1)^N = +1$
- $\Delta^{(3)}$ smaller for $(-1)^N = -1$
- $\Delta^{(4)}$ reflects average of $\Delta^{(3)}$ (N) and $\Delta^{(3)}$ (N-1)
($\Delta^{(4)}$ no additional information)

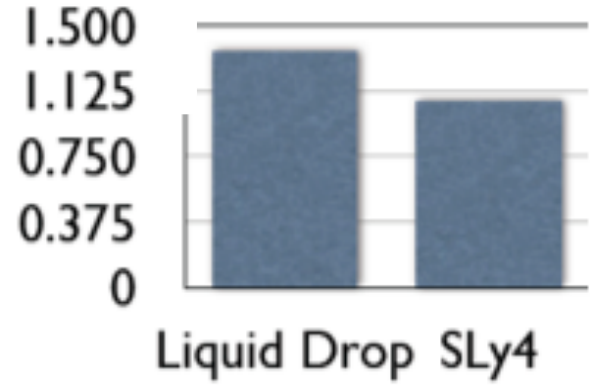


Can Microscopic Models do better than LDM?

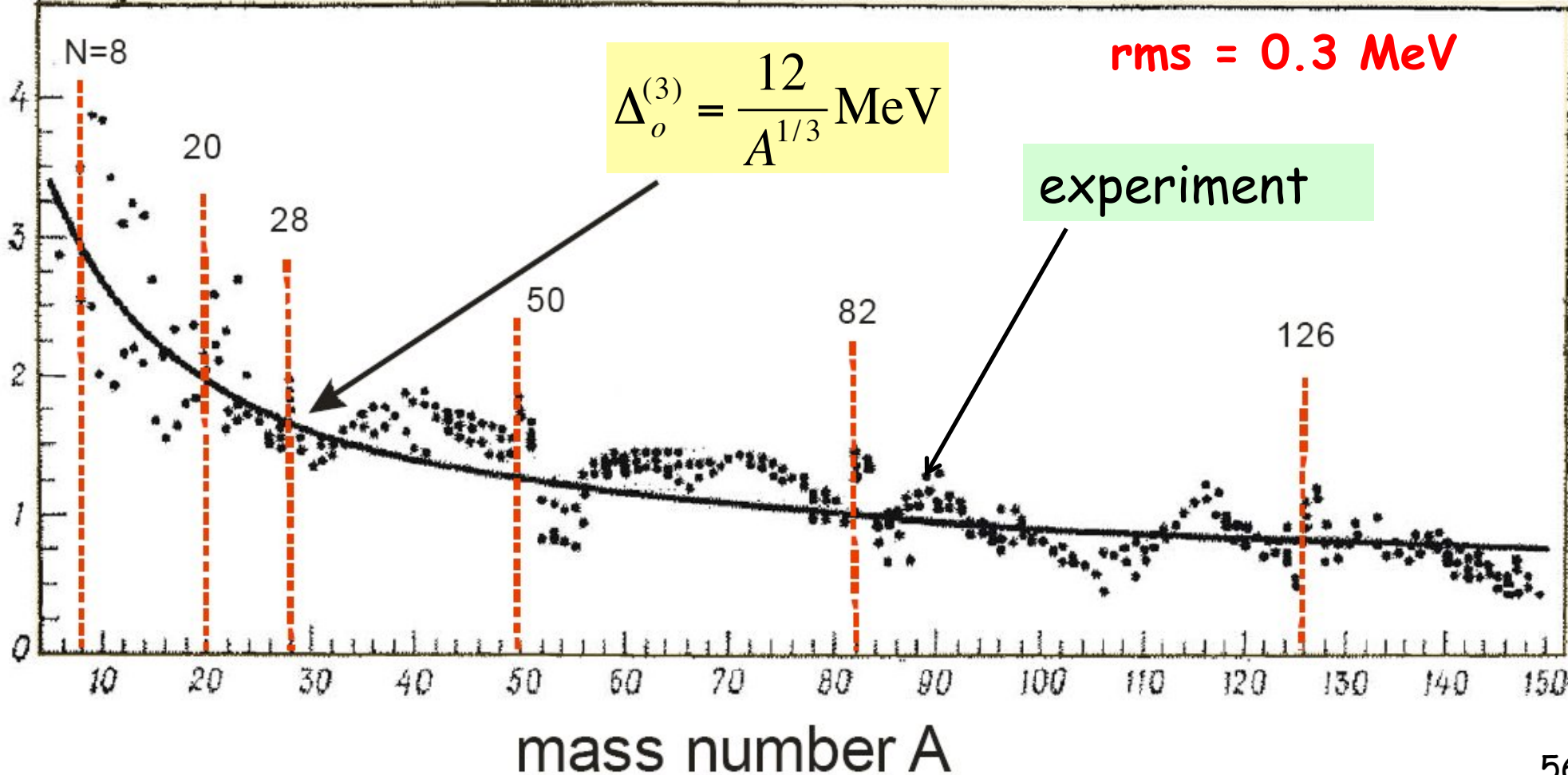
rms for binding energies



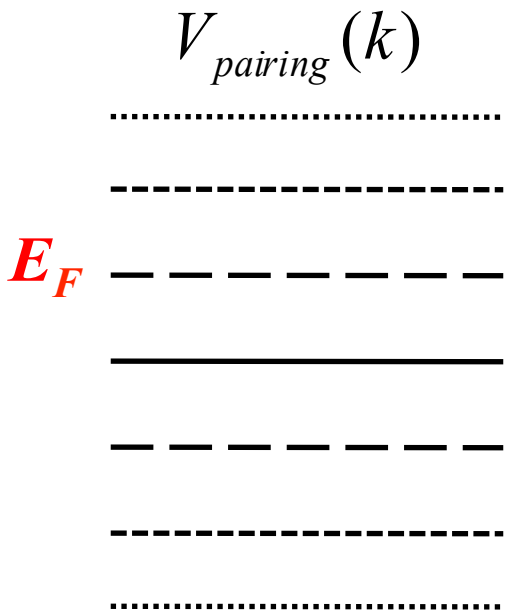
rms for separation energies



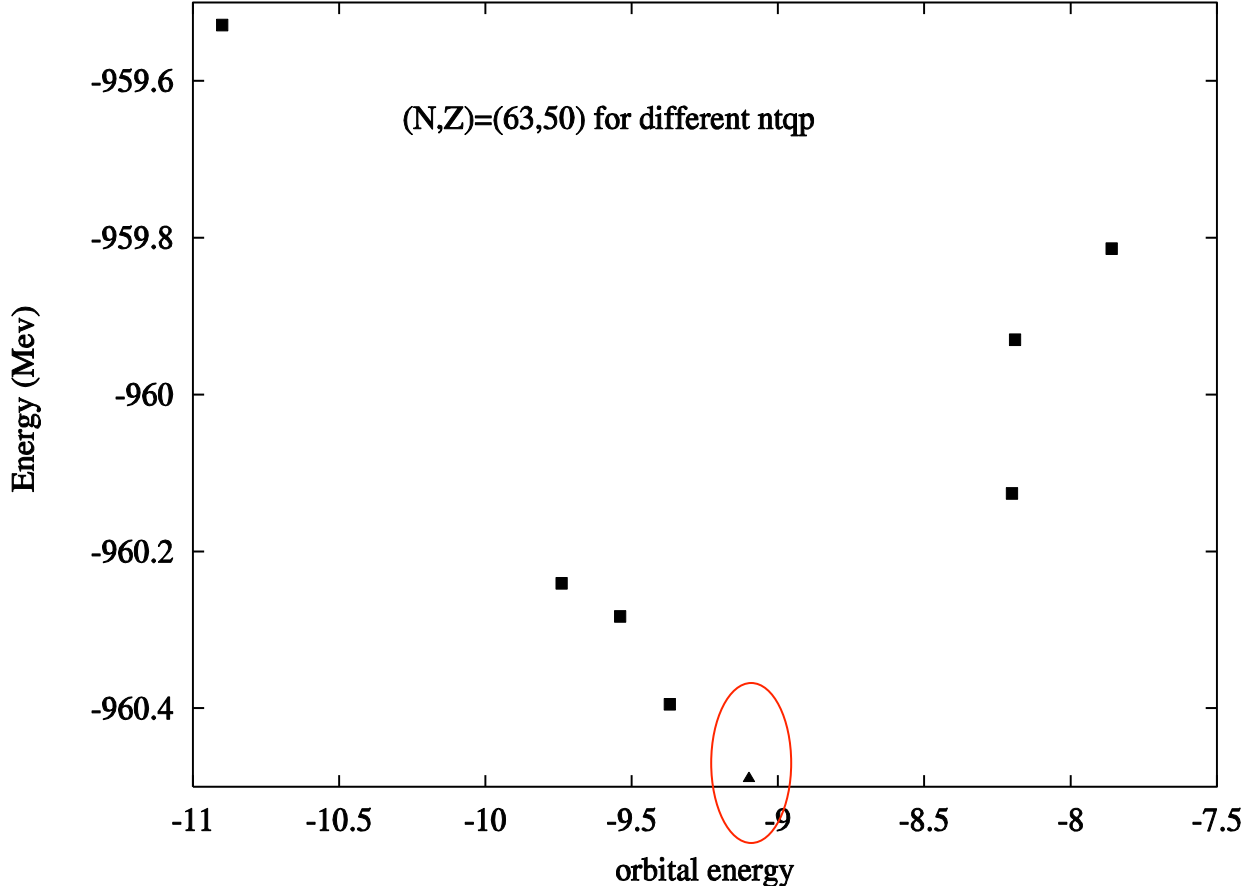
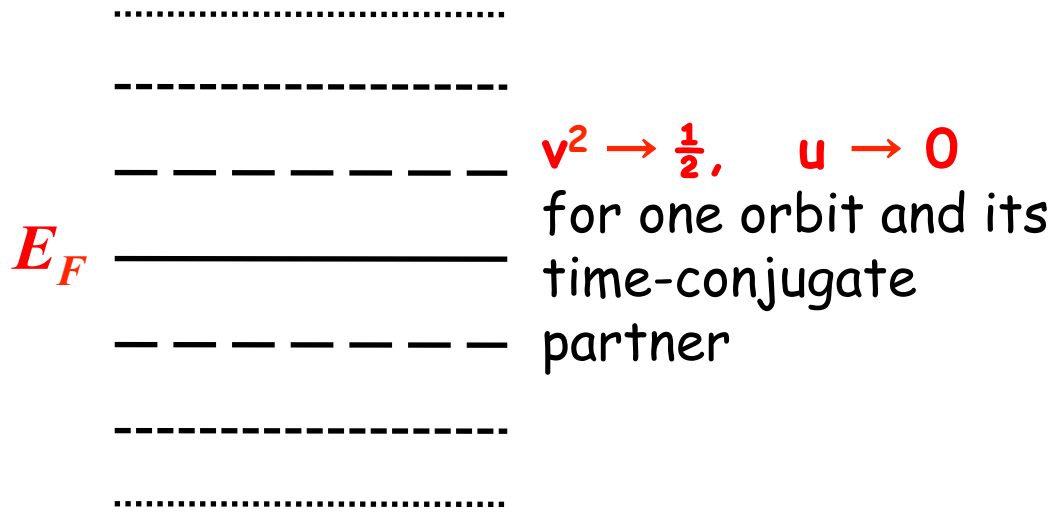
neutron pairing gap



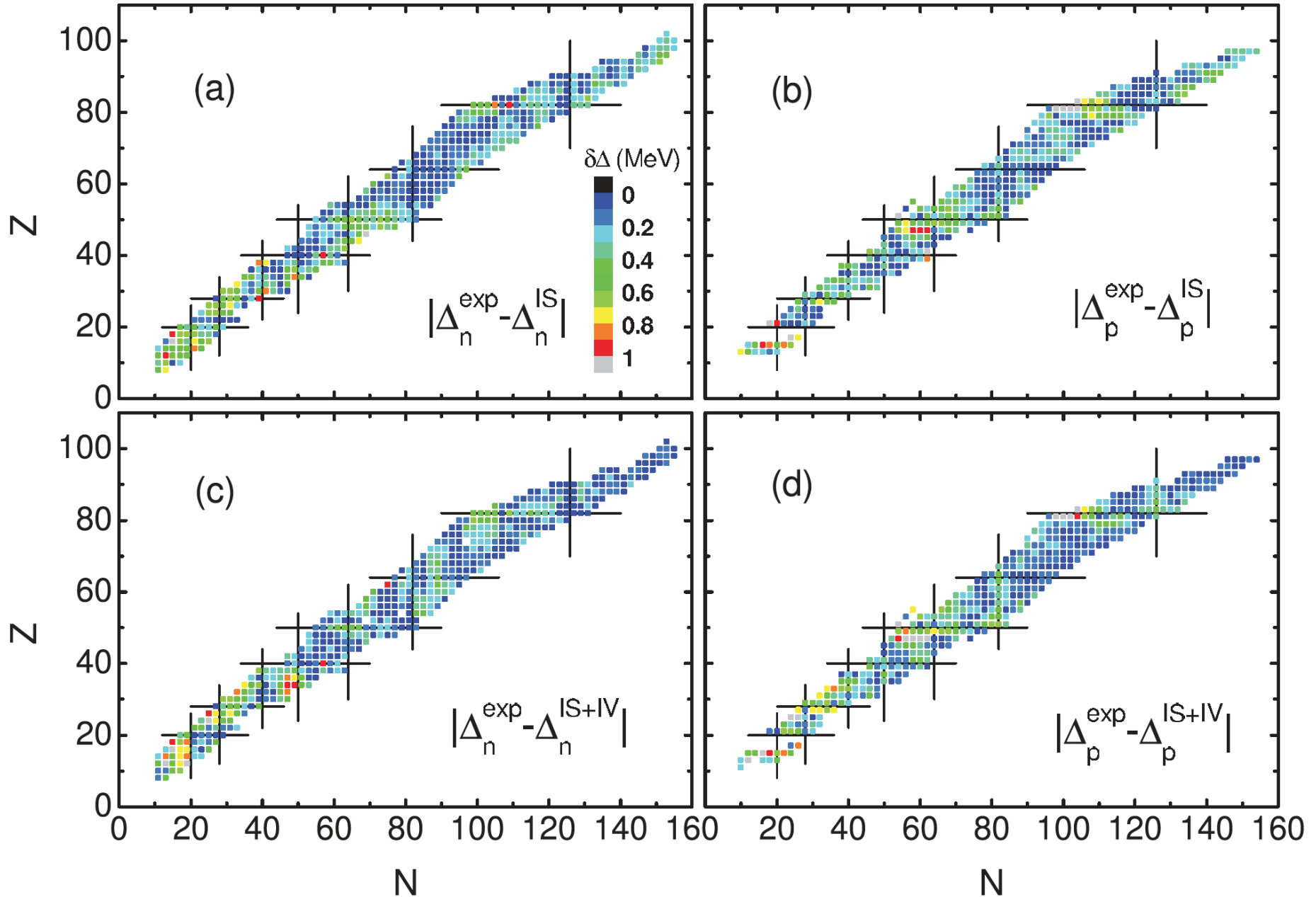
Blocking Procedure for Odd Nucleons



$\Lambda \sim 50 \text{ MeV}$



From 100 to 10^{57} nucleons - Skyrme & pairing

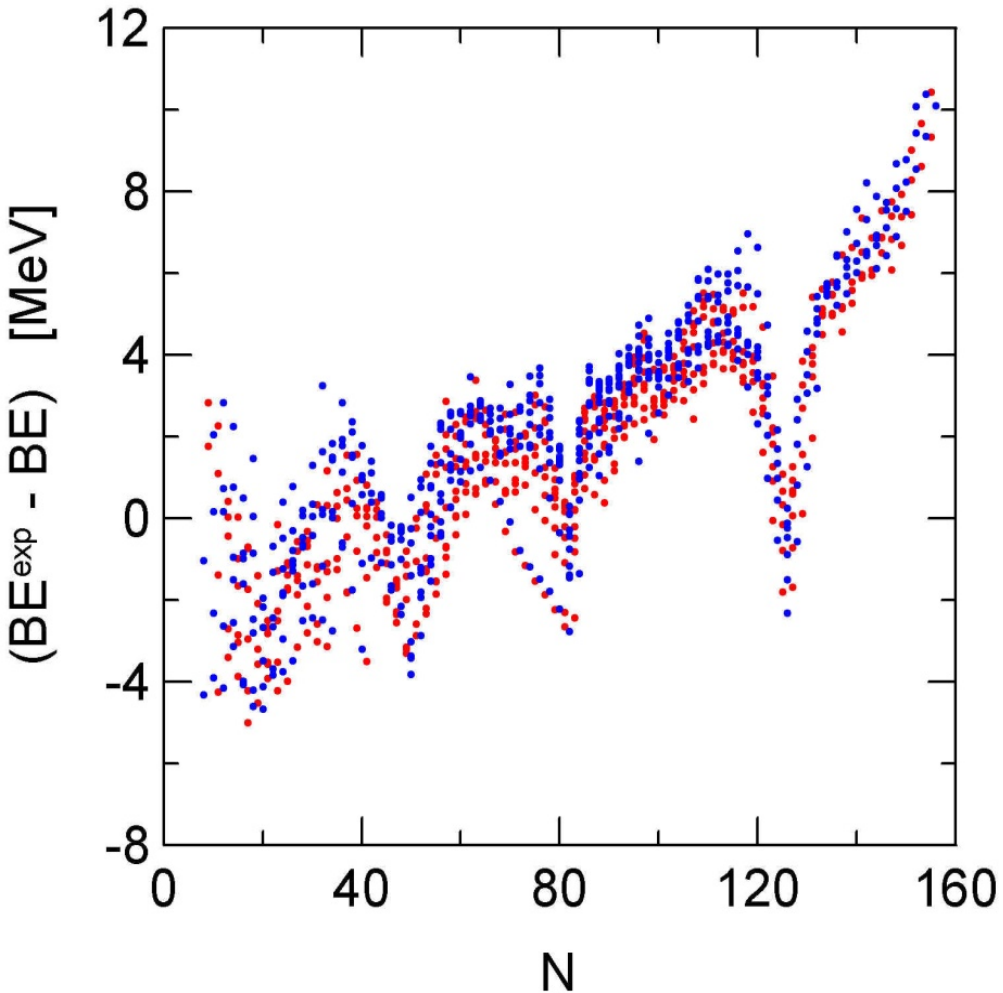


CB, Hongfeng Lu, Sagawa, PRC 80, 027303 (2009)

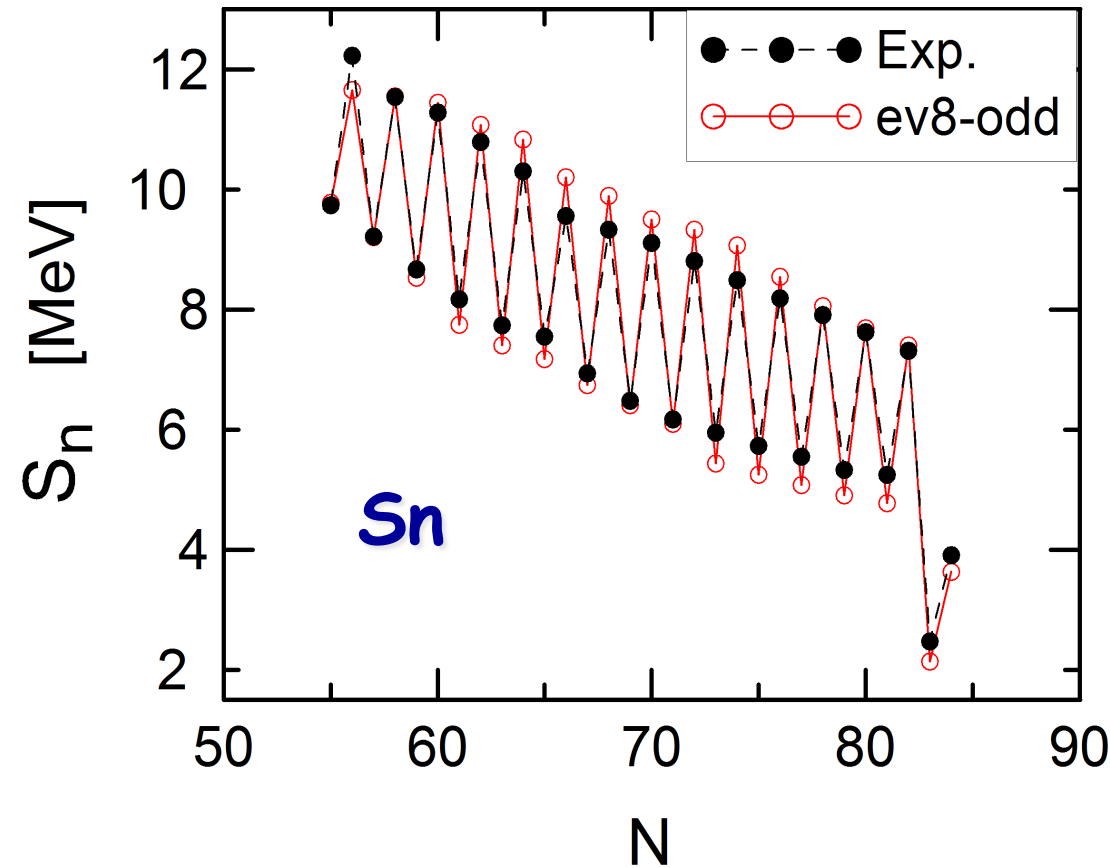
W. J. Chen, CB, F. R. Xu and Y. N. Zhang, PRC 91, 047303 (2015).

Pairing improves nuclear properties

- N-even, 521 nuclei, rms = 2.83 MeV
- N-odd, 498 nuclei, rms = 2.71 MeV



Separation energies staggering

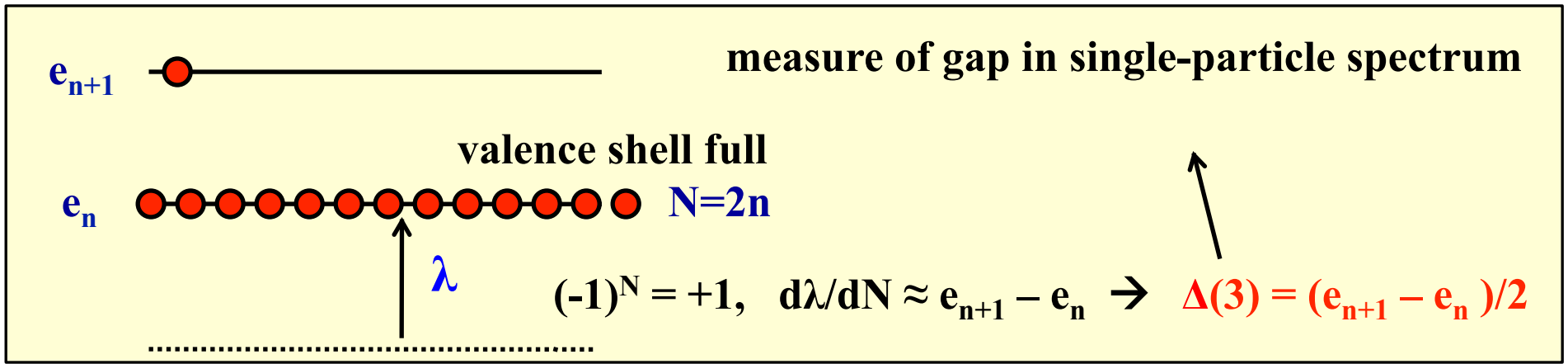
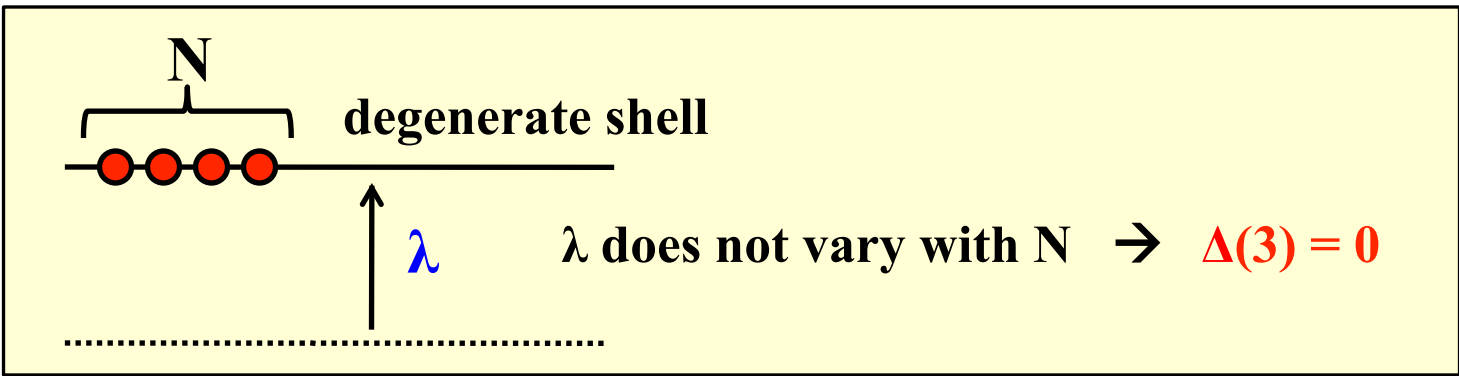


Bertsch, CB, Nazarewicz, Schunck, Stoitsov,
PRC 79, 0343306 (2009)

Pairing vs Level Properties

$$\Delta^{(3)} = \frac{1}{2}(-1)^N [B(N-1) + B(N+1) - 2B(N)] \Rightarrow 2(-1)^N \Delta^{(3)} \cong \frac{\partial^2 B}{\partial N^2} = \frac{\partial \lambda}{\partial N} = \frac{1}{g(\lambda)}$$

Fermi energy ($\lambda = \partial B / \partial N$) s.p. level density ($g(e) = dN / \partial e$)



Jahn-Teller mechanism: spherical symmetry spontaneously broken

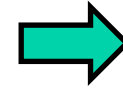
$(2j+1) \rightarrow$ double-degenerate orbits $\Rightarrow \Delta^{(3)}$ alternates for $(-1)^N = +$ and $-$

Pairing vs Level Properties

Macroscopic-microscopic model:

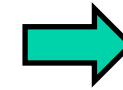
$$B = E_{sp} - \tilde{E}_{sp} + E_{macro}, \quad E_{sp} = \sum_{k=1}^A e_k$$

$$E_{macro} = \dots + a_I \frac{(N-Z)^2}{A}, \quad a_I = 23 \text{ MeV}$$



$$\Delta^{(3)} = \frac{23}{A} \text{ MeV}$$

$$\tilde{E}_{sp} \text{ contribution: } g(\lambda) = \frac{3a}{\pi^2}, \quad a \cong \frac{A}{8} \text{ MeV}$$

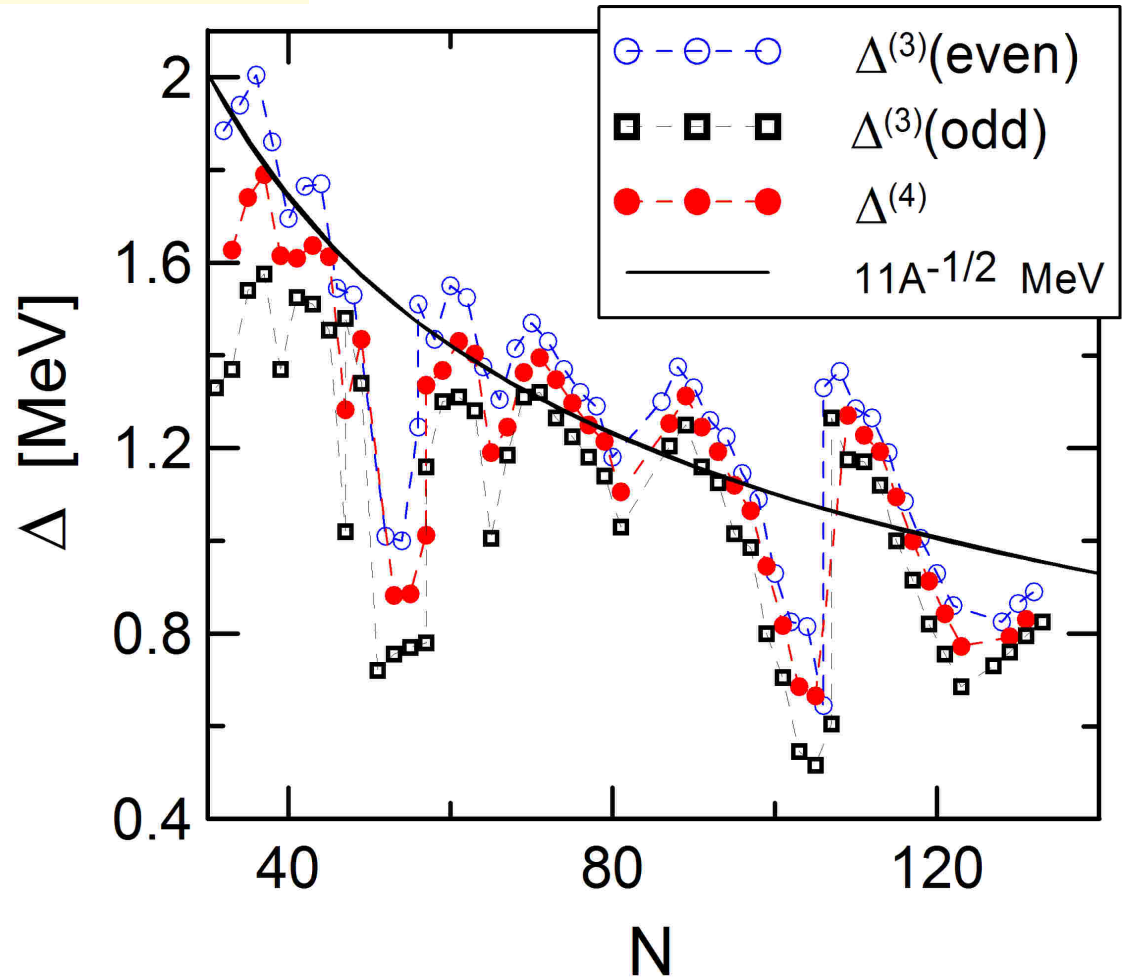


$$\Delta^{(3)} \cong -\frac{1}{g(\lambda)} \cong -\frac{25}{A} \text{ MeV}$$

$$\Delta^{(3)}(N) \cong -\frac{1}{2} \delta e$$

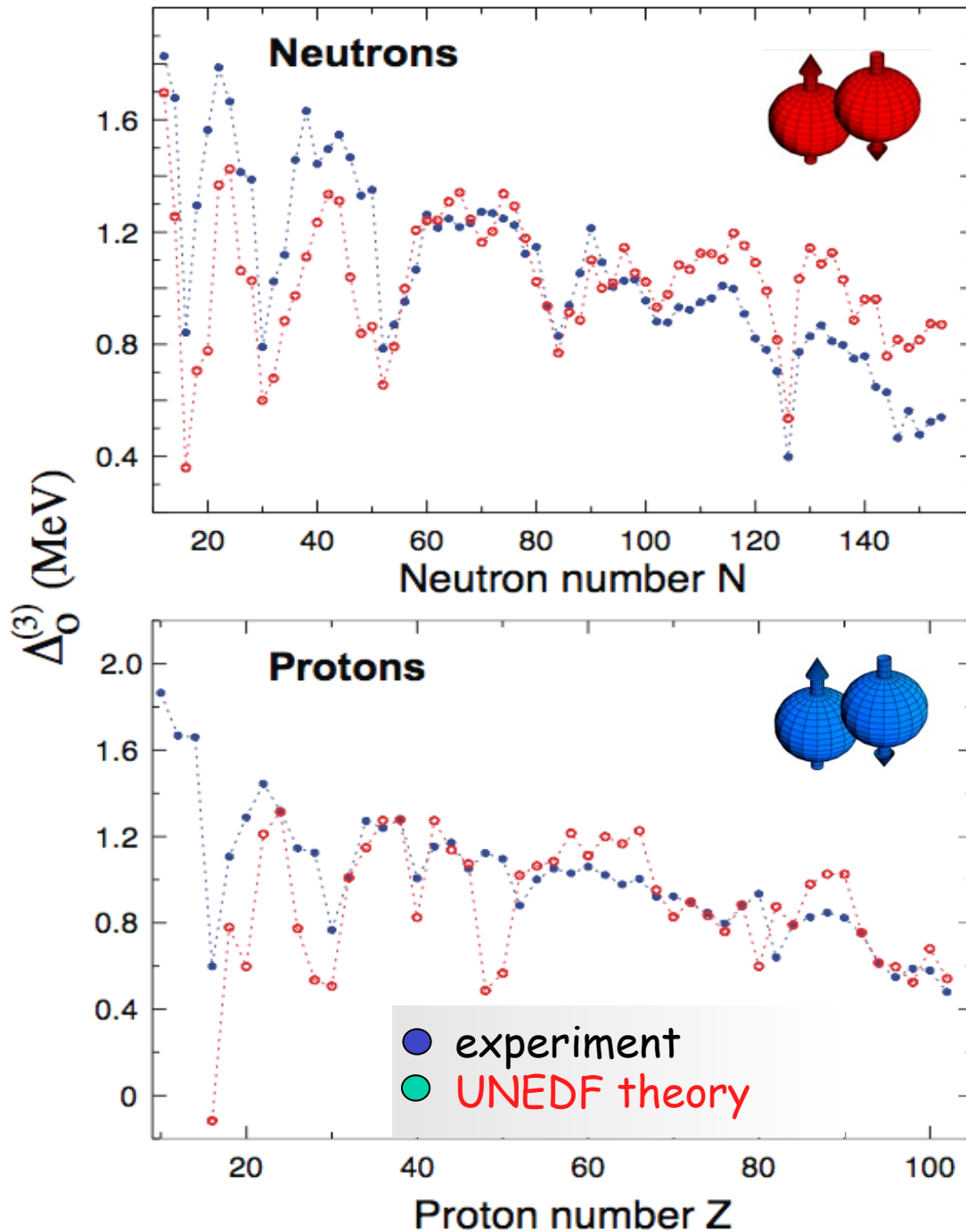
+ LDM corrections

$$2[\Delta^{(3)}(\text{even}) - \Delta^{(3)}(\text{odd})] \cong e_{n+1} - e_n$$

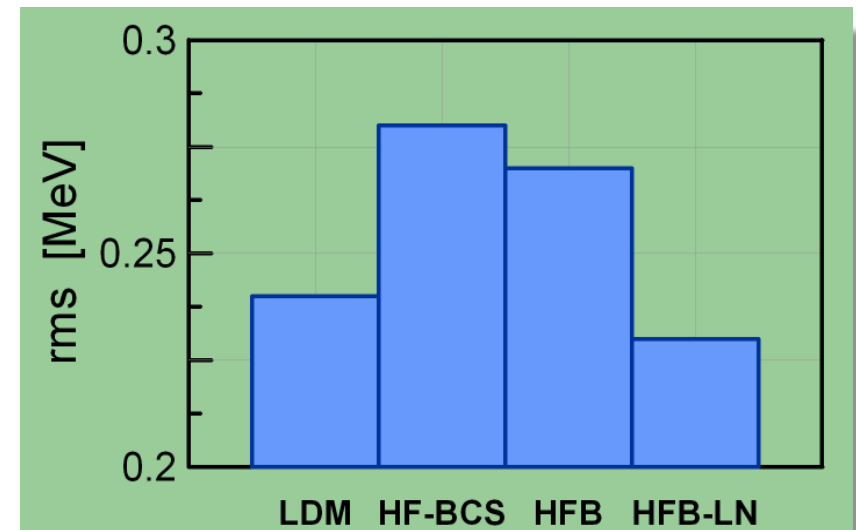


Satula, Dobaczewski, Nazarewicz,
PRL 81, 3599 (1998).

The uNclear Nuclear Pairing - UNEDF Collaboration



- Mass tables for 2,400 nuclei have been analyzed using different forms and methodologies for the pairing mechanism
- New functional forms for the pairing interaction have been proposed



$$\Delta^{(3)} = \frac{1}{2} (-1)^N [B(N-1) + B(N+1) - 2B(N)]$$

Bertsch, CB, Nazarewicz, Schunck, Stoitsov, PRC 79, 0343306 (2009)

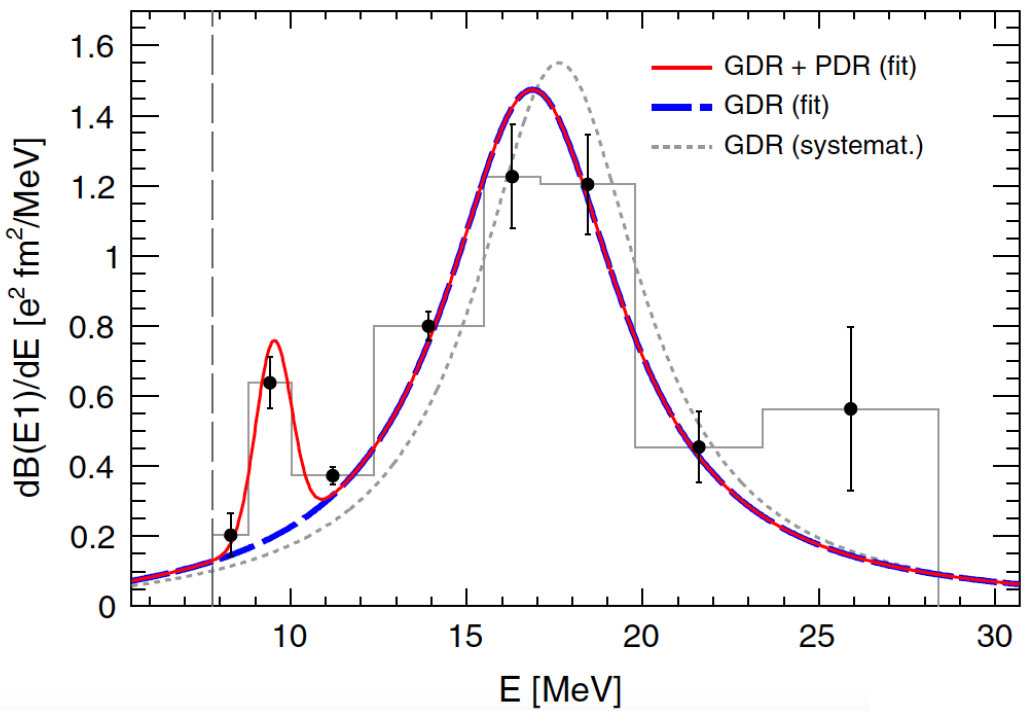
Pairing - ISGMR - Comparison to data

	nucleus	ph	pp	diff.
TAMU/ RCNP	$^{204-206-208}\text{Pb}$	SLy5	all	< 0.1
TAMU/ RCNP	^{144}Sm	SkM*	volume	- 0.1
TAMU/ RCNP	^{90}Zr	SLy5	all	+ 0.2
TAMU	^{92}Zr	SLy5	volume	- 0.4
	^{94}Zr	Skxs20	surface	+ 0.8
TAMU	^{92}Mo	SLy5	volume	- 1.6
	^{94}Mo	Skxs20	surface	+ 0.0
RCNP	$^{112-114-118-120}\text{Sn}$ [4]	Skxs20	mixed	< 0.1
	$^{122-124}\text{Sn}$ [4]	Skxs20	surface	< 0.1
	^{116}Sn [4]	SkM*	surface	< 0.1
TAMU	$^{112-124}\text{Sn}$ [35]	Skxs20	surface	\approx 0.8
	^{116}Sn [35]	Skxs20	surface	+ 0.2
RCNP	$^{106-110-112-114-116}\text{Cd}$ [6]	Skxs20	surface	< 0.1
TAMU	$^{110-116}\text{Cd}$ [46]	Skxs20	surface	\approx 0.9

Avogadro, CB,
PRC 88, 044319 (2013)

ISGMR is better reproduced with the soft interaction Skxs20 ($K_{\infty} \approx 202$ MeV), in contrast with the generally accepted value for $K_{\infty} \approx 230$ MeV.

E/M response for PDR, GDR and GQR



^{68}Ni

Rossi et al.,
PRL 11, 242503 (2013)

